MOLECULAR WEIGHT CHARACTERIZATION AND RHEOLOGY OF LIGNINS FOR CARBON FIBERS

By

GERALD WOLFGANG SCHMIDL

A DISSERTATION PRESENTED TO THE GRADUATE SCHOOL
OF THE UNIVERSITY OF FLORIDA IN PARTIAL FULFILLMENT
OF THE REQUIREMENTS FOR THE DEGREE OF
DOCTOR OF PHILOSOPHY

UNIVERSITY OF FLORIDA

1992

UNIVERSITY OF FLORIDA LIBRARIES

Copyright 1992

by

Gerald Wolfgang Schmidl

To my parents, Hans and Hilda, and to my wife, Viana

ACKNOWLEDGEMENTS

The author wishes to thank Dr. A.L. Fricke for his guidance and friendship throughout the many years required to complete this work. His extensive knowledge and experience, and his hard driving work ethic, have been very inspiring. He also wishes to thank Dr. C.L. Beatty for his friendship and advice, and for the use of his equipment. The author would also like to thank Dr. R.S. Drago, Dr. G. Hoflund, and Dr. C.W. Park for their willingness to participate in the review and critique of this dissertation, and Mr. Stan Sobczynski at the Department of Energy for providing ample funding for this project.

The members of Dr. Fricke's research group: Daojie Dong, Allan Preston, Barbara Speck, and Abbas Zaman, and fellow suffering graduate students, also deserve the author's sincere appreciation for friendship and support. The author also thanks Dr. Bill Toreki for performing the fiber carbonization work, David Bennett for his invaluable help in measuring tensile properties of the carbonized lignin fibers, and Ron Baxley, Tracey Lambert, and the office staff, for their help in solving the numerous mechanical and bureaucratic problems that frequently arose.

Finally, the author wishes to thank Tito and Adela Ostrea, his loving parents Hans and Hilda, and his wife and best friend, Viana, for their love and support during this long and arduous endeavor.

TABLE OF CONTENTS

page

ACKNOWLEDGEMENTS iv

LIST OF TABLES ix

LIST OF FIGURES x

KEY TO SYMBOLS xiii

KEY TO ABBREVIATIONS xvi

ABSTRACT xviii

CHAPTERS

1 INTRODUCTION 1

1.1 Overview 1
1.2 Research Objectives 2
1.3 Lignin 2
1.3.1 Occurrence in Wood 2
1.3.2 Structure 3
1.3.3 Lignin Utilization and Applications 5
1.4 Pulping Processes 7
1.4.1 Kraft Process 7
1.4.2 Organosolv Process 8
1.5 Carbon Fibers 9
1.5.1 Properties and Applications 9
1.5.2 Precursor Materials and Commercial Fibers 11
1.5.3 Processing Steps 12
1.5.4 Carbon Fibers from Lignin 14
1.6 Fiber Spinning 14
1.7 Need for Lignin Characterization 15
1.8 Overview of Subsequent Chapters 16

2 LIGNIN SELECTION AND PURIFICATION 17

2.1 General Considerations 17
2.2 Lignin Selection 18
2.3 Lignin Purification 20
2.3.1 Kraft Lignins 20
2.3.2 Organosolv Lignins 20
2.3.3 Storage 23

3 MOLECULAR WEIGHT CHARACTERIZATION 24

3.1 Introduction 24
3.2 SEC Theory 25
3.2.1 Separation Mechanism 25
3.2.2 Detection 27
3.2.3 Calibration 28
3.2.4 Nonsize Exclusion Effects 30
3.3 Background and Literature Review 31
3.3.1 Introduction 31
3.3.2 Traditional SEC Analyses 33
3.3.3 Association and Adsorption 34
3.3.4 Column Calibration 36
3.3.5 Multidetection and Absolute MWD 40
3.4 Experimental Work and Data Analysis 44
3.4.1 Instrumentation 44
3.4.2 Mobile Phase Selection and Preparation 46
3.4.3 Sample and Standards Preparation 46
3.4.4 SEC Runs and Data Analysis 49
3.5 Results and Discussion 50
3.5.1 General Comments on Mobile Phase Evaluation 50
3.5.2 Lignin Analysis in THF 51
3.5.3 Lignin Analysis in DMF and DMF Mixed Mobile Phases 52
3.5.4 Lignin Analysis in NaOH Solutions 55
3.5.5 Lignin Analysis in DMSO + LiBr Solutions 57
3.5.6 Column Calibration 66
3.5.7 Comparison of SEC Results with Previous Work 68
3.6 Conclusions and Recommendations 70
3.6.1 Conclusions 70
3.6.2 Recommendations for Future Work 71

4 LIGNIN THERMAL ANALYSIS 72

4.1 Introduction 72

4.2 Theory 73
4.2.1 Glass Transition 73
4.2.2 Effect of Plasticizer on T_g 75
4.2.3 DSC Principles of Operation 76
4.3 Background and Literature Review 78
4.3.1 Introduction 78
4.3.2 Early Work: Characteristic Softening Temperatures 79
4.3.3 Lignin T_g Studies 80
4.3.4 Enthalpy Relaxation 82
4.3.5 Glass Transition Behavior of Plasticized Lignins 83
4.4 Experimental Work and Data Analysis 85
4.4.1 Instrumentation 85
4.4.2 Sample Selection and Preparation 86
4.4.3 DSC Experimental Methods 87
4.4.4 Data Analysis 89
4.5 Results and Discussion 91
4.5.1 Glass Transition Temperatures for Dry Lignins .. 91
4.5.2 T_g s for Solvent Plasticized Indulin AT 95
4.6 Conclusions and Recommendations 100
4.6.1 Conclusions 100
4.6.2 Recommendations for Future Work 101

5 LIGNIN RHEOLOGY 103

5.1 Introduction 103
5.2 Rheometry Theory 104
5.2.1 Viscometric Flows and Material Functions 104
5.2.2 Steady Shear Operation 105
5.2.3 Dynamic Shear Operation and Linear Viscoelasticity 108
5.3 Background and Literature Review 111
5.3.1 Black Liquor Rheology 111
5.3.2 Polymer Rheology 111
5.4 Experimental Work 113
5.4.1 Sample Preparation 113
5.4.2 Rheometer 115
5.4.3 Testing Procedures 116
5.5 Results and Discussion 118
5.5.1 General Observations 118
5.5.2 Steady Shear Behavior 119
5.5.3 Dynamic Shear Rheometry 121
5.6 Conclusions and Recommendations 125
5.6.1 Conclusions 125

5.6.2 Recommendations for Future Work 125

6 LIGNIN FIBER SPINNING AND CARBONIZATION 127

6.1 Introduction 127
6.2 Background and Literature Review 127
6.2.1 Early Japanese Development Work 127
6.2.2 West German Process 130
6.2.3 Carbon Fibers from Black Liquor 131
6.2.4 Fiber Microstructure 132
6.2.5 Recent Development Work 133
6.3 Experimental Work 134
6.3.1 Lignin Fiber Spinning 134
6.3.2 Fiber Carbonization 136
6.3.3 Fiber Analysis 137
6.4 Results and Discussion 140
6.4.1 Thermogravimetric Analysis 140
6.4.2 Surface Morphology 142
6.4.3 Elemental Composition 146
6.4.4 Mechanical Properties 147
6.5 Conclusions and Recommendations 151
6.5.1 Conclusions 151
6.5.2 Recommendations for Future Work 152

7 OVERALL CONCLUSIONS AND RECOMMENDATIONS 154

7.1 Summary 154
7.2 Conclusions 155
7.3 Recommendations for Future Work 157

REFERENCES 159

BIOGRAPHICAL SKETCH 169

LIST OF TABLES

Table		page
1-1	Performance Properties and Application Areas of Lignin Products	6
1-2	Physical Properties and Applications of Carbon Fibers	10
2-1	Lignins Selected for this Study	19
3-1	SEC Mobile Phase Selection	47
3-2	Lignin Molecular Weights from SEC in DMSO + 0.1M LiBr at 85°C	64
3-3	Comparison of SEC Results for Mixed Hardwood Kraft and Organosolv Lignins with Literature Values	69
4-1	Hansen Solubility Parameters for Lignin Solvents	87
4-2	Temperature Program for DSC Analysis of Dry and Solvent Plasticized Lignins	89
4-3	Glass Transition Temperatures for Dry Lignins	93
6-1	Lignin Fiber Spinning Conditions	137
6-2	Lignin Fiber Carbonization Conditions	138
6-3	Elemental Composition of Lignin Carbon Fibers	147
6-4	Mechanical Properties of Lignin-Based and PAN-Based Carbon Fibers	150

LIST OF FIGURES

Figure		page
1-1	Representative Model for Native Softwood Lignin Structure	4
1-2	Lignin Monomers: p-Coumaryl Alcohol (I), Coniferyl Alcohol (II), and Sinapyl Alcohol (III)	5
2-1	Kraft Lignin Isolation and Purification Scheme	21
3-1	Typical SEC Chromatogram for a Softwood Kraft Lignin Run in DMF at 85°C on Jordi Gel Mixed Bed + 10^3 Å Columns..	53
3-2	SEC Chromatogram for a Softwood Kraft Lignin Run in DMF/EGMPE (98/2) at 85°C on Jordi Gel Mixed Bed + 10^3 Å Columns	55
3-3	SEC Chromatograms for Indulin AT Run in DMSO with Various Concentrations of Lithium Bromide at 85°C on the Jordi Gel 10^3 Å GBR Column	58
3-4	SEC Chromatograms for Selected UF Kraft Softwood Lignins Run in DMSO + 0.1M LiBr at 85°C on the Jordi Gel 10^3 Å GBR Column	60
3-5	SEC Chromatograms for Selected UF Kraft Softwood Lignins Run in DMSO + 0.1M LiBr at 85°C on the Jordi Gel 10^3 + 10^4 Å GBR Column Set	61
3-6	SEC Chromatograms for Indulin AT, Maple, and Organosolv Lignins Run in DMSO + 0.1M LiBr at 85°C on the Jordi Gel 10^3 Å GBR Column	62
3-7	SEC Calibration Curve with Narrow MWD Polysaccharide Standards for the Jordi Gel 10^3 + 10^4 Å GBR Column Set Running DMSO + 0.1M LiBr at 85°C	67

4-1	Experimental Definition for the Onset Glass Transition Temperature	90
4-2	DSC Scan for S.D. Warren Birch Kraft Lignin. Heating Rate = 10°C/min in Nitrogen	92
4-3	Effect of Lignin Polydispersity on the Breadth of the Glass Transition Region	96
4-4	Glass Transition Depression for Solvent Plasticized Indulin AT Lignin	98
5-1	Cone and Plate Geometry. (a) Steady Shear Flow; and (b) Dynamic Oscillatory Shear Flow	106
5-2	Steady Shear Rheometry of Indulin AT + 28% NMP at 80 and 100°C	120
5-3	Dynamic Oscillatory Shear Strain Sweeps of Indulin AT + 28% NMP. Frequencies were 1.0 rad/sec at 80°C, and 10 rad/sec at 100°C	122
5-4	Dynamic Oscillatory Shear Rheometry of Indulin AT + 28%NMP at 80 and 100°C	123
5-5	A Comparison of First Normal Stress Differences and Storage Moduli, from Steady Shear and Dynamic Shear Rheometry, Respectively	124
6-1	Lignin Fiber Spinning Apparatus	135
6-2	Carbonized Lignin Fiber Tensile Testing Apparatus	139
6-3	Thermogravimetric Analysis of Fibers Spun from Indulin AT + 28% NMP. Normal TGA Curve for Softwood Kraft Lignin (----) by Masse [62]. Heating Rate = 10°C/min in Nitrogen	141
6-4	SEM Micrographs for Lignin Fiber. (a) Uncarbonized "Green" Fiber; (b) Carbonized "B" Fiber	143
6-5	SEM Micrographs for "B" Carbonized Lignin Fiber	144
6-6	Tensile Test for Carbonized Lignin Fiber "A"	148

6-7 Tensile Test for Carbonized Lignin Fiber "B"..... 149

KEY TO SYMBOLS

Symbol	Definition
a	Mark-Houwink constant
C_p	Heat capacity at constant pressure, J/(g-°C)
F	Total normal force, N
G^*	Complex shear modulus, Pa
G'	Storage modulus, Pa
G''	Loss modulus, Pa
K	Distribution coefficient of solute; Mark-Houwink constant
M	Molecular weight in Mark-Houwink relationship
$\bar{M}_n$	Number average molecular weight
M_p	Peak molecular weight
$\bar{M}_w$	Weight average molecular weight
N_1	First normal stress difference, Pa
N_2	Second normal stress difference, Pa
R	Cone, plate radius, mm
r	radial position
T	Torque, N-m; Temperature, °C

T_g	Glass transition temperature, °C
T_g^o	Glass transition temperature for pure polymer, °C
T_m	Onset melting temperature, °C
T_s	Softening temperature, °C
t	Time, sec
t_R	Solute retention time, min
v	Velocity, m/sec
V_i	Pore volume, ml
V_o	Interstitial (dead) volume of SEC column, ml
V_R	Retention volume of solute, ml
V_T	Total column volume, ml
W_2	Weight fraction of diluent, g/g
α	Cone angle, rad
γ	Strain
γ_o	Strain amplitude
$\dot{\gamma}$	Shear rate, sec^{-1}
δ	Phase shift, rad; general solubility parameter, $(cal/cm^3)^{0.5}$
δ_o	Overall Hansen solubility parameter, $(cal/cm^3)^{0.5}$
δ_d	Hansen dispersion (nonpolar) parameter, $(cal/cm^3)^{0.5}$
δ_h	Hansen hydrogen bonding parameter, $(cal/cm^3)^{0.5}$
δ_p	Hansen polar parameter, $(cal/cm^3)^{0.5}$

η, η_{app}	Steady shear apparent viscosity, Pa-sec
η_o	Zero shear rate viscosity, Pa
$[\eta]$	Intrinsic viscosity, cm^3/g
η^*	Complex viscosity, Pa-sec
η'	Dynamic viscosity (real component of η^*), Pa-sec
η''	Imaginary component of η^*, Pa-sec
θ	Spherical coordinate direction
τ	Shear stress, Pa
τ_o	Shear stress amplitude, Pa
ϕ	Spherical coordinate direction
Ψ_1	First normal stress coefficient, $Pa\text{-}sec^2$
Ψ_2	Second normal stress coefficient, $Pa\text{-}sec^2$
Ω	Angular velocity, rad/sec
ω	Frequency, rad/sec

KEY TO ABBREVIATIONS

ACS	American Chemical Society
DMF	N,N-Dimethylformamide
DMSO	Dimethylsulfoxide
DRI	Differential refractive index
DSC	Differential scanning calorimetry
DV	Differential viscometry
DVB	Divinylbenzene
EDS	Energy dispersive x-ray spectroscopy
EG	Ethylene glycol
EGDME	Ethylene glycol dimethyl ether
EGMME	Ethylene glycol monomethyl ether
EGMPE	Ethylene glycol monopropyl ether
FRT	Force rebalance transducer
GPC	Gel permeation chromatography
HPLC	High pressure liquid chromatography
HPSEC	High pressure size exclusion chromatography
LALLS	Low angle laser light scattering
MW	Molecular weight

MWD	Molecular weight distribution
NMP	N-Methyl pyrrolidinone
PAN	Polyacrylonitrile
PEG	Polyethylene glycol
PEO	Polyethylene oxide
PID	Proportional, integral, and derivative
PMMA	Polymethyl methacrylate
PRT	Platinum resistive thermosensor
PS	Polystyrene
PSS	Polystyrene sulfonate
PVA	Polyvinyl alcohol
SEC	Size exclusion chromatography
SEM	Scanning electron microscopy
TBA	Torsional braid analysis
TCE	1,1,1-Trichloroethane
TEA	Triethylamine
TGA	Thermogravimetric analysis
THF	Tetrahydrofuran
UF	University of Florida
UV/Vis	Ultraviolet/visible
VPO	Vapor pressure osmometry

Abstract of Dissertation Presented to the Graduate School
of the University of Florida in Partial Fulfillment of the
Requirements for the Degree of Doctor of Philosophy

MOLECULAR WEIGHT CHARACTERIZATION AND RHEOLOGY OF LIGNINS FOR CARBON FIBERS

By

Gerald Wolfgang Schmidl

December 1992

Chairperson: Arthur L. Fricke
Major Department: Chemical Engineering

This investigation was initiated to (1) characterize purified lignins, from a statistically designed pulping experiment, and from commercial sources, for molecular weights (MW s) and molecular weight distribution (MWD) by size exclusion chromatography (SEC), to support a larger overall study of kraft black liquor physical properties, and to (2) study the feasibility of producing lignin-based carbon fibers as an alternative high value use for lignins. To support the lignin fiber spinning work, glass transition temperatures (T_g s) for dry and solvent plasticized lignins were determined by differential scanning calorimetry, and rheological properties of solvent plasticized lignins were measured by steady and oscillatory shear rheometry. Kraft softwood, kraft hardwood, and organosolv lignins were studied.

A new SEC method for comparative lignin MWD characterization was developed which consists of dimethyl sulfoxide + 0.1M LiBr running at 85 °C in a

custom made "deactivated" column, and overcomes persistent lignin association and adsorption problems. Accurate column calibration methods, such as resolution of moments, must still be investigated because calculated weight average MW s differed from fully corrected absolute values by a factor of 3-15.

Lignin T_g s ranged from 130 to 170°C, which reflect the effect of differences in pulping conditions on MW. The glass transitions were very broad, and correlated linearly with polydispersity of MW. The T_g depression for solvent plasticized Indulin AT (a kraft softwood lignin) was greater with N-methyl pyrrolidinone (NMP), a weaker hydrogen bonding solvent, than with dimethyl formamide, a stronger one.

The rheological properties of Indulin AT plasticized with NMP were measured at 80 and 100°C with a cone and plate rheometer. This material exhibited shear thinning behavior and some degree of viscoelasticity. Apparent viscosity and complex viscosity both decreased with increasing shear rate or frequency, and first normal stress difference and storage modulus both increased with increasing shear rate or frequency. These trends are the same as for synthetic polymer melts and solutions.

Single fibers of Indulin AT + 28% NMP were spun at 100 m/min at 130°C, and carbonized at 1,000°C under argon. These fibers had a carbon content of 91%, and mechanical properties--diameter, tensile strength, modulus, and elongation--of 103 ± 3.5 μm, 150 ± 20 MPa, 49.1 ± 14.4 GPa, and 0.32 ± 0.11%, respectively. Producing carbon fibers from kraft lignins is currently not a viable alternative application, but these results were encouraging, and further work in this area is recommended.

CHAPTER 1
INTRODUCTION

1.1 Overview

Lignin is a complex, amorphous, heterogeneous natural polymer, which, after cellulose, is the most abundant and important natural polymeric substance in the plant world. It is extracted from wood during pulping operations for papermaking and is the primary organic component of the black liquor byproduct. Although its primary use is as a fuel in the pulping process, other applications could include carbon fiber manufacture. In order to develop alternative applications, a thorough understanding of lignin structure/property relationships, including molecular weight characterization and rheological behavior, is necessary.

This chapter identifies the objectives of this research (Section 1.2), and briefly discusses the structure, properties, and current utilization of lignins in Section 1.3. A brief description of the dominant kraft pulping process and a newer organosolv pulping process are given in Section 1.4. An introduction to carbon fibers is given in Section 1.5 followed by a brief description of the fiber spinning process in Section 1.6. Finally, the justification for this characterization work, and a brief description of the remaining chapters, is discussed in Sections 1.7 and 1.8, respectively.

1.2 Research Objectives

This experimental study has two principal objectives: (1) to characterize purified lignins, from a statistically designed pulping experiment, and from commercial sources, for molecular weights and molecular weight distribution by SEC, and (2) to investigate the feasibility of producing carbon fibers from these lignins. These two objectives are semi-independent and reflect the dual nature of this work: basic lignin material properties characterization, and applications development for purified lignins.

The molecular weight characterization work will support a much larger overall study of kraft black liquor physical and chemical properties which will benefit the pulp and paper industry in its long term plan to more efficiently process black liquors. The development of lignin-based carbon fibers could provide an alternative high value use for lignins, as compared to its current predominantly low value fuel use. Three primary types of lignins were studied: kraft softwood, kraft hardwood, and organosolv lignins.

1.3 Lignin

1.3.1 Occurrence in Wood

Wood is a three-dimensional cellular composite structure consisting of cellulose, hemicelluloses, lignin, small amounts of extractives such as phenols, terpenes, and organic acids; and ash. Wood is not a homogeneous material; its

chemical constituents are not uniformly distributed, and there are also various types of cells. Lignin comprises approximately 18-35 weight % of wood, and is concentrated in the thickest layer of the cell wall. It provides strength to wood by serving as a matrix to hold the cellulose fibers together. There are two main categories of wood: gymnosperms (softwoods), such as spruce, fir, pine, and cedar; and angiosperms (hardwoods) such as oak, maple, and birch [71, 81].

1.3.2 Structure

Lignin has a very complex, heterogeneous, highly branched, amorphous structure which can vary significantly with morphology (location in cell), cell type (vessel versus fiber), wood type (softwood versus hardwood), and species. A representative model for this complex structure is shown in Figure 1-1. In different cell regions, lignin can be a random three-dimensional network polymer, or a nonrandom two-dimensional network polymer. Upon delignification, the properties of the solubilized macromolecules reflect the properties of the network from which they are derived [22, 37, 81] .

Three phenylpropane monomers, differing only in the number of methoxyl substituents, polymerize to form lignin. These monomers are p-coumaryl alcohol, coniferyl alcohol, and sinapyl alcohol, and are shown in Figure 1-2. Lignification is initiated when a phenolic hydroxyl hydrogen atom is abstracted by the enzyme peroxidase to form a phenoxy free radical. This phenoxy free radical can be delocalized to both aromatic and side chain carbon atoms. Because of this

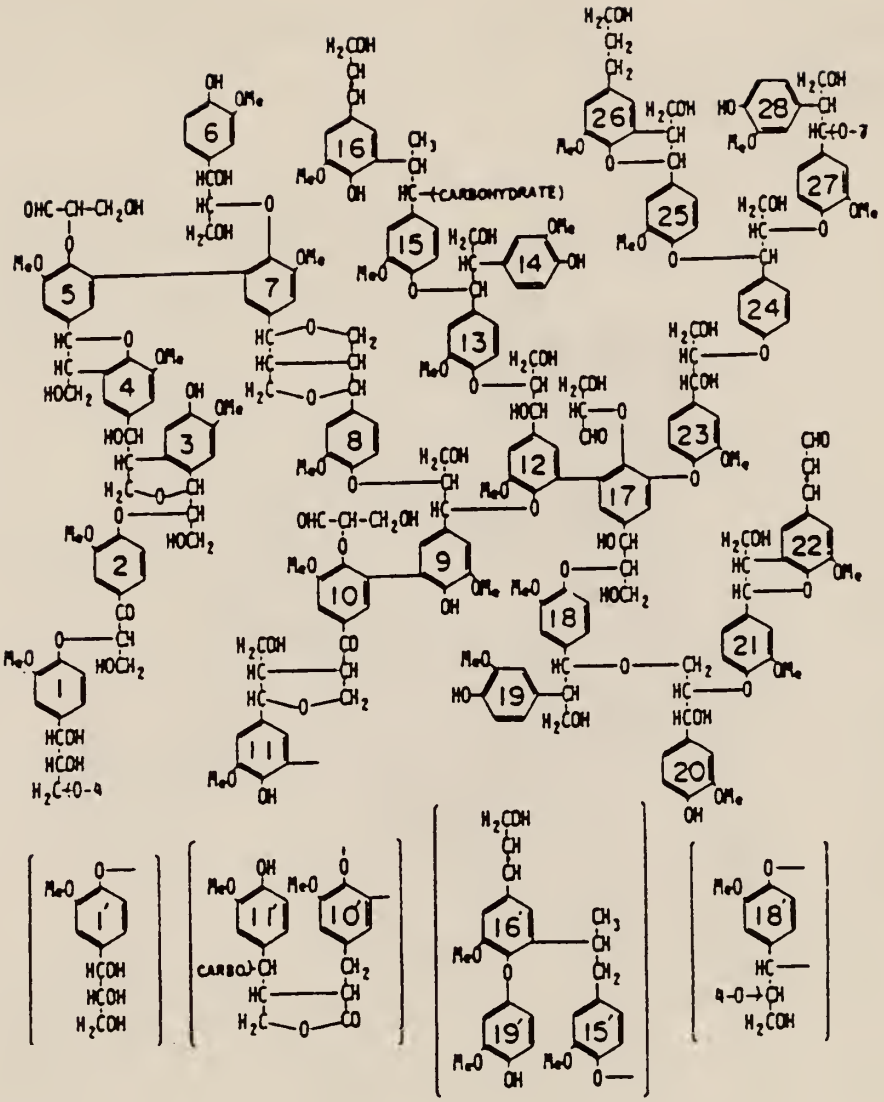

Figure 1-1. Representative Model for Native Softwood Lignin Structure. Source: Obst [71].

delocalization, coupling of these radicals can form ether linkages, carbon-carbon bonds, and bonds to more than one other phenyl propane unit. This results in the complicated lignin polymer having a crosslinked and three dimensional structure [71].

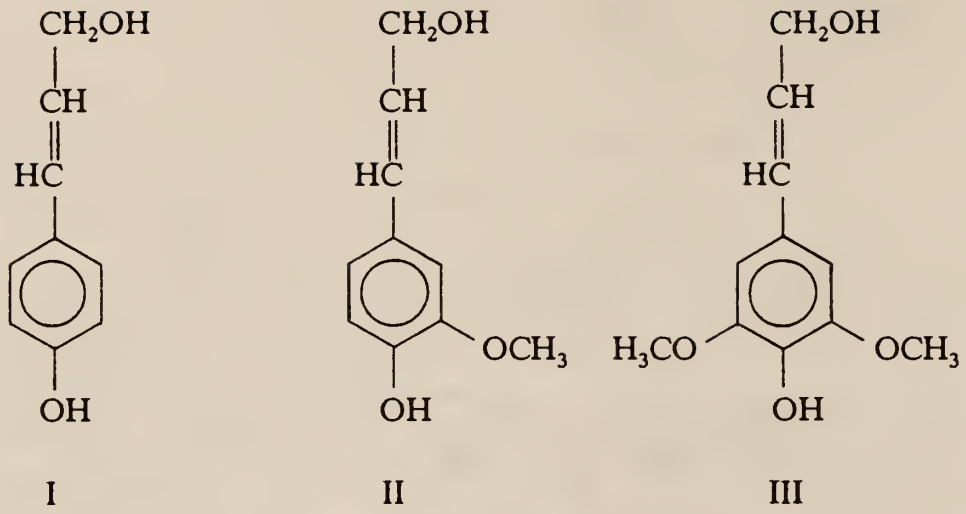

Figure 1-2. Lignin Monomers: p-Coumaryl Alcohol (I), Coniferyl Alcohol (II), and Sinapyl Alcohol (III). Source: Obst [71].

1.3.3 Lignin Utilization and Applications

Total worldwide lignin production is approximately 100 million tons/year*, and there are currently four main areas of commercial utilization: (1) as a remaining component in mechanical, high yield semi-chemical, and unbleached chemical pulps, e.g. in newsprint, (2) as a fuel, (3) as a polymeric product, and (4) as a source of low molecular weight chemicals [22]. The predominant use for lignin today is as a fuel, because recovery of the process chemicals in the dominant kraft pulping process is based on incineration of the spent black liquor, and due to the high heating value of the organic material in the spent liquor: 23.4 MJ/kg (10,070 Btu/lb) [22].

* Extrapolated from data presented by Glasser and Kelley [33].

Table 1-1. Performance Properties and Application Areas of Lignin Products.

	Performance property	Application areas
1.	Dispersing	Dispersants for carbon black, pigments, dyestuffs, clays, pesticides; cement grinding, concrete superplasticizer, gypsum wallboard, oil well drilling muds
2.	Complexing/dispersing	Boiler and cooling water treatments, micronutrients, corrosion inhibition, industrial cleaners, and protein precipitation
3.	Binding	Adhesives for board and veneer, animal feed pellets, printing inks, foundry sands, ore and coal briquettes; phenolic resin substitute, ceramics and refractories, soil conditioning
4.	Emulsion stabilizing	Asphalt, waxes, soaps, fire foam
5.	Adsorption/interfacial tension	Enhanced oil recovery
6.	Adsorption/desorption	Control release pesticides
7.	Mechanical strength	Rubber reinforcing

Sources: Fengel and Wegener [22], and Lin [56].

The utilization of polymeric purified lignins and lignin derivatives comprises only about 1-2 % of total lignin production and is generally based on the dispersing, adhesive, and surface active properties of the lignin products [22]. A summary of these diverse applications is provided in Table 1-1. High fractionation and modification costs, due to its inherent chemical and molecular weight inhomogeneity, have limited the utilization of lignin for the production of low molecular weight

chemicals and as a raw material for polymers and structural plastics [57]. At present, only vanillin and related substituted phenols are derived from lignin [22]. A potential application for lignin is as a raw material for the production of low to medium strength carbon fibers.

1.4 Pulping Processes

In pulping processes for paper manufacture, the objective is to delignify the wood and liberate the cellulose fibers from the wood cell structure. The cellulose remains behind in the pulp which is then made into paper. Lignin and other organic extractables, such as hemicelluloses and sugars, reduce the mechanical properties and optical quality of paper and are thus not desirable. Pulping of wood can be accomplished by chemical means, mechanical means, or a combination of the two.

1.4.1 Kraft Process

The dominant pulping process in use today is the kraft process which accounts for 74% of all chemical pulp production, and 58% of total pulp production [22]. In the kraft process, wood is reacted in an aqueous solution of sodium hydroxide and sodium sulfide at temperatures of 160 to 180 °C for 45 to 120 minutes in either batch or continuous digesters. The sulfide acts to promote and accelerate the dissolution of lignin while minimizing condensation reactions [1, 22].

Following digestion (pulping), the spent liquor, known as black liquor, which consists of lignin and other dissolved organics in an aqueous sodium salt solution, is

concentrated in multiple effect evaporators to increase the solids content, and then incinerated in a Tomlinson-type recovery furnace. This chemical recovery stage is an integral part of the kraft process, because it provides for recovery of the process cooking chemicals and utilization of the high heating value of the dissolved organics (especially lignin) for steam production [1, 89].

The advantages of the kraft process attest to its widespread use: it works for virtually all softwood and hardwood species, has superior delignification selectivity, results in a strong pulp, and includes a well established and relatively simple chemical recovery and regeneration system [1, 22]. Some of the main drawbacks of this process are the relatively low yields (usually 45-50%), the dark color of the unbleached pulps, the pollution problems and associated abatement costs (especially the foul odor vented to the surroundings), and the enormous capital costs for installation of a new mill [1, 22, 89]. These economic factors have been the driving force for the development of new or modified pulping processes.

1.4.2 Organosolv Process

Organosolv pulping processes encompass the use of a wide range of organic solvents, such as alcohols, glycol, phenol, organic acids, and amines, as pulping chemicals [47]. They have been actively investigated for at least the last fifty years, but none have been fully commercialized because of economic considerations. Recently, Repap Technologies, Inc., started up a 30 ton/day commercial scale pilot

plant to evaluate its ALCELL™ process [103]. It is described here primarily because it has the potential to become a major new pulping process.

In the ALCELL™ process, wood is reacted with aqueous ethanol solution containing an undisclosed catalyst. Pulping and washing take place in an extractor with three successively cleaner cooking liquors under temperature and pressure conditions of 200°C and 34 bar, respectively [103]. The spent pulping liquor is recovered and recycled for subsequent extraction, and the byproducts--lignin, wood sugars, and volatile components--are separated and concentrated for particular end uses.

The chief advantage of this process over the kraft process is that it is sulfur free, resulting in a significant reduction in environmental pollution. Capital costs for a fully commercialized system would be low compared to a kraft mill because it does not require a recovery boiler, brownstock washer, or a lime cycle. Operating costs would be comparable, however, and bleached pulps have strength properties comparable to those of kraft pulps. The primary disadvantage is that the process appears to work well only for hardwoods [59, 103].

1.5 Carbon Fibers

1.5.1 Properties and Applications

Carbon and graphite fibers have been developed over the past thirty years primarily as low density, high modulus (high Young's modulus) reinforcing elements for plastic composite materials [48]. Although originally developed for aerospace

Table 1-2. Physical Properties and Applications of Carbon Fibers.

	Physical property	Applications
1.	Physical strength, specific toughness, light weight	Aerospace: wings, control surfaces; automotive: springs, tire cords; sporting goods: skis, tennis rackets
2.	High dimensional stability, low coefficient of thermal expansion, and low abrasion	Missiles, aircraft brakes, aerospace antenna and support structures, large telescopes, optical benches, waveguides for stable high-frequency (GHz) precision measurement frames
3.	Good vibration damping, strength, and toughness	Audio equipment, loudspeakers, voice coils, pickup arms, musical instruments, robot arms
4.	Electrical conductivity	Automobile hoods, novel tooling, casings and bases for electronic equipment, EMI and RF shielding, brushes, conductive papers and plastics, electrodes, heating elements, superconducting cables
5.	Biological inertness	Blood filters, prosthetic devices, surgery and x-ray equipment, implants, tendon/ligament repair
6.	Fatigue resistance, self-lubrication, high damping	Textile machinery, general engineering, high stress bearings, flywheels
7.	Chemical inertness, high corrosion resistance	Chemical industry; nuclear field; valves, seals, gaskets, and pump components in process plants
8.	Electromagnetic properties	Large generator retaining rings, radiological equipment

Sources: Donnet and Bansal [19], Dresselhaus et al. [20], and Sittig [88].

applications, where high strength and light weight are of paramount importance, they have since been widely applied in less demanding areas, as shown in Table 1-2.

The diversity of applications for carbon fibers is a direct reflection of some of their very unique properties. The theoretical Young's modulus of graphite is estimated to be about 1,000 GPa and a representative selection of commercially available carbon fibers exhibit a range of moduli from 200 to 800 GPa, tensile strengths from 1.8 to 7.1 GPa, and strain to failure from 0.2 to 2.4% [48]. Generally, high modulus fibers have low tensile strengths and low strain to failure, and vice versa.

The high modulus of all carbon fibers is due to good orientation of the turbostratic graphite layer planes which constitute the material and also give rise to good thermal and electrical conductivity. The stability of carbon fiber reinforced structures is enhanced by a very low coefficient of thermal expansion, excellent damping characteristics, chemical inertness, and biocompatibility.

1.5.2 Precursor Materials and Commercial Fibers

Carbon fibers have been produced from a wide variety of organic precursor materials ranging from natural ones, such as wool and lignin, to synthetic polymers, such as poly methylmethacrylate (PMMA), and high performance fibers, such as Kevlar [48, 88]. Cellulosics, especially rayon, were the first material from which carbon fibers were made in the U.S. in the 1960's. Ex-rayon fibers were not competitive, however, because of very low yield and poor mechanical properties of the carbonized rayon. Today, only two precursor materials are of any commercial significance: polyacrylonitrile (PAN), a second generation material first used to make

carbon fibers in the United Kingdom in the 1960's, and mesophase petroleum pitch introduced in the 1970's [48, 88].

The commercially available carbon and graphite fibers range in price from about $20 per kg for low modulus ex-PAN fibers to over $2,000 per kg for ultra-high modulus ex-pitch fibers [20]. Most of the current applications for carbon fibers utilize high strength, low modulus ex-PAN fibers costing $20-60 per kg. Despite rapid growth in consumption in recent years, the price has not dropped significantly. This is due to the fact that the PAN precursor fiber is relatively expensive, and the yield is less than 50% [20].

Ex-pitch precursor fibers were expected to be ultimately much cheaper than those made from PAN because of lower raw material costs and higher yields. This has not happened, however, because of difficulties in preparing and spinning pitch which lead to significantly higher costs. For both ex-PAN, and ex-pitch fibers, the price increases rapidly with increasing modulus. This is partly due to the cost of heat treatment of any material near 3,000°C, and partly due to the small market for high modulus fibers. From an economic standpoint, applications requiring very high modulus fibers necessitate even more performance advantages than those which use low modulus fibers [20].

1.5.3 Processing Steps

The processing of carbon fibers has several steps which are common to all fibers made from polymeric precursors [18, 20]: (1) spinning--extrusion of polymer

melt or solution into fine fibers, (2) stabilization--conversion of fibers into a chemical form which will prevent melting or fusion of the fiber so that it can withstand higher temperature heat treatments, (3) carbonization at temperatures of approximately 1,000°C to eliminate noncarbon elements and form a material made up primarily of hexagonal networks of carbon, and (4) graphitization--further heat treatment to temperatures of up to 3,000°C to increase the degree of order in fibers and thereby achieve the ultimate mechanical properties, especially very high modulus, in the final carbon fibers.

Carbonization and graphitization stages are similar for almost all organics; the major difference being the degree of orientation and crystallinity which can be achieved at a given temperature. During one of the stages of the pyrolysis process, the precursor fibers are given a stretching treatment in order to achieve a preferred orientation along the fiber axis [18].

A high carbon yield is important for an economical process, and the significant factors in obtaining one are (1) the nature of the polymeric precursor, (2) the nature of the degradation process, (3) the capacity of the precursor for cyclization, ring fusion, and coalescence, and (4) the nature of the stabilizing pretreatment. Degradation of the precursor should involve cyclization of a mesophase type of mechanism, and the glass transition temperature of the precursor, or its stabilized intermediate form, is a critical parameter during the carbonization and graphitization processes [18].

1.5.4 Carbon Fibers from Lignin

As a raw material for carbon fibers, lignins present some distinct advantages over PAN and pitch. They are readily available, relatively inexpensive, and are structurally rich in aromatic rings. For most applications, low to medium strength carbon fibers are sufficient, and lignins could be suitable for this category of fibers. The utilization of lignins as carbon fiber precursors would be a high value added application.

1.6 Fiber Spinning

Fiber spinning is a unique polymer processing operation in which a fluid is continuously extruded through an orifice to form an extrudate of usually circular cross section. Further downstream of the die, the extrudate is contacted such that the filaments can be pulled and conveyed to further processing steps, such as stretching and carbonization in the case of carbon fibers [64].

The determination that a fluid is fiber forming is a necessary, but not sufficient, condition for the development of a spinning process [64]. The "spinnability" of a polymer melt or solution depends not only on its viscosity values, but also on its viscoelastic properties, its ability to undergo large degrees of stretching, and its mass transfer characteristics in the case of dry and wet spinning [94].

The three primary spinning processes are melt spinning, dry spinning, and wet spinning. In melt spinning, the molten polymer is simply extruded through a

spinneret die. In dry spinning, the polymer is extruded as a solution and the filament is formed by evaporation of the solvent. In wet spinning, the polymer solution is extruded into a nonsolvent which causes the filaments to coagulate [6]. Melt spinning is primarily a uniaxial extensional flow; the extensional viscosity is related to the spinning behavior. The spinning process involves a complex strain history, which, starting in the die, consists of shear, recoil (swell), and finally uniaxial stretching at a variable rate [15].

Rheological material properties thus play an important role in analyzing the spinning process. A thorough rheological characterization of the lignins is therefore necessary to investigate the feasibility of spinning fibers.

1.7 Need for Lignin Characterization

The characterization of lignins for molecular weight and rheological properties is very significant for investigating the feasibility of spinning fibers. In addition, such a database of lignin material properties would be very valuable to the pulp and paper industry because there is a great need for improvement in the recovery process, but the database required for the design of such improvements is generally lacking [26].

Lignin molecular weight has a significant effect on the physical properties of concentrated lignin solutions, e.g., black liquors, such as viscosity, boiling point elevation, and low temperature thermodynamic transitions, and these parameters are very important for improving the processing, concentration, and incineration of black liquor solutions [26].

Ongoing research on black liquor physical properties characterization is based on the premise that kraft black liquor can be treated as a polymer solution, particularly at high solids, with the behavior dominated by the lignin present. This allows the application of a wealth of polymer science theory and analytical techniques.

1.8 Overview of Subsequent Chapters

In chapter 2, the criteria for lignin selection, and the different purification schemes, are discussed. Chapter 3 covers the molecular weight characterization work with an emphasis on the development of a new analytical method for SEC. A study of glass transition temperatures for purified dry lignins and solvent plasticized lignins is presented in chapter 4, and a study of rheological properties, specifically viscoelastic properties of solvent plasticized lignins, is covered in chapter 5. Both the lignin thermal analysis, and the rheological characterization work, were performed to support the lignin fiber spinning and carbonization work. Chapter 6, then, covers some preliminary development work on lignin-based carbon fibers. Finally, overall conclusions and recommendations for this work are presented in chapter 7.

CHAPTER 2
LIGNIN SELECTION AND PURIFICATION

2.1 General Considerations

Several important criteria were considered in choosing the particular lignins for the various aspects of this study. These factors included the wood species, availability of the black liquor raw material or purified lignin, pulping method, and the suitability of commercial and special research lignins.

The importance of choosing lignins from a variety of both hardwood and softwood species is self-evident. Numerous species of trees are pulped for papermaking in different parts of the U.S. In the Northeast and North Central U.S., major hardwoods include birch, maple, beech, aspen, poplar, and oak; and major softwoods include pines, balsam fir, spruce, and hemlock. In the Western U.S., alder is the major hardwood, and douglas fir, ponderosa, sugar, and lodgepole pines, cedar, firs, spruce, larch, and hemlock are the major softwoods. Finally, in the Southeastern U.S., the major hardwoods are gums, tulip poplar, sycamore, oaks, and hickory; and the major softwoods are yellow, loblolly, slash, longleaf, and shortleaf pines [84].

The kraft process is by far the dominant pulping process, and kraft lignins, from raw kraft black liquors, are therefore of significant commercial importance, and are readily available from pulp and paper companies and from a specially designed

and constructed pilot plant in the Department of Chemical Engineering at the University of Florida. Lignins from organosolv pulping could also be investigated and are readily available from Repap Technologies, Inc. and its pilot plant scale ALCELL™ organosolv pulping process.

Many researchers, however, have used special, noncommercial lignins, such as those obtained by steam explosion followed by organic solvent extraction, ball mill grinding, and other methods, for analytical studies such as this one [e.g. 10]. These lignins are not readily available, however, and are not very representative of industrial lignins. Therefore, because of the commercial nature of this project, the emphasis should be on studying kraft lignins.

2.2 Lignin Selection

In consideration of the above discussion, three distinct types of lignins were chosen for this study: softwood kraft lignins, hardwood kraft lignins, and an organosolv lignin which consisted of mixed hardwoods. Table 2-1 lists all of the lignins studied, their wood species, sources, and pulping conditions. Identification codes for each of these lignins are listed in column one and will be used in subsequent chapters. In general, detailed information regarding the pulping conditions for the industrially obtained lignins was not available.

The lignins obtained from pulping activities at the University of Florida Pulp and Paper pilot plant in our own research group form part of a controlled, statistically designed pulping experiment in which the four parameters of cooking

Table 2-1. Lignins Selected for this Study

Lignin (Code)	Form[a]	Source[b]	Species	Pulping Conditions[c]
Indulin AT (IND)	L	W	Loblolly pine	κ# = 95-100
Mixed hardwood kraft (WHK)	L	W	Mixed hardwood: oak, sweet gum	κ# = 25
Birch kraft (WBK)	BL	SDW	Somersett paper birch	κ# = 14.7, H = 1,400, EA = 13.0%, S = 30%
Maple kraft (WMK)	BL	SDW	Michigan sugar maple	κ# = 15.0, H = 1,414, EA = 13.5%, S = 30%
ABAFX011,012 (FX11)	BL	UF	Southern slash pine	κ# = 107, t = 40 min, T = 330°F, EA = 13%, S = 20%
ABAFX015,016 (FX15)	BL	UF	Southern slash pine	κ# = 61.1, t = 80 min, T = 330°F, EA = 16%, S = 20%
ABAFX025,026 (FX25)	BL	UF	Southern slash pine	κ# = 18.5, t = 80 min, T = 350°F, EA = 16%, S = 35%
ABAFX027,028 (FX27)	BL	UF	Southern slash pine	κ# = 77.5, t = 80 min, T = 330°F, EA = 13%, S = 20%
ABAFX037,038 (FX37)	BL	UF	Southern slash pine	κ# = 43.3, t = 80 min, T = 350°F, EA = 13%, S = 35%
ABAFX043,044 (FX43)	BL	UF	Southern slash pine	κ# = 51.1, t = 60 min, T = 340°F, EA = 14.5%, S = 27.5%
ABAFX055,056 (FX55)	BL	UF	Southern slash pine	κ# = 29.4, t = 60 min, T = 340°F, EA = 17.5%, S = 27.5%
Organosolv (RO)	L	R	Mixed hardwood: 50% maple, 25% aspen, 25% birch	See ALLCELL™ process description, section 1.4.2

Notes: [a] L = lignin, BL = black liquor.

[b] W = Westvaco, North Charleston, SC; SDW = S.D. Warren, Westbrooke, ME; UF = University of Florida pulp and paper pilot plant, Gainesville, FL; R = Repap Technologies, Inc., Valley Forge, PA.

[c] κ# = Kappa number: a numerical value representing the amount of residual lignin in the pulp.

H = H-factor: a numerical value that represents time and temperature as a single variable in the kraft (alkaline) cooking process [89].

EA = effective alkali: NaOH + ½Na_2S, expressed as equivalent weight of Na_2O [89].

S = sulfidity: the percentage ratio of Na_2S to NaOH + Na_2S, expressed as equivalent weight of Na_2O [89].

time, temperature, effective alkali (EA), and sulfidity (S) are investigated. The effect of varying these parameters on the physical properties of the resulting black liquors forms the basis of the industrially important black liquor physical properties characterization work [26]. The pilot plant is described in detail by Fricke [28].

2.3 Lignin Purification

2.3.1 Kraft Lignins

Most of the kraft lignins in this study had to be isolated and purified from kraft black liquors which are very complex mixtures of fibrous materials, dissolved organics (lignins, hemicelluloses, sugars, acids, resins, and other extractables), and inorganic salts. The purification scheme developed by D.J. Dong* is shown in detail in Figure 2-1 and involves a lengthy series of acid precipitation, redissolution, washing, and drying steps. The final dried lignin obtained is then approximately 98+% pure with low molecular weight organic acids and bound sulfur as its major remaining impurities. Lignins that were already obtained as dried powders were further purified by performing only the last few steps of the purification scheme.

2.3.2 Organosolv Lignins

The purity of the organosolv lignin, as received, was 97-98%, and a suggested purification scheme to remove the major impurities (low molecular weight sugars and

---

* Dong, D.J. Personal Communication (1992).

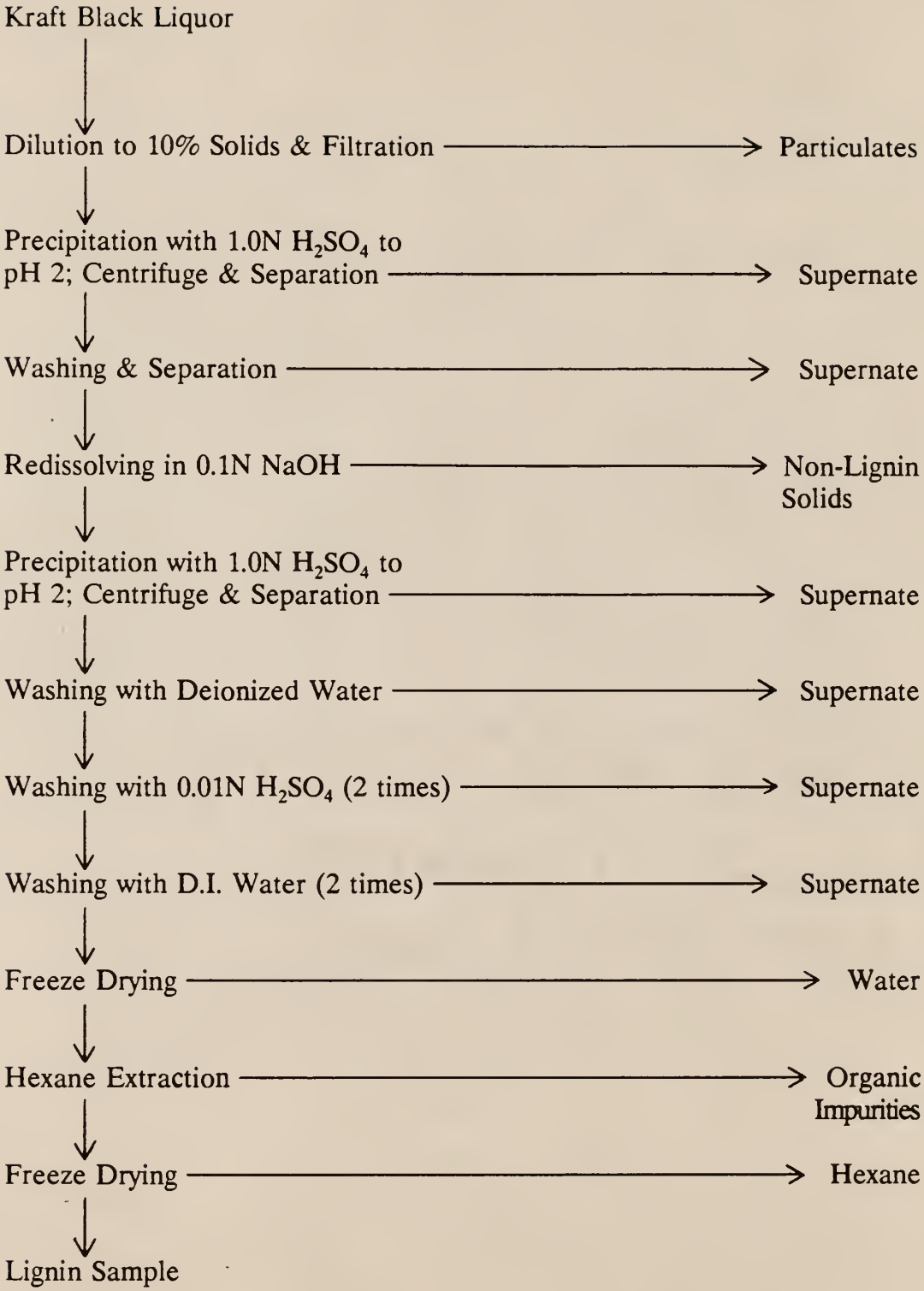

Figure 2-1. Kraft Lignin Isolation and Purification Scheme.

resin acids) consisted of a graded solvent extraction progressing from completely nonpolar to very polar: petroleum ether, ethyl ether, ethyl acetate, acetone, anhydrous methanol, and 90% methanol/10% water*. This extraction scheme was modified by the author to the following: n-hexane, 1,1,1-trichloroethane, acetone, and methanol (all from Fisher Scientific, Inc., Orlando, FL) based on their ready availability and higher boiling temperatures.

The graded solvent extraction was performed on only one organosolv lignin sample using a Soxhlet apparatus according to standard procedures [85]. A porous alumina thimble was initially charged with 26.5 g of vacuum dried lignin. Each extraction step was run for 4-5 hours, and the lignin remaining in the thimble was then vacuum dried to remove residual solvent prior to moving on to the next solvent.

Qualitative observations, such as color changes in the extracting solvents, indicate that a multitude of organic compounds were extracted from the lignin. Initially, all of the solvents were clear. In the first extraction, n-hexane turned yellow, and an orange-yellow solid precipitated when the solution cooled. The TCE in the second extraction turned a deep reddish brown, and large flocs of precipitate formed after several days. The acetone in the third extraction became cloudy and turned dark brown, and in the fourth extraction, the methanol turned dark reddish brown. The masses of lignin remaining after each step were not consistent, but did indicate that very little was extracted in the n-hexane step, and substantial amounts were extracted in each of the remaining three steps. Although samples of extracting

*Cronlund, M., Repap Tech., Inc. Personal Communication (3 April 1991).

solvent from each step were retained for future chemical analysis, this has not yet been done. An overall yield for this extraction was only on the order of 10%.

2.3.3 Storage

The purified lignins were stored in the dark in capped glass sample vials sealed with Parafilm®, and over a two year period, no color changes in the lignin samples were noticed. The raw black liquors were kept refrigerated at close to 0°C to minimize degradation reactions.

CHAPTER 3
MOLECULAR WEIGHT CHARACTERIZATION

3.1 Introduction

Lignin has been extensively studied and characterized [e.g. 34]. However, molecular weights determined by a large number of investigators exhibit an extremely wide range of values. This can be attributed to the multiplicity of extraction techniques, the wide variety of wood species, different purification procedures, and different analytical techniques that have been employed.

Analytical techniques for measuring molecular weights of polymers fall into two general classes: "absolute" methods such as vapor pressure osmometry (VPO) and low angle laser light scattering (LALLS), and "secondary" methods such as size exclusion chromatography (SEC), also known as gel permeation chromatography (GPC). Absolute methods allow the determination of true values for the number average molecular weight ($\overline{M}_n$), and the weight average molecular weight ($\overline{M}_w$), from VPO and LALLS, respectively. Size exclusion chromatography is much more versatile and allows the determination of all the molecular weight averages, as well as the molecular weight distribution (MWD). However, these values have only relative meaning because they are dependent on the calibration scheme employed.

Although SEC can only provide relative molecular weight values, it is a very rapid and convenient technique as compared to VPO and LALLS which are very laborious and time consuming methods. Both VPO and LALLS require very careful experimental technique and numerous corrections for nonideal behavior. For example, Kim [52] demonstrated that measurements of lignin $\overline{M}_w$ by LALLS must be made at or above the Theta temperature for the lignin-solvent pair and that nonideal optical phenomena significantly affect the results. One experimental determination of $\overline{M}_w$ by LALLS requires six separate measurements: the effect of polymer concentration on solution refractive index, the effect of polymer concentration on light absorption at the particular wavelength used, light scattering of the solvent, excess light scattering of the solution, light polarization, and scattered light flourescence. From these data, corrections for optical effects can be made and $\overline{M}_w$ determined.

In this study, SEC was primarily used to determine the average molecular weights and the MWD of lignins, and a novel calibration procedure was investigated to overcome the limitations mentioned above.

3.2 SEC Theory

3.2.1 Separation Mechanism

In SEC, separation is accomplished by injecting the polymer solution into a continuously flowing solvent stream which passes through one or more columns packed with highly porous, sub 10 μm rigid gel particles and then detecting the

fractionated sample as it elutes from the column. The polymer molecules are separated in the column packing according to their molecular size or hydrodynamic volume in solution. The degree of retention of the polymer molecules in the pores is the phenomenon which affects the separation. Smaller molecules are retained to a greater degree than larger ones, and, as a result, the largest size molecules elute from the column first followed by successively smaller molecules [55, 105].

This fractionation process is entropy driven and based on the concentration gradient of solute that exists between the stationary mobile phase within the pores of the gel particles and the interstitial flowing mobile phase. Solute permeation into the pores is associated with a decrease in entropy because solute mobility becomes more limited inside the pores of the column packing. The SEC separation is controlled by the differential extent of permeation, not the differential rate of permeation. Solute diffusion in and out of the pores is rapid enough with respect to the flow rate to maintain an equilibrium solute distribution. SEC is an equilibrium entropy controlled size exclusion process [105].

The volume of solvent at which a solute elutes from the column or the volume of liquid corresponding to the retention of a solute on a column is known as the retention volume. This can be related to the physical parameters of the column as follows:

$$V_R = V_o + KV_i \tag{3-1}$$

where V_R is the retention volume of the solute, V_o is the interstitial volume (dead volume) of the column, V_i is the pore volume, and K is the distribution coefficient

based on the relative concentrations between the two phases. The total column volume V_T is given by

$$V_T = V_o + V_i \tag{3-2}$$

Therefore, the retention volume is expressible in terms of the two measurable quantities V_o and V_T as

$$V_R = V_o(1-K) + KV_T \qquad for\ 0<K<1 \tag{3-3}$$

The void volume corresponds to the total exclusion of solute molecules from the pores. Between V_o and V_T, solute molecules are selectively separated based on their molecular size in solution. If molecules elute beyond V_T, corresponding to K > 1, separation is no longer achieved by a size exclusion mechanism, but rather, solute is retained on the column support by an affinity mechanism such as adsorption.

3.2.2 Detection

The fractionated sample is usually detected by means of a mass concentration detector such as a differential refractive index (DRI) detector, or an ultraviolet/visible (UV/Vis) absorption spectrophotometer. Both of these detectors continuously monitor the mass of sample eluting from the column set by measuring the difference in refractive index, or light absorption, respectively, between the fractionated sample solution and pure solvent (or air for UV/Vis). This differential property is then directly proportional to the mass of sample present.

UV/Vis detectors generally operate in the wavelength range of 190-600 nm and are significantly more sensitive than DRI detectors. However, UV/Vis detection

requires the sample to have an ultraviolet or visibly active chromophore which is not active at the same wavelength as the solvent.

3.2.3 Calibration

Calibration in SEC involves converting a chromatogram into a molecular weight distribution curve. Narrow standard calibration has traditionally been the method of choice, but universal calibration and broad standard calibration have also been used, especially with the development of sophisticated computer software for data analysis. Finally, resolution of moments, which is a numerically demanding method, also appears very promising.

In narrow standard calibration, narrow MWD polymer standards, with polydispersities less than 1.1, are used to generate volume retention curves. A one-to-one correspondence of peak retention volume with peak molecular weight (M_p) of the standard is made, and a plot of log M_p versus retention volume generates a primary molecular weight calibration curve which is usually cubic in form:

$$\log M_p = a + bV + cV^2 + dV^3 \qquad (3\text{-}4)$$

where a, b, c, and d are constants that usually differ by at least an order of magnitude.

The chromatogram for the unknown sample is then divided up into discrete volume (or time) intervals and molecular weight values, M_i, are assigned to each sample slice as a function of the elution volume (or time) in accordance with (3-4). The various molecular weight averages are then calculated by the usual formulas

[105]. A serious limitation of this method is the lack of well characterized narrow MWD standards for many polymers such as lignin. Thus, only an apparent MWD curve for the sample polymer is possible.

Universal calibration is an empirical method utilizing the concept of hydrodynamic volume which can be expressed in terms of the product of the intrinsic viscosity, $[\eta]$, and the molecular weight, M, of the polymer sample. When plotted as log $[\eta]$M versus elution volume, SEC calibration curves for different types of polymers merge into a single plot. This behavior is theoretically sound. When separation occurs strictly by size exclusion involving only entropy changes, polymers of different chemical structures, but the same hydrodynamic volume, will elute at the same retention volume from any given SEC column set. However, significant deviations between experiment and theory, due to possible reversible adsorption, crosslinking, and extensive branching, for example, can exist [41, 43, 105].

The relationship between molecular weight and intrinsic viscosity is given by the empirical Mark-Houwink equation:

$$[\eta] = KM^a \tag{3-5}$$

where K, and a are the Mark-Houwink constants. These constants vary with polymer type, temperature, and solvent, and accurate values are difficult to obtain experimentally. For polymers with a three dimensional network structure, such as lignin is believed to have, universal calibration is not valid [41, 105].

Broad standard calibration can be an integral MWD method, which utilizes the complete MWD curve of the polymer standard, or linear calibration methods

which use only the average molecular weight values of the polymer standard but assume a linear approximation of the calibration curve [105]. Although both approaches are valid, the linear calibration methods are more versatile and pose no restrictions on the MWD shape of the standards.

In the linear method, an iterative procedure is used to determine values for the coefficients a and b in (3-4) (c and d are zero) such that computed molecular weight values are in agreement with the known values for the polymer standard. The resolution of moments method is a generalization of the integral broad standard calibration technique except that no set form for the distribution is assumed [26, 66]. The objective is to generate a third order calibration equation such as (3-4) by determining values of the constants a, b, c, and d such that $\bar{M}_n$ and $\bar{M}_w$ computed from the chromatogram match two known values of $\bar{M}_n$ and $\bar{M}_w$, from absolute measurements, specified for the sample polymer. This technique requires calculation of the moments of the distribution and involves a complex and iterative numerical optimization procedure. The calibration equation obtained by this method will be valid for a specific type of polymer and set of operating conditions.

3.2.4 Nonsize Exclusion Effects

The separation mechanism described above applies only to ideal size exclusion behavior. Since solute-solvent-matrix interactions govern SEC elution behavior, nonsize exclusion effects must frequently be taken into account or eliminated in order to achieve ideal SEC behavior [4].

There are a multitude of possible nonsize exclusion effects which can lead to nonideal SEC behavior. These include solute/packing enthalpic interactions, intermolecular solute association, intramolecular electrostatic effects, concentration effects, polymer shear degradation, ultrafiltration, hydrodynamic effects, polymer chain orientation and deformation, and peak dispersion [4]. Further nonideal effects can arise from the use of mixed mobile phases such as preferential solvation of the polymer [4].

Enthalpic interactions that can occur between polymer and packing can result in polymer adsorption to the gel matrix. These interactions include ion exchange, ion inclusion, ion exclusion, hydrophobic interactions, hydrogen bonding, dispersion (London) forces, dipole interactions, and electron-donor-acceptor interactions [4].

The mobile phase is usually chosen to eliminate these effects so that it is a good solvent for the polymer and whose solubility parameter, δ, is close to that of the gel. This results in both polymer and packing being well solvated and potential adsorptive sites on both being deactivated. If $\delta_{gel} > \delta_{solvent}$, normal phase adsorption will occur, and if $\delta_{gel} < \delta_{solvent}$, the packing will act as a reversed phase packing. If $\delta_{gel} = \delta_{solvent}$, size exclusion will be the dominant separation mechanism [4].

3.3 Background and Literature Review

3.3.1 Introduction

Since it was first developed in the 1960's, SEC has been applied to the characterization of lignins. Consequently, an extensive body of work exists which

encompasses a wide range of mobile phases, column chemistries, and lignins. Likewise, a very broad range of lignin molecular weights has been reported: from less than 1,000 for some kraft lignins, to over 100,000 for some lignin sulphonates [24, 25]. The diversity of this research effort is a direct reflection of the inherent molecular complexity of lignin and the difficulty in counteracting unfavorable lignin-column-solvent interactions in order to achieve true size exclusion behavior.

The main advantage of SEC is its ease of use and rapid sample analysis, and the main limitation is that it provides only relative molecular weight data. Various calibration techniques have therefore been employed in an attempt to overcome this limitation and achieve absolute molecular weight characterization for lignins. A discussion of these calibration procedures is therefore a very significant and integral part of the overall picture of lignin SEC characterization work.

It is difficult to make direct one-to-one comparisons among the many studies in the literature because of the unique character of each lignin-column-solvent set. The interactions among each of the three components govern lignin's elution behavior and therefore the particular mobile phases, column packing materials, and lignins and their method of preparation, that each group of investigators have employed, are very significant. Because of the extensive nature of this topic, a thorough review of the available literature is not practical. Therefore, only significant highlights are discussed below.

3.3.2 Traditional SEC Analyses

Traditional SEC analyses of kraft lignins, organosolv lignins, and lignosulphonates have been carried out on a variety of gel packing materials including polysaccharide, or more specifically, polydextran based gels, on acrylate polymer based gels, on silica based columns, and on polystyrene divinylbenzene (PS-DVB) copolymer gel columns.

The polydextran columns (Sepharose, or Sephadex type by Pharmacia) have been used with aqueous mobile phases [25, 97], and polar organic mobile phases such as DMF [11, 12, 13, 54, 70]. The acrylate gels (PW series by Toyo Soda Manufacturing Co.) are semi-rigid high performance gels and have been used with aqueous mobile phases [73]. The silica based packing (Waters Associates Bondagel column) has been used with polar organic mobile phases [98], and the PS-DVB copolymer gel columns (Waters μ-Styragel, Ultrastyragel for example) have been used with polar organic mobile phases, principally THF [10, 40, 51, 74].

For high pressure (high performance) SEC, PS-DVB gels, with THF as mobile phase and polystyrene narrow MWD standards for calibration, have become the most widely used SEC system. This is probably due to the good compatibility between THF and the PS-DVB gel (in terms of solubility parameters) [4]. Sample detection is usually by means of differential refractive index or ultraviolet absorption at 280 nm.

3.3.3 Association and Adsorption

Lignin association in the mobile phase and reversible adsorption to the gel packing have been widespread and troublesome nonsize exclusion effects. Both of these two phenomena involve complex and often little understood interactions among the lignins, mobile phases, and column gels. The nonideal SEC behavior accompanying these effects results in erroneously high apparent MW's for association, and erroneously low MW's for adsorption.

Previous investigators have almost universally used chemically modified lignin samples to minimize both adsorption and association effects, and added salts to polar organic mobile phases, such as DMF, to minimize association effects. These derivatized lignins have been methylated, acetylated, silylated, or hydroxypropylated at the free phenolic hydroxyl positions where hydrogen bonding interactions are believed to occur. The main concern with this procedure is that quantitative derivitization is difficult, and derivitized lignins have altered conformations and different elution profiles than nonderivitized ones.

Association can occur in both aqueous solutions at pH < 12-13, and in organic mobile phases at temperatures below the Theta or Flory temperature for the respective lignin-solvent pair [52]. Many investigators recognized this phenomenon [10, 13, 74]. In higher fractional polarity solvents such as DMF, lignin-lignin associative interactions are high, resulting in bimodal or multimodal elution profiles. These associative effects produce peaks of very high apparent molecular weight with some elution beyond the exclusion limit of the column set [10].

Many investigators have been limited to ambient temperature conditions for lignin SEC experiments with DMF and have therefore been unable to overcome the association effects solely by operating above the Theta temperature for this system (about 80°C for kraft softwood lignins in DMF [52]). They have therefore resorted to adding lithium salts (0.1M LiBr or LiCl) to DMF mobile phases which effectively broke up lignin association complexes and changed the multimodal elution profiles to a single broad peak profile.

Connors et al. [13] using Sephadex columns at ambient temperature, showed that molecular association was disrupted for LiCl concentrations in DMF of between 0.0001M and 0.001M. The added salt was theorized to prevent association by shielding dipoles in the individual molecules. Further studies showed that when the fractions from the bimodal molecular weight distribution of lignins were collected and rechromatographed, the materials from the higher and lower end of the distribution were chemically different though not vastly different in molecular weights. Since acetylated lignins displayed similar elution patterns, molecular association was not due to hydrogen bonding [13].

Pellinen and Salkinoja-Salonen [74] ran derivatized and underivatized lignin samples and model compounds in THF on PS-DVB based columns. They believed that polymeric lignins would not associate because they observed that underivatized model compounds neither absorbed on to the gel nor underwent intermolecular association. Free hydroxyl groups in the lignins and the model compounds were derivatized to eliminate hydrogen bonding between the target molecules.

Adsorption of lignins to the column gel has been a common observation for PS-DVB based columns with DMF mobile phases. Because of its structure with many free phenolic hydroxyl groups, lignin is attracted to the aromatic rings of the gel through the unshared electron pairs on the oxygen atoms. Adsorption can be hydrophilic or hydrophobic and leads to an underestimation of the MW's. In aqueous mobile phases, ionic interactions are due to the polyelectrolytic nature of lignins [74].

3.3.4 Column Calibration

Column calibration has been a persistent problem which has limited the applicability of SEC for obtaining accurate and realistic MW values for lignins. The primary calibration methods that have been employed are the use of narrow MWD polymer standards, principally polystyrene, the use of lignin model compounds, and the use of narrow fractions of lignin samples whose molecular weights have been determined by ultracentrifugation. Absolute MWD determination by multidetection and universal calibration methods will be discussed in Section 3.3.5.

Column calibration with narrow MWD polymer standards, such as polystyrene, poly methyl methacrylate (PMMA), polyethylene oxide (PEO) or others, is the most straightforward technique and has been widely used [e.g. 10]. Polystyrene standards in relatively nonpolar mobile phases, such as THF, are ideally suited for PS-DVB gels. However, in polar mobile phases such as DMF, polystyrenes reversibly adsorb to the PS-DVB gel matrix resulting in increased retention times [10, 31, 51]. More

polar polymer standards such as PEO and PMMA adsorb to a lesser extent and are more suitable for DMF. In aqueous mobile phases, polystyrene sulfonates have been used [73, 97].

Regardless of the standard used, there is a common limitation to this technique: the structure and conformation of the standard is very different from that of the sample lignins; all of the commercially available narrow MWD standards are linear polymers, whereas lignin is highly branched and spherical. This results in lignin molecular weights as determined by narrow standard calibration that are as much as an order of magnitude too low as compared to values determined by absolute methods.

In addition to polystyrene standards, many investigators have used monodisperse lignin model compounds to calibrate their column sets [11, 12, 40, 51, 54, 73, 74]. Connors [11], and Connors et al. [12] used 15 different lignin model compounds to calibrate Sephadex columns in DMF. These model compounds spanned the molecular weight range of 168 to 1,076 and consisted of various substituted and derivitized phenyl propane oligomers which represent some of the functional groups of lignin. They found a good correlation between molecular weight and elution volume or partition coefficient.

Kristersson et al. [54] investigated the elution properties of lignin model compounds (guaiacylglycerol, pinoresinol, dihydrodehydrodiisoeugenol), carbohydrates, and low molecular weight lignin carbohydrate compounds which spanned the molecular weight range of 180 to 990. These were run in dioxane-water

(1:1), and DMF on Sephadex columns. They found that all of the compounds eluted essentially according to molecular size in DMF, but not in dioxane-water.

Using both lignin model compounds and polystyrene standards, Himmel et al. [40] calibrated their column set in terms of hydrodynamic radius by determining the effective hydrodynamic radius as a function of molecular weight. They analyzed steam exploded aspen lignins in a dioxane/chloroform mixed mobile phase on PS-DVB based columns, and concluded that the relationship of molecular weight to hydrodynamic radius, specific for each polymer-solvent system, must still be determined by a direct method.

Pellinen and Salkinoja-Salonen used low molecular weight lignin model compounds such as vanillin and vanillic acid [73], and various substituted methoxy phenols in the molecular weight range of 154 to 638 that were representative of different structures and functional groups typical for lignin [74]. These model compounds were run underivitized and as acetylated and silylated versions.

Calibration with the model compounds gave somewhat higher values of $\bar{M}_n$ and lower values of $\bar{M}_w$ than PS calibration, but both calibrations gave similar low values of $\bar{M}_n$ for the underivitized samples. The elution volume depended on MW as well as on the derivitization of the lignin model compounds, and the polydispersity was smaller when the model compound calibration was used. The chief limitation is the lack of high MW lignin model compounds for calibration [74].

Johnson et al. [51] compared the elution behavior of lignin model compounds and model polymers in THF and DMF on PS-DVB based gel columns. The lignin

samples were organosolv aspen lignins that had been quantitatively acetylated. In high fractional polarity solvents made with DMF, the derivitized lignin model compounds and lignin model polymers adsorbed less than the PS standards.

Linear lignin model polymers, and derivitized and underivitized lignins, exhibited similar associative behavior in polar solvents (e.g. DMF) which decreased with the addition of 0.1M LiBr. None of the low MW lignin model compounds, derivitized or not, clearly exhibited associative behavior in polar solvents. Chromatograms of mixtures of well defined low MW lignin model compounds, ether bonded lignin model polymers and acetylated lignins in polar solvents appeared to be merely additive [51].

A calibration technique that circumvents the vexing problem of structural and conformational inhomogeneity between the sample lignins and the polymer standards is the use of narrow fractions of sample lignins whose molecular weights have been determined by some absolute method such as LALLS or ultracentrifugation. In this way, the elution behavior of both the standards and the samples should be identical, and this method should theoretically provide absolute MW values.

Obiaga and Wayman [70], Forss et al. [25], and Wagner et al. [97], among others, have used this method. Obiaga and Wayman [70] analyzed a spruce lignosulfonate in dimethyl sulfoxide (DMSO) on a Sephadex column which they calibrated with only three lignin fractions whose molecular weights had been measured by ultracentrifugation. This calibration curve was shifted and rotated to correct for skewing and axial dispersion. For the sample, $\overline{M}_w$ as determined by SEC

and sedimentation equilibrium differed by only 4%. Forss et al. [25] calibrated Sephadex columns with both kraft lignin fractions and lignosulfonate fractions, which had been characterized by light scattering, for analysis in aqueous mobile phases.

The serious disadvantage of this method is the inordinate amount of time required to determine the molecular weights of the lignin fractions for calibration. Both LALLS and ultracentrifugation are laborious and tedious procedures.

3.3.5 Multidetection and Absolute MWD

Several groups of investigators have utilized a dual detection system for SEC that incorporates both a DRI detector and a LALLS detector [29, 53, 87], or a DRI detector and a differential viscosity (DV) detector for universal calibration [42, 43, 86, 87]. Both approaches are sophisticated attempts to obtain absolute MW values while bypassing the use of unsuitable calibration standards.

The on-line SEC-LALLS system makes it possible to overcome the calibration problem and continuously calculate the molecular weight of the molecules eluting from the column set. However, complex problems are associated with this method that make its application to lignin analysis difficult. All three groups of investigators encountered experimental difficulties with LALLS detection, particularly optical effects such as sample flourescence, absorption, and polarization, which must be corrected for.

Kolpak et al. [53] analyzed several softwood lignins from spent kraft pulping liquors in THF on PS-DVB gel columns. They compared their online results with

static (stand alone) LALLS measurements and found that static LALLS measurements for one of the lignins were much higher than SEC/LALLS MW values: $\bar{M}_w$ = 17,300 for static LALLS versus $\bar{M}_w$ = 10,650 for SEC/LALLS. They attributed this large discrepancy to sample aggregation in THF.

Froment and Pla [29] studied acetylated derivatives of dioxane extracted spruce lignin, alkali black cottonwood lignin, and organosolv black cottonwood lignin in THF on PS-DVB gel columns. In order to correct for the optical effects mentioned above, at least three recorder traces were made for each sample: vertical and horizontal components of the scattered light (polarization correction), transmitted light (absorption correction), and the concentration profile (DRI scan); and a flourescence filter was used. Froment and Pla [29] recognized that this method was very promising, but also full of difficulties.

In the third highlighted study, Siochi et al. [87] analyzed four hydroxypropyl derivatives of organosolv red oak, and aspen hardwood lignins, and a Westvaco mixed kraft hardwood lignin. Their system consisted of a Waters 150C HPSEC with a DRI detector in series with a Chromatix KMX-6 LALLS detector and in parallel with a Viscotek Model 100 DV detector. Their mobile phase/column system was the same as in the other two studies: THF at 30°C and PS-DVB gel columns. Siochi et al. [87] also concluded that in order to use LALLS detection, corrections for sample absorbance, flourescence, and beam polarization must be made; optical effects gave them erroneously high calculated $\bar{M}_n$ s from SEC/LALLS, as compared to values measured directly by VPO.

Absolute molecular weight determination by universal calibration is a well established technique, and with the recent development of differential viscosity detectors for SEC, the molecular weight and intrinsic viscosity measurements can now be made online in real time.

Himmel et al. [43] studied four different acetylated aspen hardwood lignins that had been obtained by ball milling and solvent extraction, steam explosion followed by alkaline extraction, organosolv pulping followed by water extraction of the associated sugars, and dilute sulfuric acid hydrolysis followed by sodium hydroxide extraction. These samples were run in THF at ambient temperature on PS-DVB gels. Narrow MWD standards such as polystyrenes, polybutadienes, PMMA's, and low molecular weight lignin model compounds (synthetic phenyl tetramers) were found to fit universal calibration.

They concluded that differential viscosity was a valuable detection method, but that the MW values for these lignins needed to be compared to absolute values obtained from LALLS and VPO. A limitation of these SEC-based "absolute" MW measurements is the narrow concentration window available for analysis. Also, due to the lack of available appropriate MW, composition, and branched polymer standards, the limits of fit for universal calibration to complex biopolymers such as lignin could not be judged [43].

Siochi et al. [86, 87] investigated the feasibility of using SEC/DV for absolute molecular weight determination of hydroxypropylated derivatives of red oak, aspen, and hardwood kraft lignins. These were run in THF at 30°C on Waters

Ultrastyragel columns in a Waters 150C HPSEC with both DRI and DV detectors. Narrow MWD polystyrene calibration standards were used, and "absolute" reference $\overline{M}_n$ values were obtained from VPO to check the validity of the universal calibration method.

All the lignins had $\overline{M}_n$ values in the range of 1,100 to 2,000, and values obtained from SEC/DV compared favorably to those obtained from VPO. These lignins also demonstrated time dependent association in THF at 30°C: $\overline{M}_n$ increased by 20% in two days. Changes in the absolute molecular weight distributions in all the experiments confirmed that time dependent association occurs in lignin derivatives in THF. They concluded that SEC/DV is a reliable and convenient technique for obtaining average molecular weights and the absolute MWD for lignins [86, 87].

Himmel et al. [42] used three hydrodynamic methods to determine unknown lignin MW's: SEC, universal calibration, and sedimentation equilibrium. They analyzed acetylated aspen hardwood lignins in THF on a set of μ-Spherogel columns (PS-DVB based) with pore sizes of 10^4, 10^3, and 500 Å.

Conventional SEC with polystyrene calibration produced the lowest MW estimates for the four lignins, whereas both universal calibration and sedimentation equilibrium produced similar MW estimates that were 1.5-2.5 fold higher. The higher apparent MW's from universal calibration, relative to SEC, are consistent with the concept of lignin being a branched polymer, because branched polymers of higher MW may occupy the same hydrodynamic volume as linear polymers of lower

molecular weight. These low MW acetylated aspen lignins appeared to fit universal calibration [42].

3.4 Experimental Work and Data Analysis

3.4.1 Instrumentation

The experimental setup for the SEC work consists of a Waters 150C ALC/GPC integrated high pressure liquid chromatography system, and an outboard Waters 486 UV/Vis tunable absorbance detector (Waters Division of Millipore Corp., Milford, MA), interfaced with a NEC APC IV computer workstation which runs the Maxima 820 software for HPLC and GPC data acquisition and processing (Dynamic Solutions Division of Millipore Corp., Ventura, CA). The mobile phase is supplied by a Kontes integrated HPLC mobile phase handling system (Kontes, Vineland, NJ) which has a five liter capacity and is capable of solvent filtration, degassing by sparging with an inert gas, and mobile phase storage.

The 150C is a fully programmable, self contained unit which includes a high pressure pump, 16 sample carousel, automatic injector, DRI detector, and column oven. It has complete temperature control to 150°C over the full analysis sequence of sample injection, fractionation, and detection. The UV/Vis detector was installed at a later date in series with, and upstream from, the DRI detector. This unit is a single channel detector with a wavelength range of 190-600 nm. For more detailed information, the reader is referred to the respective operator's manuals [99, 100].

Three sets of analytical columns, employing different chemistries, were used to investigate a wide variety of solvents as possible lignin mobile phases. For THF, a set of three Ultrastyragel columns (Waters Division of Millipore Corp., Milford, MA): 10^4 + 10^3 + 100 Å pore sizes, were connected in series. For DMF and other polar organic mobile phases, we used a set of two Jordi Gel columns: Mixed Bed + 10^3 Å pore sizes connected in series, and for aqueous and polar organic mobile phases, we used a set of Jordi Gel 10^3 + 10^4 Å GBR columns (Jordi Associates, Inc., Bellingham, MA).

The Ultrastyragel columns contain a highly crosslinked styrene divinylbenzene copolymer gel and measure 30 cm long by 7.8 mm internal diameter (i.d.). The Jordi Gel columns contain a highly crosslinked poly-DVB gel and measure 50 cm long by 10 mm i.d., except the 10^4 Å GBR column which is 25 cm long by 10 mm i.d. Although all of these columns are temperature stable up to 150°C, the polymer gel bed in all of the Jordi Gel columns does not shrink or swell appreciably upon solvent changeover, whereas the Ultrastyragel ones may if the difference in solvent polarities is significant. This limits the application of the Ultrastyragel columns to mobile phases with similar polarities. In the GBR column, the crosslinked poly-DVB gel has been modified by adding glucose amine groups to the aromatic rings and the alkane chains. This deactivates the aromatic rings toward adsorption interactions and makes the gel compatible with both aqueous and polar organic mobile phases.

3.4.2 Mobile Phase Selection and Preparation

Selection of the proper mobile phase and column chemistry for lignin analysis has been the major emphasis in the development of an effective SEC method. Table 3-1 lists the wide variety of pure and mixed solvents, together with several column chemistries, that have been investigated in order to overcome the nonsize exclusion behavior, particularly adsorption to the column gel in polar organic mobile phases, that lignins exhibit with most common mobile phase/column systems.

Preparation of the mobile phase was a straightforward process: solvents were vacuum filtered through 0.45 or 0.50 μm pore size nylon or teflon membrane filters (Gelman Sciences, Inc., Ann Arbor, MI), then degassed by sparging with helium for 15-20 minutes while pulling a vacuum, and then stored under a helium blanket of 1-2 psig in the Kontes mobile phase reservoir. All of the solvents were either HPLC grade or Certified ACS grade and were obtained from Fisher Scientific Co. (Orlando, FL), except ethylene glycol monopropyl ether (EGMPE) and NMP, which were obtained from Eastman Kodak (Rochester, NY). Mixed solvents were prepared on a volume basis prior to filtration. For each new mobile phase, the column set was equilibrated (usually overnight) at 0.1 or 0.2 ml/min until at least three column volumes had eluted.

3.4.3 Sample and Standards Preparation

For the lengthy methods development process of mobile phase evaluation and selection, several older softwood kraft lignins [27], Indulin AT, and organosolv lignin

Table 3-1. SEC Mobile Phase Selection

No.	Mobile Phase[a]	Temp. (°C)	Column Set[b]
1	THF	30, 45	U
2	DMF	50, 80, 85	JG
3	DMF + LiBr (0.05, 0.1M)	80, 85	JG
4	DMF + 2% TEA	85, 100	JG
5	DMF / DMSO (95/5)	85	JG
6	DMF / EGMPE (90/10, 95/5, 98/2, 99/1)	85, 100	JG
7	DMF / EG (95/5, 97/3, 98/2)	85, 100	JG
8	DMF + 2% EGDME	85	JG
9	DMF / EGMME (95/5, 98/2)	85, 100	JG
10	EGMME	85	JG
11	DMF + 10% Pyridine	85	JG
12	DMF / N-butanol (90/10)	85	JG
13	Pyridine	60, 85	JG
14	DMF / TCE (50/50, 90/10)	55, 60	JG
15	DMF / Toluene (91/9) + 0.05M LiBr	85	JG
16	DMF / NMP (95/5)	85	JG
17	DMF + 1.1% Pyrogallol	85	JG
18	KOH (0.1, 1.0M)	40, 50, 60	GBR
19	DMF / 1.0M KOH (50/50)	40, 80	GBR
20	NaOH (0.1, 0.2, 0.3, 0.5M)	40, 50	GBR
21	DMSO	85	GBR
22	DMSO + LiBr (0.01, 0.05, 0.1, 0.15, 0.2M)	85	GBR

Note: [a]Solvent abbreviations defined in Key to Abbreviations.
[b]U = Ultrastyragel, JG = Jordi Gel, and GBR = Jordi Gel GBR.

were used as test samples. For promising mobile phases, e.g. 0.2M NaOH, and DMSO + 0.1M LiBr, all of the lignins listed in Table 2-1 were prepared and analyzed. Because of the wide variety of mobile phases and column chemistries that have been investigated, several different narrow MWD polymer standards were required for effective SEC calibration. For THF, polystyrene standards were used, and for DMF based mobile phases, polyethylene oxide, polyethylene glycol and poly methyl methacrylate standards were used. For aqueous mobile phases and DMSO + LiBr, polysaccharide standards (linear polymaltotrioses) were used. All of the standards were obtained from Pressure Chemical Co. (Pittsburgh, PA).

Lignins were vacuum dried for several hours prior to preparing the sample solutions, and both samples and standards were weighed out on a Sartorius electronic balance with 0.1 mg resolution (Göttingen, Germany). Solutions of lignins and standards were prepared in the respective mobile phase in 25 ml volumetric flasks at approximate concentrations of 1-2 g/L (0.1-0.2% w/v), and 1 g/L (0.1% w/v), respectively. Lignins normally dissolved within one hour, while standards were allowed to thoroughly dissolve overnight. Usually, two or three standards, differing by at least a factor of five in nominal molecular weight, were combined in one flask.

Samples and standards were filtered through 0.45 μm pore size nylon or teflon Acrodisc syringe filters (Gelman Sciences, Inc., Ann Arbor, MI) into 4 ml sample vials for loading into the sample carousel for automatic injection in the 150C. As a precaution against association in some mobile phases at room temperature, lignin

samples were filtered 'hot', at close to the SEC run temperature, by preheating both the sample solutions and the glass syringes.

3.4.4 SEC Runs and Data Analysis

Final operating conditions for the 150C were established for running DMSO + 0.1M LiBr, as the preferred mobile phase, on the Jordi Gel GBR columns. Initially, only the 10^3 Å column was used, but to complete this study, the 10^4 Å column was also installed. A nominal flow rate of 1.1 ml/min (actual flow rate approximately 1.03 ml/min), analysis temperature of 85 °C, injection volumes of 50 μl and 100 μl for lignins and standards, respectively, and two injections per sample were used. Run times were 30 minutes for the 10^3 Å column, and 45 minutes for the 10^3 + 10^4 Å column set. Proper injection volumes for both samples and standards were determined by monitoring the peaks' retention time shifts with respect to decreasing injection volume until no further shift occurred, or until the signal-to-noise ratio became unacceptably low.

The UV/Vis and DRI detectors were connected in series which enabled dual detection of the lignin samples and the polymer standards. However, only the lignins displayed any UV absorbance in the transparent range of the mobile phase, and their mass distributions were therefore monitored by UV at 280 nm, while the polymer standards were monitored by DRI. The greater sensitivety of the UV/Vis detector allowed for lower lignin injection volumes, and the 0.15 min time lag between the two detectors was accounted for in the standards' retention times. Lignin molecular

weights were then calculated from the sample chromatograms by means of third order narrow standard calibration curves with correlation coefficients of 0.995 or greater. These MW calculations were cutoff on the low side at a calibration MW of 50.

3.5 Results and Discussion

3.5.1 General Comments on Mobile Phase Evaluation

The mobile phases listed in Table 3-1 represent a systematic approach to developing a suitable mobile phase/column combination. This lengthy evaluation process became the main emphasis in the development of an effective SEC analytical method for lignins because of the experimental problems that were encountered. The complex chemical interactions in lignin-column-mobile phase systems frequently resulted in nonideal SEC elution behavior for lignins.

The experimental difficulties, such as association and adsorption, that many previous investigators experienced, have also been observed in this study. General results for the preliminary evaluation (mobile phases 1-17 in Table 3-1) were often very inconsistent and not reproducible. This merely adds to the wealth of seemingly contradictory and confusing SEC analyses of lignins. Derivitization of the lignins is a common procedure to minimize some of these undesirable interactions; however, this was not done in this study. The key element was selecting the proper column chemistry (stationary phase) in combination with a compatible and effective lignin solvent system.

The discussion of the experimental difficulties encountered in the evaluation of the various mobile phases is an important aspect of this method development because it addresses the major problems inherent in the SEC analysis of lignins. Three mobile phase/column groupings were considered: THF, DMF and DMF mixed mobile phases, and aqueous mobile phases (principally NaOH); run on Ultrastyragel, Jordi Gel, and Jordi Gel GBR columns, respectively. Results for lignins run in DMSO + LiBr on the Jordi Gel GBR columns are discussed separately.

3.5.2 Lignin Analysis in THF

THF was a logical mobile phase to start with because it has been frequently used in the past by many other investigators. In addition, our set of Ultrastyragel columns, which were purchased with the 150C, came packed in THF. This system of THF with PS-DVB column chemistry and calibration with narrow MWD polystyrene standards is widely used for nonpolar polymers, but was not satisfactory for our analysis of lignins.

The major problem with this system was the very poor discrimination among different molecular weight lignin samples (as determined by VPO and LALLS). All of the lignins had essentially the same elution profiles with the same retention times. Consequently, based on the polystyrene calibration, they all had nearly identical average molecular weights. Another problem was the sometime limited solubility of lignins in THF. The causes of this inconsistent behavior were not pursued, but it was

later surmised that the solubility of lignins in THF is strongly affected by the amount of water present as an impurity.

3.5.3 Lignin Analysis in DMF and DMF Mixed Mobile Phases

DMF has also been widely used as a mobile phase for lignins--it is more polar than THF and is a very good lignin solvent. However, the Ultrastyragel columns could not be run in DMF because of the appreciable shrinkage in the gel, especially for the 100 Å column, which would result from a THF to DMF solvent changeover. Therefore, the Jordi Gel columns were purchased for running DMF, and subsequent organic mobile phases, because of the greater versatility of this gel for running different polarity solvents.

The common result for these DMF based mobile phases has been lignin adsorption on to the poly-DVB stationary phase resulting in abnormally long retention times and unrealistically low molecular weights. An example of this behavior is shown in Figure 3-1 for a typical softwood kraft lignin. Note how the elution profile of the polymer peak is interrupted by the sharp negative peak which is probably water and identifies the total permeation limit (low MW resolution limit) of the column. Occasionally, normal looking chromatograms were observed, however, these were not reproducible.

The mechanism for lignin adsorption probably involves attraction by the π electrons of the aromatic rings in the gel for unshared electron pairs in hydroxyl and ether groups in lignin. During kraft pulping, lignin undergoes significant structural

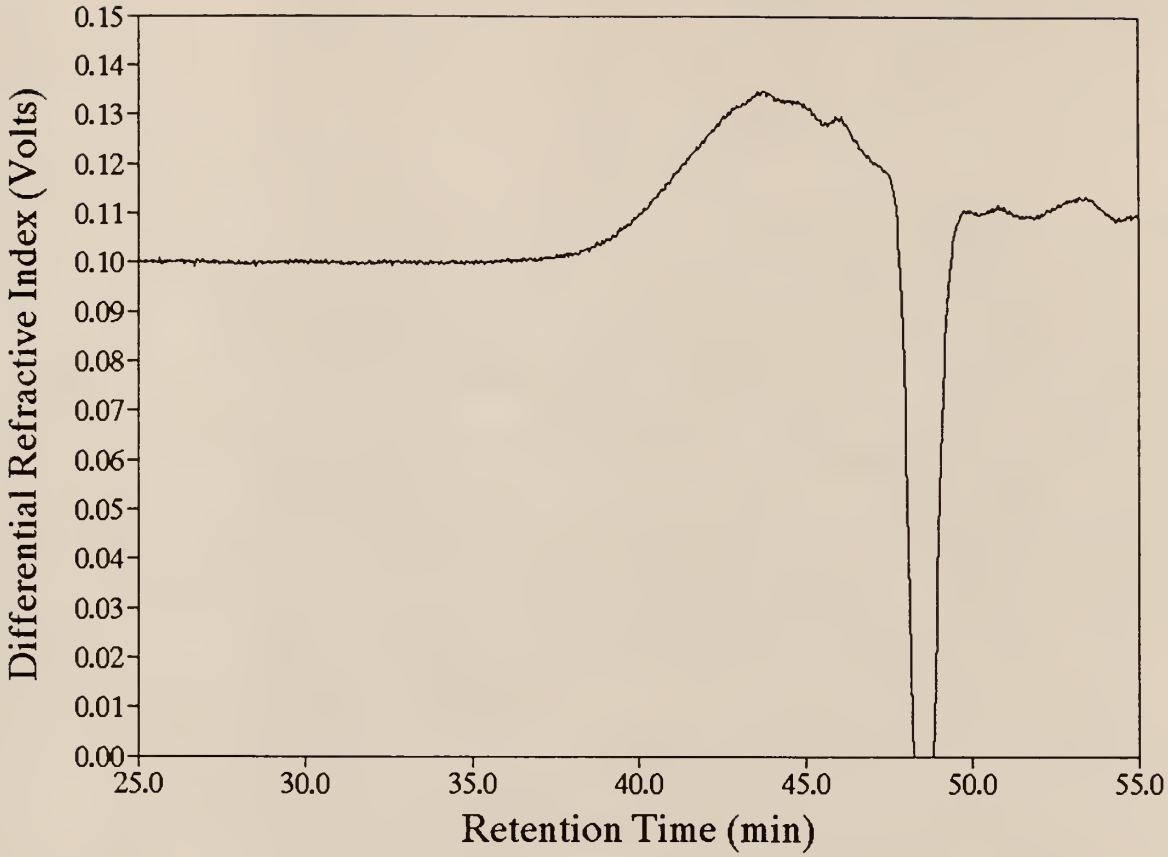

Figure 3-1. Typical SEC Chromatogram for a Softwood Kraft Lignin Run in DMF at 85°C on Jordi Gel Mixed Bed + 10^3 Å Columns.

degradation followed by condensation reactions which partially counterbalance the degradation and result in a structure which is very rich in phenolic hydroxyl and methoxy groups [9]. Numerous adsorption sites for interaction with the aromatic rings in the gel are therefore available.

The polarity of DMF, relative to that of lignin and the gel, must also play a role in this elution behavior, because in THF, adsorption was not observed. The overall Hansen solubility parameters, δ_o s, for DMF, THF, and the PS-DVB gel are 12.1, 9.5, and 9.1 $(cal/cm^3)^{1/2}$, respectively [4, 21,]. We expect that δ_o for the poly-

DVB gel is very similar to that for the PS-DVB gel. THF has thus approximately the same δ_o value as the gel, whereas DMF is significantly more polar than the poly-DVB gel, and this polarity difference can promote lignin adsorption on to the gel.

Our approach for overcoming lignin adsorption has been to investigate mixed mobile phases where a minor solvent possessing unshared electron pairs is added to DMF so that it will preferentially adsorb to the gel instead of lignin. These cosolvents are listed in Table 3-1 and include ethylene glycol (EG) and several of its derivatives--ethylene glycol monopropyl ether (EGMPE), ethylene glycol dimethyl ether (EGDME), and ethylene glycol monomethyl ether (EGMME); and others such as triethyl amine (TEA), n-butanol, and pyrogallol (1,2,3-trihydroxy benzene). This strategy differs from the more common approach of derivatizing lignins to tie up free phenolic hydroxl groups as many previous investigators have done.

Chromatograms for lignins in these mobile phases generally also show adsorption behavior, but on occasion have demonstrated a combination of both adsorption and association behavior as seen in Figure 3-2 for a softwood kraft lignin run in DMF/EGMPE (98/2) at 85°C. Note the sharp main peak, small secondary peak, low MW tail, and small adsorbing peak, which is due to low MW lignin fragments that are rich in phenolic hydroxy and methoxy groups. However, for all of the mobile phases run on the Jordi Gel column set, any elution profiles that appeared normal, and were relatively free from nonideal effects, were not reproducible.

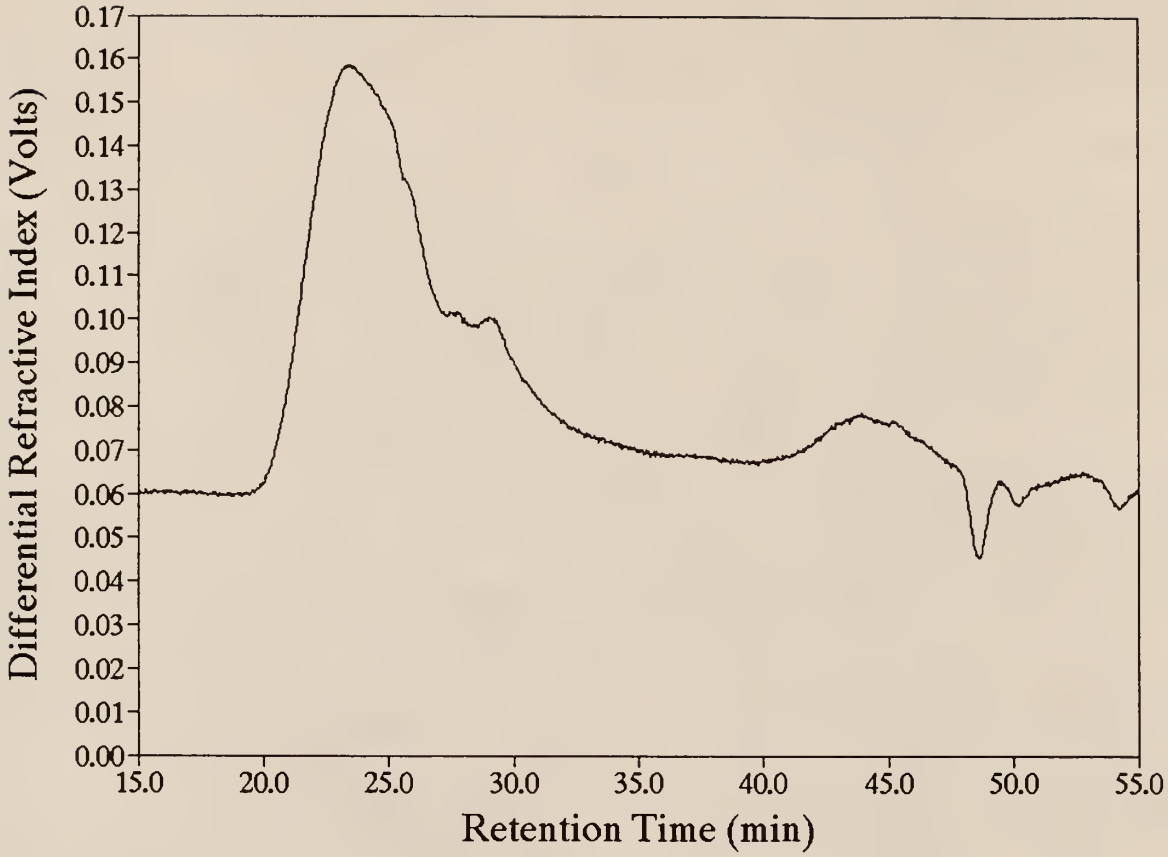

Figure 3-2. SEC Chromatogram for a Softwood Kraft Lignin Run in DMF/EGMPE (98/2) at 85°C on Jordi Gel Mixed Bed + 10^3 Å Columns.

3.5.4 Lignin Analysis in NaOH Solutions

Aqueous SEC provided a different, and potentially promising analytical approach since lignins are readily soluble in strong alkaline solutions, and do not associate in solution above a pH of 13. This switch to aqueous mobile phases, though, required an entirely new column chemistry, and Jordi Associates, Inc. provided us with a specially modified poly-DVB column which had been specifically

designed to minimize sample adsorption and be compatible with aqueous mobile phases.

Elution profiles for lignins run in aqueous NaOH on the Jordi Gel GBR column show excellent reproducibility and are characterized by very sharp and narrow peaks, but with no resolution among the different MW lignins. As with THF, all of the samples had nearly identical retention times, and based on polysaccharide calibration, they had essentially identical molecular weights. For the seven lignins from the University of Florida pulping experiment, $\overline{M}_w$ s were only 3,537 to 3,698 as compared to $\overline{M}_w$ s from LALLS measurements of 18,920 to 83,000.

In the strong alkaline solutions that were investigated: 0.1-0.5M NaOH (pH 13.0 to 13.7), both lignins and gel have electrolytic character. Hydroxide groups on both must be partially or completely ionized at these high pH s. As the NaOH concentration was increased, the eluting lignin peaks (both Indulin AT and organosolv) were systematically shifted to longer retention times and gradually broadened and lost their distinctive sharpness. Lignin molecules must become more compact and assume a progressively more spherical shape as the solution ionic strength is increased. This minimizes their hydrodynamic volume and leads to longer retention times. Lignins were probably more ionized, and had a higher charge density, than the gel, and therefore experienced a salting in effect and were trapped in the pores of the gel for progressively longer times as the NaOH concentration was increased due to charge repulsion from the mobile phase.

Aside from the poor MW resolution discussed above, these strong aqueous NaOH solutions were also unsuitable from the perspective of equipment compatibility. The quartz cell in the DRI detector, and the quartz windows in the UV/Vis detector, were attacked by NaOH and resulted in a costly failure of the DRI detector. The refractometer cell, especially the reference side where the solution is stagnant, had to be flushed regularly with deionized water to slow down this degradation process. Another, less serious problem, was persistent leakage from tubing connections and fittings. It was exceedingly difficult to maintain tight connections that were repeatedly broken and reassembled.

3.5.5 Lignin Analysis in DMSO + LiBr Solutions

Polar organic solvents, such as DMSO, were once more investigated, but this time using the GBR columns where lignin adsorption was not a problem. Dimethyl sulfoxide is a very good lignin solvent, but we discovered that lignins associate very strongly in it. Lithium bromide salt was added to the mobile phase to break up these associated complexes, and Figure 3-3 shows some examples of the dramatic changes in elution profiles for Indulin AT in DMSO with various concentrations of LiBr.

The sharp bimodal distribution for Indulin AT in DMSO changes to a single, more rounded, and nearly symmetrical peak in DMSO + 0.1M LiBr, and in DMSO + 0.2M LiBr, the peak exhibits retarded elution behavior, and is skewed to the low MW end. At this salt concentration, lignin molecules are being trapped in the pores

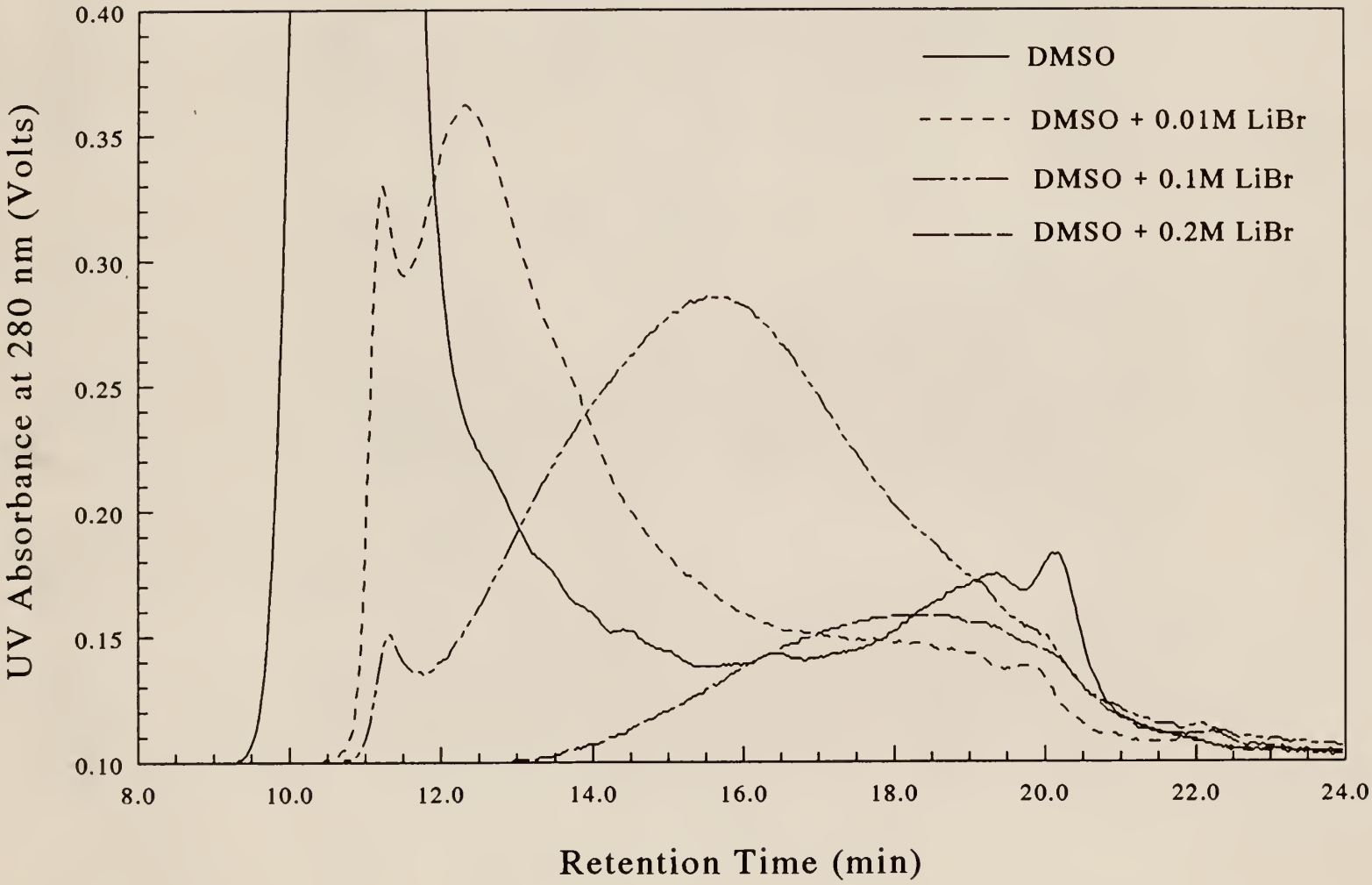

Figure 3-3. SEC Chromatograms for Indulin AT Run in DMSO with Various Concentrations of Lithium Bromide at 85°C on the Jordi Gel 10^3 Å GBR Column.

of the gel by a 'salting in' mechanism. Based on this comparison, DMSO + 0.1M LiBr was selected as the appropriate mobile phase.

Association of lignins in polar organic solvents is a complex and regrettably common phenomenon. It is dependent on temperature, as well as other parameters, and can be eliminated by raising the analysis temperature to above the solute-solvent system's Theta temperature. For example, Kim [52] established that the Theta temperature for softwood kraft lignin-DMF systems is 80 °C. Below this temperature, association becomes progressively more pronounced.

The significant lignin association in DMSO at 85 °C is quite unexpected. However, the actual temperature of the UV/Vis detector is not 85 °C, but room temperature, because it is outside the 150C SEC and the mobile phase exits the temperature controlled cabinet of the 150C SEC, passes through the UV/Vis detector, and then returns into the 150C SEC to pass through the DRI detector before going to waste. The solution cools very rapidly, and then heats back up and equilibrates rapidly because there is no visible drift in the baseline signal from the DRI detector. The association kinetics must be more rapid than the dissociation kinetics because the bimodal elution behavior was also observed at the DRI detector. The mode of association appears to be one of smaller molecules associating to form much larger conglomerates resulting in a distinctive bimodal distribution.

Representative chromatograms for selected lignins are presented in Figures 3-4, 3-5, and 3-6, and demonstrate the versatility of this mobile phase-column combination in separating a wide variety of lignins.

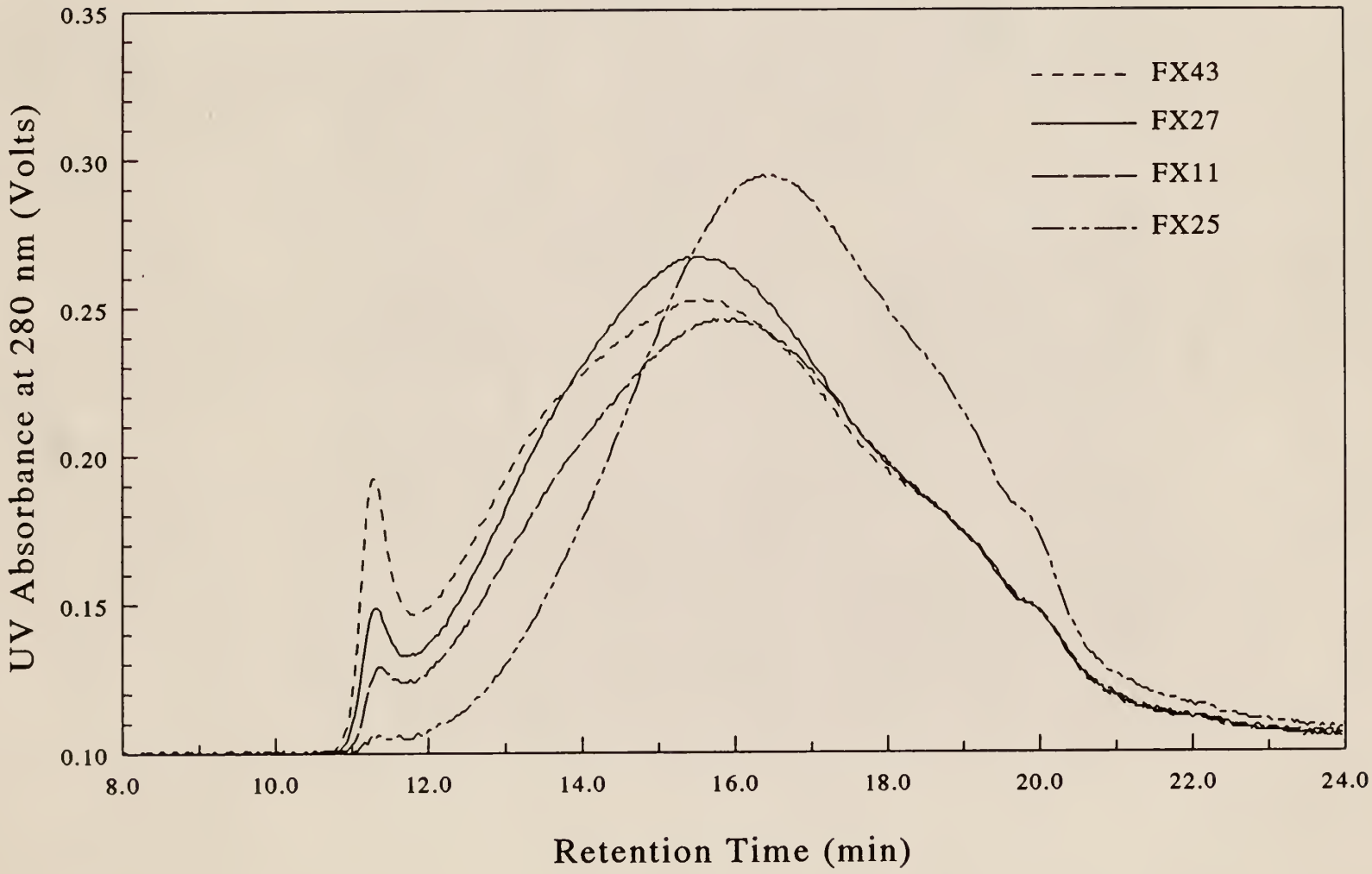

Figure 3-4. SEC Chromatograms for Selected UF Kraft Softwood Lignins Run in DMSO + 0.1M LiBr at 85°C on the Jordi Gel 10^3 Å GBR Column.

Figure 3-5. SEC Chromatograms for Selected UF Kraft Softwood Lignins Run in DMSO + 0.1M LiBr at 85°C on the Jordi Gel 10^3 + 10^4 Å GBR Column Set.

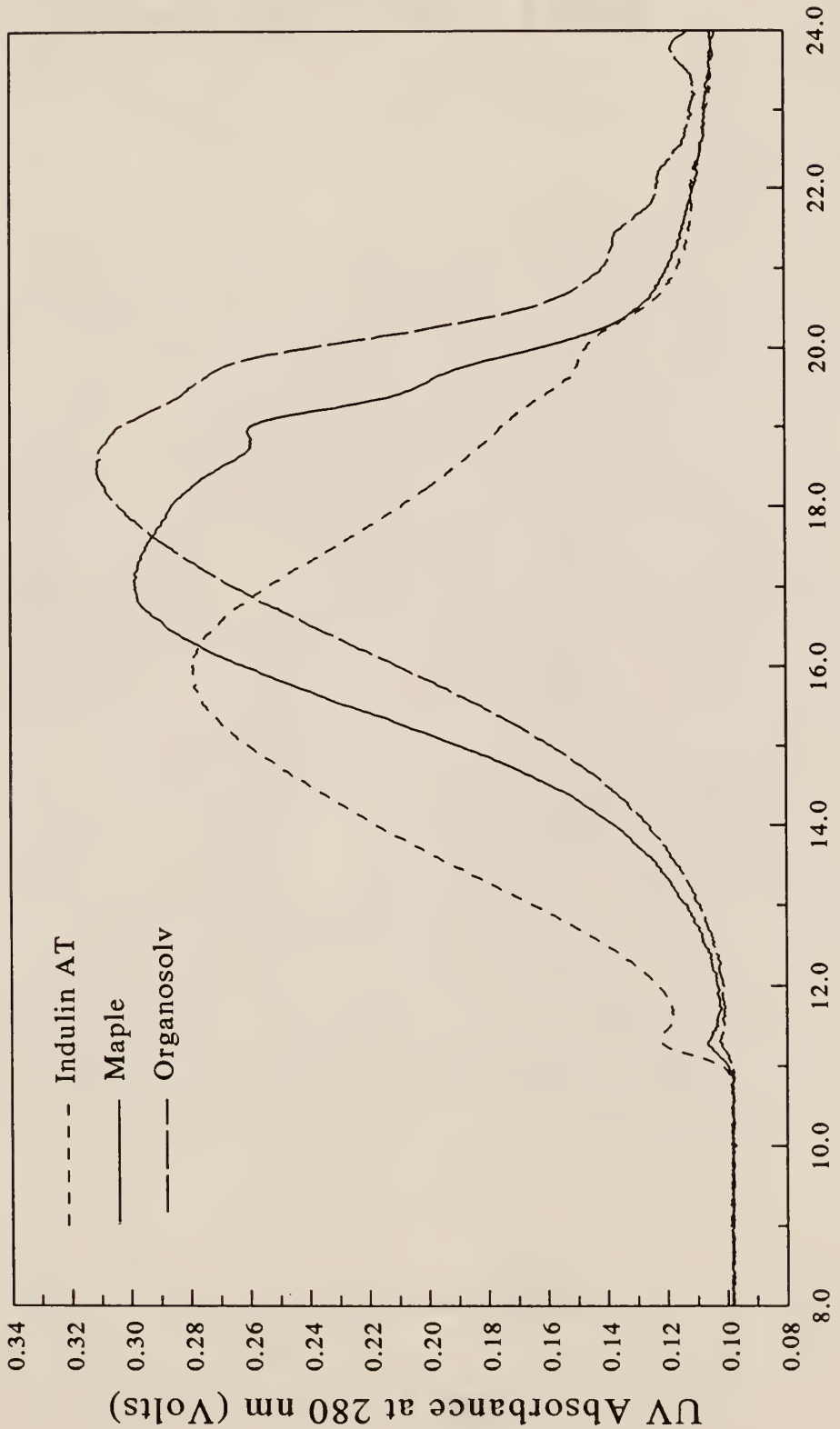

Figure 3-6. SEC Chromatograms for Indulin AT, Maple, and Organosolv Lignins Run in DMSO + 0.1M LiBr at 85 °C on the Jordi Gel 10^3 Å GBR Column.

In Figure 3-4, elution profiles for four softwood kraft lignins from the UF pulping experiment--FX11, FX25, FX27, and FX43--are very similar and have the same general shape, but different retention times. There are some subtle differences though: FX43 is slightly skewed to the high MW side, and FX25 is noticeably skewed to the low MW side. All four have a small shoulder at t_R = 20 min where oligomeric lignin fragments are eluting. These characteristics are representative of of all the lignins studied and reflect the different molecular weight distributions resulting from the different pulping conditions. All of the kraft softwood lignins from the UF pulping experiment are from the same species of wood, and therefore should, on average, be the same chemically. Molecular weights for the complete set of lignins are summarized in Table 3-2.

All of the lignins also exhibit the same sharp initial peak at t_R = 11.3 min in Figure 3-4. This was thought to be due to some small amount of very high MW unresolved material that was being excluded from the 10^3 Å GBR column. With both 10^3 + 10^4 Å GBR columns in use, the shapes of the elution profiles for the same four lignins, presented in Figure 3-5, are essentially identical to those in Figure 3-4, except that the sharp initial peaks, which are now definitely being separated, have decreased in magnitude relative to the main peaks.

In Figure 3-6, the elution profiles for three different types of lignins: kraft softwood (Indulin AT), kraft hardwood, and organosolv, are significantly different. The Indulin AT has a nearly symmetric profile, whereas the maple lignin is skewed to the low MW side, and the organosolv lignin is skewed to the high MW side. All

Table 3-2. Lignin Molecular Weights from SEC in DMSO + 0.1M LiBr at 85°C.

Lignin	$\overline{M}_n$ [a]	$\overline{M}_w$	$\overline{M}_w/\overline{M}_n$	$\overline{M}_{wLALLS}$ [b]	$\overline{M}_{wLS}/\overline{M}_{wSEC}$
Indulin AT	1,582 1,332	6,058 5,142	3.829 3.859	49,380	8.15 9.60
Mixed Hardwood	997	3,357	3.360		
Birch	1,148	3,128	2.725	29,710	9.50
Maple	1,196	3,229	2.700	12,900	4.00
ABAFX011 & 012	1,483 1,387	6,263 6,411	4.224 4.621	19,630	3.13 3.06
ABAFX015 & 016	1,750 1,521	8,519 8,687	4.868 5.711	83,000	9.74 9.55
ABAFX025 & 026	1,217 1,155	3,951 3,910	3.246 3.385	58,880	14.9 15.1
ABAFX027 & 028	1,672 1,519	7,298 7,960	4.365 5.242	21,930	3.00 2.76
ABAFX037 & 038	1,368 1,251	5,352 5,589	3.912 4.468	18,920	3.54 3.39
ABAFX043 & 044	1,696 1,543	8,677 9,672	5.116 6.269	42,930	4.95 4.44
ABAFX055 & 056	1,581 1,516	6,552 7,149	4.144 4.718		
Organosolv					
As received	809	2,403	2.970		
N-hexane fraction	840	2,477	2.948		
TCE fraction	977	2,905	2.973		
Acetone fraction	944	2,763	2.926		
Methanol fraction	954	2,907	3.047		

Note: [a] For lignins with two MW entries, the upper number corresponds to runs on the Jordi 10^3Å GBR column only, and the lower entry corresponds to runs on the Jordi 10^3 + 10^4 Å GBR column set.
Calibration with narrow MWD polysaccharide standards; MW calculations were cut off at a calibration MW of 50.

[b] Fully corrected $\overline{M}_w$ values were determined by Daojie Dong (unpublished data) from LALLS.

three lignins also have a slight shoulder on the low MW side at t_R = 19.5 min, and the maple lignin has a second, and very substantial, shoulder at t_R = 18.8 min. These different profiles are primarily due to the different pulping conditions, and to the general structural differences between softwood and hardwood lignins.

The extent of delignification (pulping) was much greater for the maple lignin than for Indulin AT, based on their respective Kappa numbers: 15.0 versus 95-100, respectively. Consequently, the molecular weights of the maple lignin would be significantly lower than for the Indulin AT, as seen in Table 3-2. Pulping conditions for the organosolv are not known, but based on the low MW s, the delignification was probably very complete. Softwood and hardwood lignins have different concentrations of primary and secondary ether bonds in their structures, and these experience different depolymerization kinetics during the pulping reactions.

The three kraft hardwood lignins, despite being from different species--mixed hardwood (oak and sweet gum), birch, and maple--have nearly identical elution profiles, such as the one for maple displayed in Figure 3-6, and very similar average molecular weights, as seen in Table 3-2. This is not surprising because both the maple and birch lignins were pulped under identical conditions, as listed in Table 2-1.

All five of the organosolv samples exhibit the same elution profiles as the one displayed in Figure 3-6, and only modest increases (about 17%) in both $\bar{M}_n$ and $\bar{M}_w$ between the first two fractions: original, and n-hexane, and the remaining three fractions: TCE, acetone, and methanol. Thus, the lengthy purification/extraction

procedure for the organosolv lignin did not significantly alter its average molecular weights and MWD, as seen by the values listed in Table 3-2.

3.5.6 Column Calibration

The MW data presented in Table 3-2 is based on a third order calibration of the Jordi Gel GBR columns using narrow MWD polysaccharide standards, which are unique and have not yet been used by others for lignin analysis. A sample calibration curve for the 10^3 + 10^4 Å column set is presented in Figure 3-7.

The polysaccharide standards are linear molecules, and unfortunately, this calibration method suffers from some of the same limitations that have plagued previous investigators using polystyrenes and other linear polymers: the molecular structure of the polysaccharides, and hence their elution behavior, are very different from that of the highly branched lignins. Consequently, calculated MW values based on this calibration can vary significantly from absolute values as seen by the comparison of $\overline{M}_w$ values from SEC and LALLS in Table 3-2.

The $\overline{M}_w$ values determined by LALLS have been fully corrected for optical effects--sample flourescence, anisotropy, and absorption--and are 3-15 times greater than the corresponding values from SEC, as seen in the last column in Table 3-2. More significantly, there is also no correlation between the two sets of values, and no constant factor that can be used to relate the SEC values to the LALLS values. We believe that these $\overline{M}_w$ values from LALLS are accurate because in a forthcoming study by Dong [17], $\overline{M}_w$ values for several kraft softwood lignins measured in three

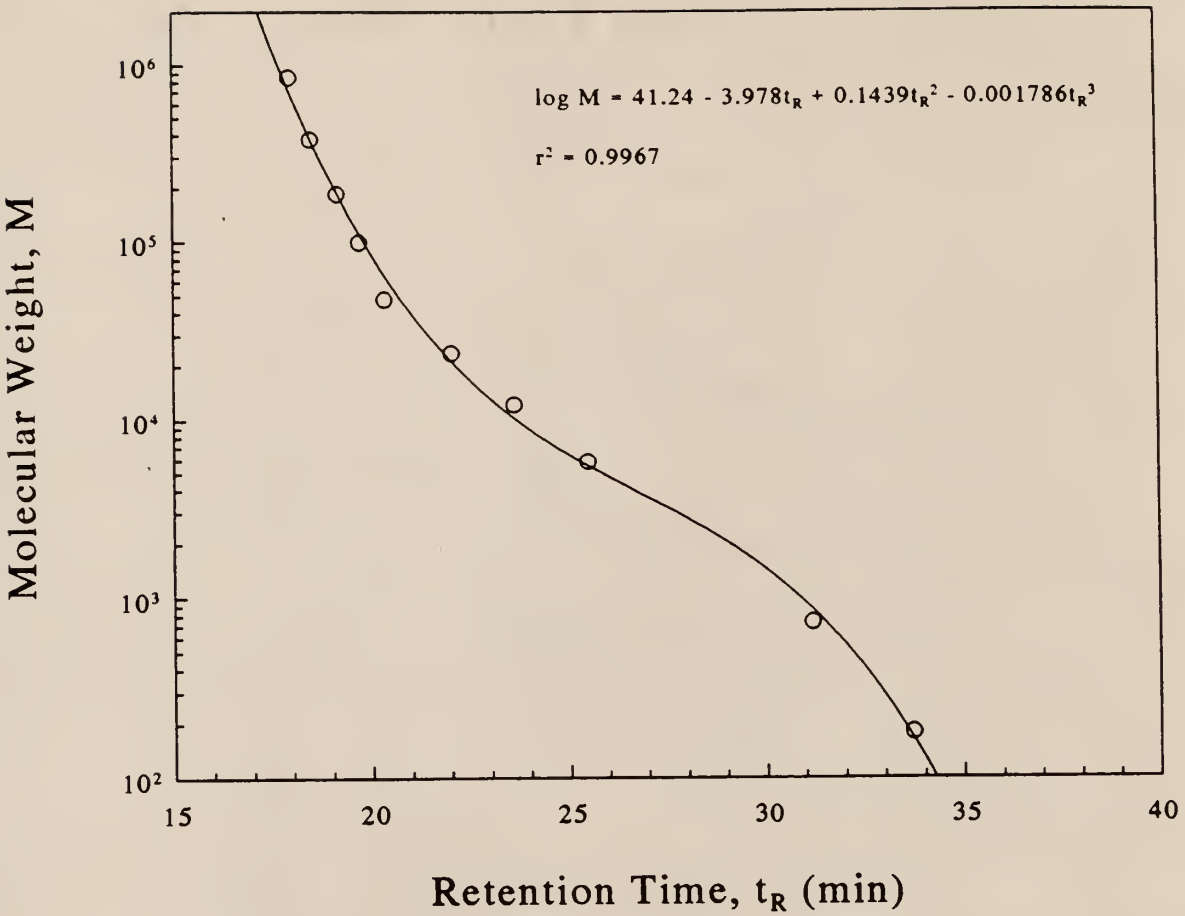

Figure 3-7. SEC Calibration Curve with Narrow MWD Polysaccharide Standards for the Jordi Gel 10^3 + 10^4 Å GBR Column Set Running DMSO + 0.1M LiBr at 85°C.

different solvents: 0.1N NaOH, DMF, and pyridine, were within 10% of each other. Narrow standard calibration, is thus only suitable for determining relative MW data for lignins, unless well characterized lignin MW fractions are used as standards, which is a very tedious approach.

An alternative calibration procedure, such as resolution of moments, which was briefly described in section 3.2.3, is therefore needed. This calibration procedure

was the intended extension of this SEC study, but has not yet been investigated because the necessary absolute $\overline{M}_n$ values for these lignins have not yet been measured by VPO. Resolution of moments should be pursued for the whole set of kraft softwood lignins from the UF pulping experiment where an entire range of carefully controlled pulping conditions has been investigated.

3.5.7 Comparison of SEC Results with Previous Work

Comparing calculated MW values for lignins from different studies is difficult, and not very meaningful, because of the uniqueness of the lignin-column-solvent conditions in each study. Our thoroughly executed, statistically designed pulping experiment has not been duplicated by other investigators, and therefore, results for these UF kraft softwood lignins cannot be compared directly with those from other studies. Two of the commercially available lignins that we have studied--the mixed hardwood kraft lignin from Westvaco, Inc., and the hardwood organosolv lignin from Repap Technologies, Inc.--have also been analyzed by Siochi et al. [87], albeit using a different mobile phase, column chemistry, and calibration procedure. Selected results from these two studies are compared in Table 3-3.

Siochi et al. [87] derivatized their lignins to avoid nonideal interactions, and ran them in THF on PS-DVB gel columns and used narrow MWD polystyrene standards to construct a universal calibration curve. Their calculated $\overline{M}_n$ and $\overline{M}_w$ values from SEC/DV are 60% and 37% higher than our respective values, for the Westvaco mixed hardwood kraft lignin, and 97% and 99% higher than our $\overline{M}_n$ and

Table 3-3. Comparison of SEC Results for Mixed Hardwood Kraft and Organosolv Lignins with Literature Values.

Lignin	$\overline{M}_n$	$\overline{M}_w$	$\overline{M}_w/\overline{M}_n$
Mixed Hardwood (WHK)	997	3,357	3.36
HPL Mixed Hardwood[a]			
(VPO)[b]	1,499		
(SEC/LALLS)	3,711	17,120	4.61
(SEC/DV)	1,597	4,589	2.87
Organosolv (RO)	809	2,403	2.97
HPL Aspen[a]			
(VPO)	1,393		
(SEC/LALLS)	4,004	24,070	6.01
(SEC/DV)	1,591	4,783	3.01

Note: [a] HPL Mixed Hardwood, and HPL Aspen are the hydroxypropyl derivatives of the Westvaco mixed hardwood kraft lignin, and the aspen organosolv lignin from Repap Technologies, Inc., respectively. VPO and SEC runs were performed in THF. Data is from Siochi et al. [87].
[b] Method abbreviations are defined in Key to Abbreviations.

$\overline{M}_w$ values, respectively, for the organosolv lignin. Their SEC/LALLS results are too high because they did not perform a beam polarization correction, but the polydispersities for the two lignins from the two studies agree very well. These large discrepancies are not serious, and this comparison should be viewed as having only relative value.

3.6 Conclusions and Recommendations

3.6.1 Conclusions

In this study, after a lengthy mobile phase/column selection process, a new, and relatively simple, SEC characterization method for kraft lignins has been developed which does not require derivatization of the lignins to overcome adsorption interactions. The following conclusions were then reached:

1. The elution behavior of lignins is complex and reflects its peculiar and complicated chemistry. Selection of the proper mobile phase and column chemistries is critical to achieving good elution behavior and minimizing nonideal effects, such as adsorption interactions.
2. The preferred mobile phase is DMSO + 0.1M LiBr running at 85°C on Jordi Gel GBR columns with sample detection by UV at 280 nm.
3. The GBR series of columns, with their deactivated gel structures, has been an important development in this work because unfavorable lignin adsorption interactions have been minimized, and consequently, the need to derivatize lignins, in order to overcome these interactions, has been eliminated.
4. Accurate and convenient column calibration methods must still be investigated. The narrow MWD polysaccharide standard calibration procedure, while convenient, resulted in $\overline{M}_w$ s for kraft lignins being

lower by a factor of 3-15 as compared to fully corrected $\overline{M}_w$ values determined by LALLS.

3.6.2 Recommendations for Future Work

This SEC method is still not fully functional because the calibration procedure only yields relative MW data. Several experimental problems still need to be addressed in future work, and based on the discussion above, the following recommendations were made:

1. The remaining UF kraft softwood lignins should be run in DMSO + 0.1M LiBr to determine their MWD s.
2. Once absolute $\overline{M}_n$ values for these kraft softwood lignins have been measured by VPO, the resolution of moments calibration procedure should be pursued in order to develop more accurate column calibrations.

CHAPTER 4
LIGNIN THERMAL ANALYSIS

4.1 Introduction

Thermal analysis is a very broad area, and within the scope of this study, we have restricted it to the measurement of glass transition temperatures for purified lignins and for solvent plasticized lignins. Lignins are amorphous polymers and upon heating undergo a glass transition which is due to the onset of chain segment motion. Glass transition behavior is characteristic of any amorphous polymer and is accompanied by abrupt changes in physical properties, such as free volume, heat capacity, and thermal expansion coefficient [68].

Differential scanning calorimetry, (DSC), is the method of choice for measuring glass transition temperatures. Although it is not as accurate as a good adiabatic calorimeter (1-2% vs. 0.1%), DSC's accuracy is adequate for most uses, it is a very rapid and convenient technique, and is the method used in this study [6].

In the remainder of this chapter, the theory of the glass transition phenomenon, and the operating principles for DSC, are discussed in section 4.2. Previous investigations into the glass transition behavior of lignins, including plasticized lignins, are discussed in section 4.3. The experimental work and data analysis are described in section 4.4, and the results and discussion are presented in

section 4.5. Finally, conclusions and recommendations for future research are given in section 4.6.

4.2 Theory

4.2.1 Glass Transition

The glass transition for amorphous polymers corresponds to the onset of liquidlike motion of long segments of molecules, characteristic of the rubbery state, as the material is heated. Conversely, as the material is cooled through the glass transition, molecular configurations are frozen into a glassy state [6]. These phenomena occur at the glass transition temperature, T_g.

Below the T_g, amorphous polymers exhibit many of the properties associated with ordinary inorganic glasses, including hardness, stiffness, brittleness, and transparency, and demonstrate only local molecular motion, such as vibration and rotation. Above the T_g, large scale segmental chain motion is evident [6]. Because polymers are generally polydisperse materials, the glass transition is not sharp and occurs over a range of temperature. The T_g is then defined as some intermediate temperature within this range.

The glass transition phenomenon is usually explained by considering theories based on free volume concepts and thermodynamics. In free volume theory, the degree of molecular mobility is considered dependent on the intermolecular void spaces, i.e. free volume, between polymer chains present in the material. This free

volume decreases with decreasing temperature until the glass transition is reached where molecular mobility is no longer allowed [6, 62].

Below the T_g, the amount of free volume remains constant as the temperature is decreased. The large scale molecular motion of polymers above the T_g requires more free volume than the short range excursions of atoms in the glassy state. This rise in relative free volume with increasing temperature leads to the abrupt change in observed volume expansion coefficient at the glass transition [6, 62].

From a thermodynamic perspective, the glass transition phenomenon is often referred to as a second order or apparent second order transition because of the discontinuity that exists in the second derivative of the Gibbs free energy at the transition temperature:

$$C_p = -T\left(\frac{\partial^2 G}{\partial T^2}\right)_P \qquad (4\text{-}1)$$

where C_p is the heat capacity at constant pressure, G is the Gibbs free energy, T is temperature, and P is pressure.

This discontinuity exists because the heat capacity of the glass is always lower than that of the liquid at the same temperature and because there is no latent heat in stopping translational molecular motion [104]. DSC provides a measure of the heat capacity, and therefore it can readily measure this transition temperature [62]. However, this analogy with thermodynamic second order transitions is a poor one because it implies more thermodynamic significance than the transition warrants [6].

In practice, the glass transition is very much a kinetically dominated event which reflects the temperature region where the time scale for molecular motion becomes comparable to that of the experiment. The T_g therefore does not have a unique value, but occurs over a range of temperature and depends on the rate of heating or cooling, e.g. annealing versus quenching [79]. Other factors which affect the Tg are the material's $\bar{M}_n$ and the molecular weight distribution. Plasticization lowers the T_g by incorporating low molecular weight diluents. Chain branching lowers the T_g (higher concentration of chain ends increases free volume), but crosslinking raises the Tg because it lowers the free volume [6].

4.2.2 Effect of Plasticizer on T_g

It is well established that adding a low molecular weight diluent or external plasticizer to an amorphous polymer lowers its T_g. This phenomenon occurs because the free volume of a low molecular weight liquid is very large relative to that of a polymer at the same temperature and pressure. The overall free volume of the mixture is therefore increased resulting in a reduction of the T_g [63]. Plasticizers can also reduce secondary polymer-polymer bonding and can themselves form secondary bonds to the polymer molecules thus increasing the free volume available for polymer mobility and thereby lowering the T_g [80].

The lowering of the T_g for most systems is directly proportional to the diluent concentration in the polymer. The widely accepted empirical equation relating the T_g depression to the diluent content is given by Ferry [23]:

$$T_g = T_g^o - kW_2 \tag{4-2}$$

where T_g^o is the T_g for the pure polymer, W_2 is the weight fraction of diluent (g/g), and k is an empirical constant. This linear relationship is valid at relatively low dilution (<20%) if diluent and polymer are compatible, whereas a parabolic function is required to cover the entire range of diluent concentrations [82]. Fujita and Kishimoto [30] derived an analagous equation based on the iso-free volume concept:

$$T_g = T_g^o - \frac{\beta}{\alpha} W_2 \tag{4-3}$$

where α is the difference in thermal expansion coefficient above and below the transition temperature and has a constant value of 4.8×10^{-4} per degree, and ß is a parameter representing the contribution of the diluent to the increase in free volume. For various low molecular weight solvents in several common synthetic polymers, values of ß ranged from approximately 0.10 to 0.30 [30].

4.2.3 DSC Principles of Operation

DSC is a comparative analytical technique in which the differential thermal behavior between a sample and a reference is continuously monitored and controlled according to a time or temperature program. For the Perkin-Elmer DSC 7 instrument used in this study, this general operational principle is known as power compensated DSC.

This instrument contains two control loops, one for average temperature control and the other for differential temperature control. The average temperature circuit measures and controls the temperature of the sample and the reference holders to conform to a predetermined temperature program. The temperature difference circuit compares the temperatures of the sample and reference holders and proportions power to the heater in each holder so that the temperatures remain equal. Thus, when the sample undergoes a thermal transition, power is supplied to the two heaters as necessary to correct any temperature difference between them, and a signal proportional to this differential power is plotted versus the time or the temperature [6, 75, 101].

Platinum resistance heaters and thermometers are used in the DSC 7 to accomplish the temperature and energy measurements which are made directly in energy units (milliwatts) providing a true electrical energy measurement of the peak areas [75]. The area under a peak is then directly proportional to the thermal energy absorbed or released in the transition [101]. Some of the physical transitions that therefore can be observed by DSC are crystallization, crystalline orientation, melting, heat capacity, glass transition, heat of reaction, and polymer structure [68].

Numerous factors affect the characteristics of thermograms. Some of these are instrument related and fixed, such as the design characteristics of sample and reference holders, and others are operator adjustable such as the sample size and mass and the heating rate. Other sample related factors include the heat capacity, packing density, particle size, and thermal conductivity.

The two main factors of sample mass and heating rate must be varied in order to strike an optimum balance between the two opposing criteria of resolution and sensitivity. Increasing the sample mass increases the sensitivity, but decreases the resolution and vice versa. Slower heating rates result in increased resolution of minor thermal effects, while faster heating rates yield a larger signal-to-noise ratio and greater sensitivity, resulting in larger peaks. Reversible transition temperatures, such as fusion temperatures, are essentially independent of heating rate, whereas irreversible transformation temperatures, such as glass transition temperatures, are heating rate dependent [68].

For a given set of operating conditions, i.e. heating rate, type of sample pan, and cooling medium in the reservoir, the energy axis (y-axis), and the temperature axis (x-axis) must be calibrated with a standard material, such as indium, having a known transition temperature (melting temperature), and a known energy of transition (heat of melting).

4.3 Background and Literature Review

4.3.1 Introduction

A modest body of work covering the thermal analysis of purified lignins for glass transition temperatures, and reporting a wide range of T_g s exists in the literature. Lignin is an inherently complex material, and this range of T_g values can be attributed to the variety of wood species that have been studied, the various extraction and purification techniques that have been employed, and the different

analytical procedures that were followed. Because of these experimental differences, direct comparisons of T_g s from different studies are not very meaningful.

Although DSC is currently the method of choice, other techniques that have been used include measuring softening temperatures by monitoring the collapse of a column of powdered lignin in a capillary, and torsional braid analysis (TBA). In TBA, a glass braid impregnated with the lignin sample is subjected to free torsional oscillations during programmed heating. From these oscillations, changes in the relative rigidity and damping and damping index reveal primary and secondary transitions, such as melting or glass transitions, in the polymer [101].

4.3.2 Early Work: Characteristic Softening Temperatures

Goring [35] was one of the first to investigate lignin's glass transition behavior by measuring a characteristic softening temperature (T_s) for various softwood and hardwood lignins and lignin sulphonates. His apparatus consisted of a capillary with a weighted plunger in which a sample of lignin powder was compressed under a constant load. The entire apparatus was immersed in an oil bath, and the extent and rate of collapse of the column of powdered lignin were measured as a function of temperature. The softening temperature was then defined as the temperature at which the powder collapsed into a solid plug.

These lignins displayed softening temperatures in the range of 130 to 190°C and were plasticized by water which decreased the T_s and to some extent also sharpened the transition. Two of the lignins were also plasticized by absorbed

organic solvents such as ethanol, benzene, pyridine, and dimethyl sulfoxide [35]. The T_s also increased with increasing lignin molecular weight: T_s = 127°C for $\bar{M}_w$ = 4,300, and T_s = 176°C for $\bar{M}_w$ = 85,000 [36]. This behavior is analogous to that for synthetic amorphous polymers.

Lignin softening temperatures, while indicative of a physical transition in the lignin, are not exactly analagous to the glass transition temperature. Softening temperatures may be more closely associated with the onset of rubbery flow, which is caused by the slippage of long range entanglements of molecular chains, rather than the glass transition, which would normally commence at somewhat lower temperatures [44].

4.3.3 Lignin T_g Studies

In a review by Nguyen, et al. [68], values of T_g for different lignins varied from 80°C for spruce dioxane lignin to 235°C for a softwood sodium lignosulphonate. For several kraft softwood lignins, organosolv lignins, and lignin sulphonates, T_g s were affected by thermal history. Two T_g s were observed for heat treatments below 132°C, but only one was observed for heat treatments above 132°C. For two observed T_g s, the lower T_g increased with increasing heat treatment temperature. The T_g s for a fractionated thiolignin varied almost linearly with molecular weight from 109°C to 124°C, and the presence of methoxy groups decreased the T_g, whereas the presence of hydroxyl groups increased it [68].

In his master's thesis, Masse [62] used DSC to determine T_g s of several kraft softwood lignins obtained from a statistically designed pulping experiment. As with previous work, he found the glass transition region to be very broad: generally 50 °C from 120 to 170 °C. The T_g values were 144-148 °C and were determined graphically as the midpoint of the transition region. Since there is significant experimental error in estimating the endpoints of the transition region, there was no significant difference in the glass transition temperatures determined above.

In a comparative study, Yoshida et al. [106] used both DSC and TBA to investigate the glass transition behavior of a softwood kraft lignin which was fractionated by successive extraction with organic solvents. Molecular weights of the lignin fractions were determined by SEC on an acetylated sample. For the unfractionated lignin, $\bar{M}_n$ = 1,400, and $\bar{M}_w$ = 39,000; for the lignin fractions, $\bar{M}_n$ = 450-5,800, and $\bar{M}_w$ = 620-180,000. The DSC experiments were run with 10 mg disc shaped samples at a heating rate of 10 °C/min under nitrogen, and the TBA samples were run at a heating rate of 2 °C/min for thermal pretreatment and analysis [106].

The T_g increased with increasing molecular weight from 32 to 173 °C, and the temperature range of the glass transition increased significantly with an increase in molecular weight and molecular weight distribution [106]. This is well known behavior for many polymers. The T_g values estimated from TBA agreed closely with those measured by DSC. However, results obtained by TBA may be influenced by the macrostructure of the material [44].

Compared to most synthetic polymers, the T_g of lignins is high. Yoshida et al. [106] believe that this is due to the large degree of hydrogen bonding and stiffness of the main polymer chain. They also observed enthalpy relaxation for the two lower molecular weight fractions, indicating a higher degree of molecular mobility for these fractions than for the higher molecular weight ones.

4.3.4 Enthalpy Relaxation

In an attempt to reconcile the widely varying T_g data for lignins, Rials and Glasser [78] focused their attention on the phenomenon of enthalpy relaxation. Lignin is extremely sensitive to thermal history and enthalpy relaxation is responsible for much of the disagreement of lignin T_g values reported in the literature [78].

In their study, Rials and Glasser [78] investigated a variety of softwood and hardwood lignins obtained by kraft pulping, steam explosion, and organosolv pulping, and two hydroxy propyl lignin derivatives. Molecular weights of the lignins were low: $\overline{M}_n$ = 500-1,300, and M_w = 1,400-7,700, and glass transition temperatures, measured by DSC, ranged from 90 to 172°C for the nonderivatized lignins, and 58 and 87°C for the two hydroxy propyl lignin samples.

Enthalpy relaxation occurs when polymers are annealed at sub-T_g temperatures. As the annealing time is increased, molecular motion becomes more restricted by the reduction of free volume, and the heat capacity of the material in the glassy region is decreased. The onset of the glass transition is shifted to slightly higher temperatures. This indicates a reduction in vibrational freedom for lignin

which suggests that organization of polymer chains may play a role in the relaxation as well as changes in free volume [78].

The annealing temperature had a strong effect on the enthalpy relaxation. The rate of enthalpy relaxation reached a maximum at about 15°C below the T_g before dropping off sharply as the annealing temperature approached the T_g. This point essentially identifies the onset of the glass transition with a higher equilibrium free volume reducing the extent of relaxation in the system [78].

Rials and Glasser [78] concluded that lignins and lignin derivatives undergo enthalpy relaxation at sub-T_g temperatures, and that the relaxation rate depended on the sub-T_g annealing temperature. There was no effect of lignin's phenolic hydroxy functionality on enthalpy relaxation. Previously, it was believed that differences in the rate of enthalpy relaxation were attributable to hydrogen bonding involving phenolic hydroxy groups.

4.3.5 Glass Transition Behavior of Plasticized Lignins

An extensive investigation of the thermoplasticization of lignin with synthetic organic plasticizers was carried out by Sakata and Senju [82]. Their objective was to determine the effectiveness of certain synthetic plasticizers on lignin with an application toward utilization of plasticized waste lignins as adhesives for fiberboard manufacture.

They studied four series of plasticizers: dialkyl phthalates, trialkyl phosphates, aliphatic acid esters, and other compounds such as camphor. The number of carbon

atoms in the alkyl residues of the plasticizers varied from one to twelve. Both a thiolignin, and a dioxane lignin were studied, and thermal softening temperatures were measured in an apparatus similar to the one used by Goring [35].

For both lignins, T_s values were reduced significantly with a decrease in the number of carbon atoms in the alkyl residue of the plasticizer, and the maximum plasticizing effect was achieved when the solubility parameter of the plasticizer approached that of the lignin (about 11 $(cal/cm^3)^{1/2}$). Small amounts of water lowered the T_s considerably, but above the 10 wt. % level, had no further effect. The combination of plasticizer with water had a synergistic effect and produced the largest drop in the softening temperature [82].

In a more recent study, Irvine [44] used DSC to investigate the thermoplasticization of lignin with water. He studied a ball-milled hardwood lignin (Eucalyptus regnans) which had been alkali pretreated and extracted with aqueous acetone. In order to prevent evaporation of water from the plasticized samples during analysis, they were sealed with polyurethane film which was crimped along with the lid onto the aluminum sample holder. The other dry samples were run in open or loosely lidded pans [44].

Glass transition temperatures decreased dramatically for small amounts of water (<5 wt. %) present. The dry lignin had a T_g of 138°C, and the 5 wt. % water plasticized lignin had a T_g of 72°C. This rapid decrease soon bottomed out and the T_g remained constant at 45°C for water contents greater than about 18 wt. % [44].

Irvine [44] reasoned that since lignin has hydroxyl and other polar groups it has the potential to be plasticized by a strongly polar hydrogen bonding solvent such as water. This process is believed to involve the reversible replacement of intermolecular hydrogen bonds by hydrogen bonded water linkages. As the water content increases, The T_g will shift to lower temperatures until, at a water content determined by the concentration of accessible hydrogen bonding sites within the polymer, no appreciable further lowering of the transition occurs.

4.4 Experimental Work and Data Analysis

4.4.1 Instrumentation

The thermal analysis work on both the dried lignins and the solvent plasticized lignins was performed on a Perkin-Elmer DSC 7 differential scanning calorimeter interfaced with a Perkin-Elmer 7500 computer workstation (Perkin-Elmer Corp., Norwalk, CT). The DSC 7 is equipped with a drybox and a coolant reservoir capable of handling ice water or liquid nitrogen for subambient operation. A detailed description of the instrument may be found in the DSC 7 system manual [75].

Dry nitrogen purge gas for both the sample chamber and the drybox is supplied by a gas distribution system. Lignin samples were dried in a Lab Line Duo Vac Oven (Lab Line Instruments Inc., Melrose Park, IL) and weighed out on a Mettler M150 electronic balance with a resolution of 0.001 mg (Mettler Instruments, Inc., Hightstown, NJ).

4.4.2 Sample Selection and Preparation

Several purified lignins, described in Table 2-1, were run as dried samples. These included Indulin AT, Westvaco mixed hardwood kraft lignin, birch kraft lignin, a softwood kraft lignin from the University of Florida pulping experiment, and an organosolv lignin. These lignins were vacuum dried at 50-60°C for at least several hours to remove some of the adsorbed moisture and then stored in a dessicator. They were then loaded into standard aluminum sample pans for analysis.

The thermal analysis of solvent plasticized lignins was designed to investigate the effect of different lignin solvents on the T_g of the resulting plasticized samples. Since lignins can interact by means of hydrogen bonding, solvents were selected to represent a range of hydrogen bonding capacities while maintaining approximately the same overall Hansen solubility parameter, δ_o, which is a decomposition of the Hildebrand parameter into three terms representing different contributions to the energy of mixing. This 3-parameter solubility assumes that the cohesive energy arises from dispersive, permanent dipole-dipole interactions, and hydrogen bonding forces

$$\delta_o^2 = \delta_d^2 + \delta_p^2 + \delta_h^2 \qquad (4\text{-}4)$$

where δ_d is the dispersive (nonpolar) term, δ_p is the polar term, and δ_h is the hydrogen bonding term [8]. These solvents are listed in Table 4-1. Ethylene glycol (EG), despite its significantly higher δ_o value, was chosen as a replacement for EGMME because of its relatively high boiling point.

Table 4-1. Hansen Solubility Parameters for Lignin Solvents.

Solvent	T_b (°C)	Solub. Parameter $(cal/cm^3)^{1/2}$ δ_o	δ_h
EGMME	124	12.0	7.9
DMF	153	12.1	5.5
EG	198	16.3	13.5
NMP	202	11.2	3.5

Sources: Barton [5], and Eastman Kodak Co. [21].

The plasticized lignin samples were prepared for only one lignin: Indulin AT because it had the highest T_g. Starting from a relatively dilute solution (approximately 33 g/L) in 4 ml sample vials, the solvent was gradually evaporated under heat and vacuum, while the total weight of the mixture was periodically monitored, until the desired solvent concentration was achieved. Four concentrations were prepared for each Indulin AT/solvent combination. The samples were ground up in their vials to make them reasonably uniform before loading into standard aluminum sample pans for analysis.

4.4.3 DSC Experimental Methods

The development of experimental methods for running both the dry and the plasticized lignins had to address several major issues: the optimum sample mass and heating rate had to be determined, adsorbed moisture on the lignin samples had to be evaporated off, and a consistent temperature program (a series of heating, cooling, and isothermal hold steps) had to be developed. This last issue is very

important because all of the samples should experience the same thermal history, to insure that all residual stresses and molecular orientations in the material are eliminated, prior to measuring their T_g s.

Based on substantial preliminary work, a heating rate of 10°C/min, and a sample size of 10-12 mg were chosen for both the dry and the plasticized lignins. To develop the temperature programs, preliminary scans were run for each of the lignins to roughly establish the location of the glass transition region, and the boundary conditions for the heating and cooling steps and the isothermal holds which allow for thermal equilibration between heating and cooling steps.

The general temperature program is outlined in Table 4-2. Steps 2 and 3 promote drying of the lignins by driving off adsorbed water. Unfortunately, for some plasticized lignins, significant amounts of solvent also evaporated which had to be corrected for. Steps 2 and 4 are a thermal conditioning procedure, and following step 4, at least one sample for each lignin was quickly weighed to determine its weight loss during heating. Although some runs were stopped here, most were continued by loading the sample back in the DSC and proceeding on to step 5. The cooling and heating rates in steps 4 and 6, respectively, are equal to insure a uniform sample thermal history. At least two samples were run for each lignin, and T_g s were then determined from the final heating scans.

The coolant reservoir, which functions as a heat sink, was loaded with tap water for running the dry lignins, but ice water was used for running the plasticized ones because of the lower T_g s. Ice water coolant required a continuous purge of the

Table 4-2. Temperature Program for DSC Analysis of Dry and Solvent Plasticized Lignins.

Step	Description of Thermal Event
1	Isothermal hold at 30-50°C for 2 min. following sample loading into DSC.
2	Heating at 40°C/min to above end of glass transition region (dry lignins); to 120-130°C for plasticized lignins.
3	Isothermal hold for 2-3 min. at final temp. in step 2.
4	Cooling at 10°C/min. to 50°C (dry lignins), or to 20-30°C (plast. lignins).
5	Isothermal hold for 2-3 min. at final temp. in step 4.
6	Heating at 10°C/min. to above end of transition region.
7	Isothermal hold for 1 min. at final temp. in step 6.

glovebox with dry nitrogen gas to prevent condensation. The sample chamber was always purged with dry nitrogen gas.

The temperature axis was periodically calibrated with an indium metal standard (onset T_m = 156.60 °C) according to the operating instructions [75], and baseline drift was compensated for by the baseline optimization feature in the software.

4.4.4 Data Analysis

The glass transition temperature for each sample was determined graphically as an onset T_g, by locating the intersection of a tangent drawn to the initial baseline and the steepest portion of the curve in the transition region, directly from the plot of differential power versus temperature as illustrated in Figure 4-1. This onset T_g

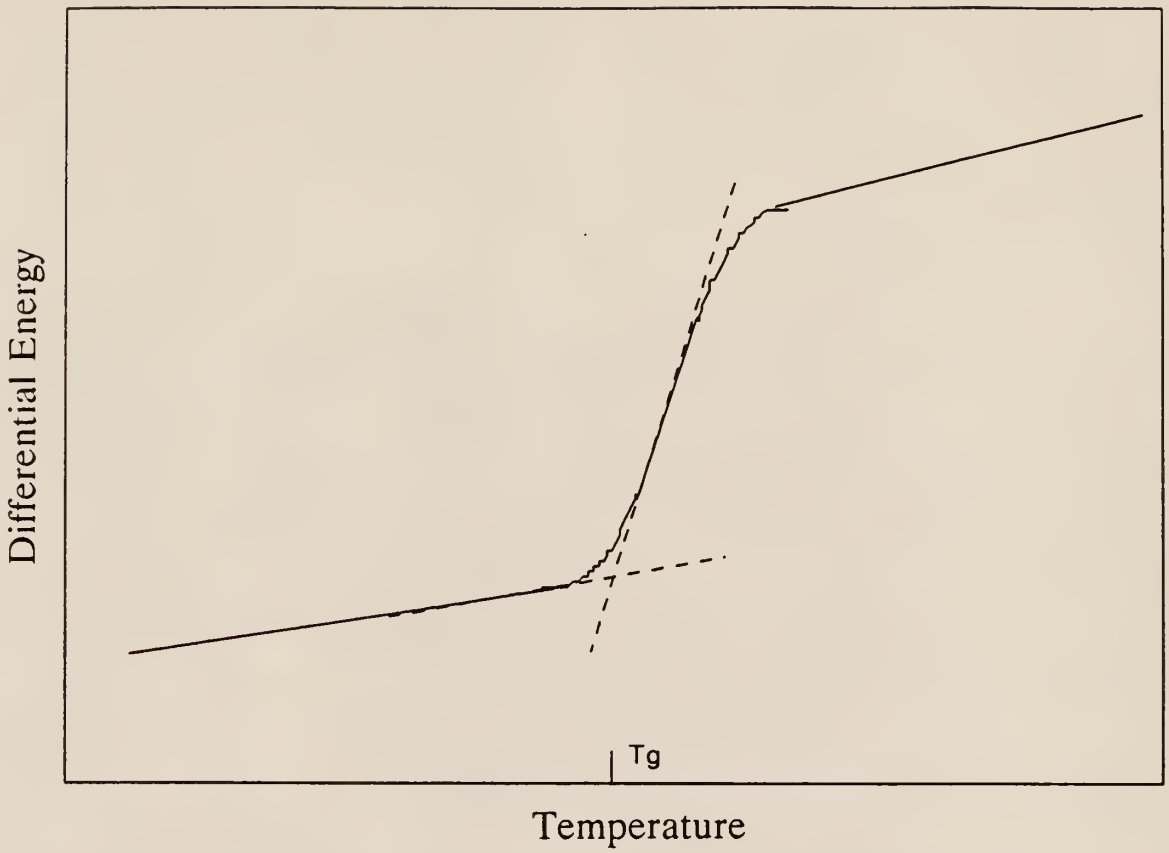

Figure 4-1. Experimental Definition for the Onset Glass Transition Temperature.

allows for a uniform comparison among lignins, because many lignins start to decompose immediately above the transition region making it difficult to identify a post-transition baseline, and therefore, the upper end of the transition region.

For the solvent plasticized lignins, weight loss due to evaporation of absorbed water and solvent during the heating was corrected for by regression analysis of the weight loss versus concentration data. In this way, a more accurate value for the solvent loading in the Indulin AT was determined.

4.5 Results and Discussion

4.5.1 Glass Transition Temperatures for Dry Lignins

A representative DSC scan for lignin is presented in Figure 4-2 and displays the characteristic behavior for all of the lignins studied: a linearly increasing baseline following initial equilibration, a broad transition region where the curve goes through an inflection point, and a relatively linear post transition baseline. This behavior is proportional to the changes in lignins' heat capacity with temperature. The pre- and post-transition baselines denote increases in heat capacity due to sensible heating, and the glass transition region denotes the abrupt and dramatic change in heat capacity due to latent heat effects. For some of the lignins, particularly those with high T_g s, the post transition baseline is difficult to identify because thermal degradation begins in this region.

For all of the scans run on this DSC, the differential heat flow (y-axis scale) is positive for endothermic transitions, and negative for exothermic transitions. The size of the transition (e.g. in mW) is relative to the mass of sample present, and transition energies of 1-2 mW for a 10 mg sample were routinely observed.

Glass transition temperatures for all of the dry lignins investigated in this study, and several lignins selected from the literature for comparison, are presented in Table 4-3. The large variation in T_g s, and the breadth of the transition regions for the various lignin samples, reflects the wide range of species, pulping conditions, and resultant lignin molecular weights that have been encountered. Because of the

Figure 4-2. DSC Scan for S.D. Warren Birch Kraft Lignin. Heating Rate = 10°C/min in Nitrogen.

Table 4-3. Glass Transition Temperatures for Dry Lignins.

Lignin[a]	T_g (°C)	T_g Range (°C)	ΔT at T_g (°C)	ΔC_p at T_g[b] (J/g°C)	$\overline{M}_n$[c]	$\overline{M}_w/\overline{M}_n$
IND	171	138-206	68	0.96	1,582	3.829
WHK	161	137-196	59	0.86	999	3.360
WBK	132	121-165	44	0.40	1,148	2.725
FX43	149	113-200	87	0.71	1,696	5.116
RO as received	78	58-109	51	0.61	809	2.970
RO n-hexane fraction	81	67-111	44	0.69	840	2.948
RO TCE fraction	84	67-123	56	0.58	977	2.973
RO acetone fraction	84	66-125	59	0.63	944	2.926
RO methanol fraction	83	63-120	57	0.67	954	3.047
Kraft Softwood Lignin[d]	134	121-171	50			
Indulin AT[e]	169				1,300	3.31
Organosolv Aspen[e]	97				600	3.50
Japanese Cypress[f]	124	109-157	48	0.57		

Note: [a] Lignin identification codes defined in Table 2-1.
[b] Values determined graphically from the DSC scans.
[c] $\overline{M}_n$ and $\overline{M}_w/\overline{M}_n$ determined by SEC.
[d] Data from Masse [62]. The T_g value has been adjusted to an onset T_g.
[e] Data from Glasser et al. [32]. Organosolv aspen lignin obtained from Repap Technologies, Valley Forge, PA.
[f] Solvent extracted with dioxane; data from Hatakeyama et al. [39].

difficulty in determining the endpoints of the transition region, differences in T_g s of less than 2 to 3 °C are not significant.

Comparing T_g values for several of the lignins listed in Table 4-3, we see excellent agreement for the two Indulin AT samples, and reasonably close agreement for our FX43 sample, and the kraft softwood lignin sample from Masse [62], which were both obtained as part of a statistically designed pulping experiment. Glass transition temperatures for the two organosolv samples--the RO 'as received' lignin and the organosolv aspen lignin are not in very good agreement, however. Finally, all of the lignins investigated here are to some extent degraded, and have lower T_g s, than native lignins in dry wood, which have estimated T_g s at least as high as 205 °C [2].

Values of the change in lignin heat capacity over the glass transition region, ΔC_p at T_g, have also been included in Table 4-3, but are only rough estimates because they were determined graphically from the individual DSC scans without first running a standard material. These ΔC_p values for the four kraft lignins vary considerably with $\overline{M}_n$, but not in any clear pattern, and the five organosolv fractions are relatively consistent along with their $\overline{M}_n$ values, and compare favorably with the literature value for the Japanese cypress lignin.

The $\overline{M}_n$ s and polydispersities for these lignins, from SEC results, are also provided in Table 4-3. The T_g s for the kraft lignins do not correlate well with $\overline{M}_n$ or $1/\overline{M}_n$ because the molecular weights are probably too low. Similarly, Masse observed for narrow MWD polystyrene standards that a linear correlation of $\overline{M}_n$

values with T_g existed only for the higher $\overline{M}_n$ (> 50,000) standards [62]. For the five organosolv lignin fractions, we see small, but distinct differences in $\overline{M}_n$ values between the 'as received', and n-hexane extracted samples; and the TCE, acetone, and methanol extracted samples, but only a small difference in T_g s between the first and second groups. This is probably due to the very low $\overline{M}_n$ values in general.

The breadth of the transition region, ΔT at T_g, does correlate very well, however, with the lignin's polydispersity. For the four kraft lignins--IND, WHK, WBK, and FX43--a linear fit of the T_g range versus the polydispersity data gives a correlation coefficient (r^2) of 0.9924, as seen in Figure 4-3, although a parabolic fit is even better. The five organosolv lignin fractions exhibit essentially the same ΔT values, which are compatible with their nearly identical polydispersities.

This relationship between ΔT at T_g, and the polydispersity, can be explained if we consider the glass transition as the onset of large scale molecular motion. For polydisperse materials, the different MW fractions will undergo the transition at different temperatures resulting in a broader transition region, whereas narrow MWD polymers will display a much narrower transition region because all of the molecules will experience the transition at approximately the same temperature.

4.5.2 T_g s for Solvent Plasticized Indulin AT

Of the lignins analyzed, Indulin AT was chosen for the plasticizer studies because it had the highest T_g as a dry material and would provide the largest temperature range for observing the T_g depression caused by solvent plasticization.

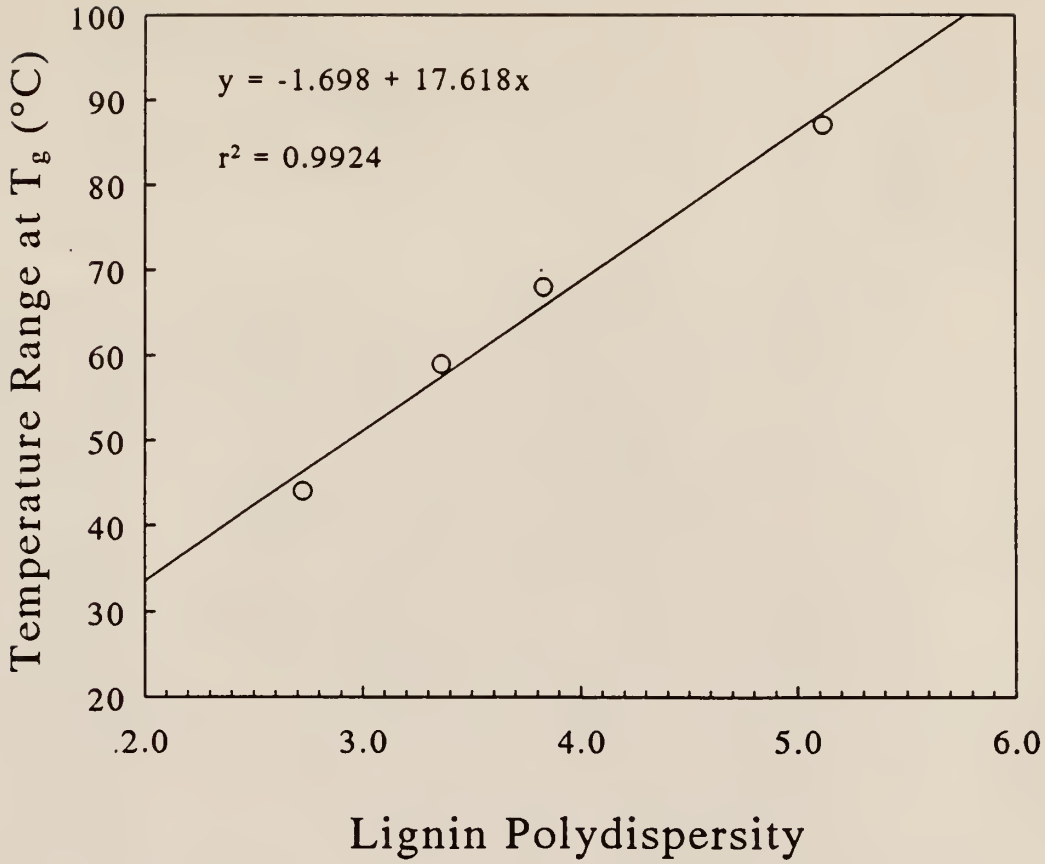

Figure 4-3. Effect of Lignin Polydispersity on the Breadth of the Glass Transition Region.

For T_g s too close to, or below, room temperature, liquid nitrogen, instead of ice water, must be used as the coolant in the DSC in order to achieve a stable baseline prior to reaching the transition region. This is a much more complex experimental situation and was therefore avoided. During initial evaluation of the plasticizing solvents, EGMME was replaced by ethylene glycol because EGMME had too low of a boiling point and nearly all of it evaporated during the initial sample heating step in the analysis procedure.

DSC scans for the plasticized Indulin AT samples have the same general shape as the one in Figure 4-2, but the actual transitions were more difficult to identify because of greater baseline drift. Despite a continuous nitrogen purge of the sample glovebox, occasional moisture condensation in and around the sample oven block is a common occurrence when ice water, instead of room temperature water, is used in the coolant reservoir.

Reproducible transitions were observed for only the NMP and DMF plasticized samples. Scans for the ethylene glycol plasticized samples were generally very noisy and did not clearly show any transitions. Although all three are lignin solvents, EG is much less effective because of its much higher viscosity and may not be uniformly distributed in the samples. Ethylene glycol also has much higher overall solubility, and hydrogen bonding, parameters than the other two, and these factors may also account for the very noisy and inconsistent DSC scans. The breadth of the glass transition region was 35-67 °C, but there was no consistent pattern with respect to solvent type or concentration. This is lower than for some of the dry lignins and may be due to the increased baseline drift.

Glass transition temperatures for the solvent plasticized Indulin AT samples, as a function of the corrected solvent concentrations, are presented in Figure 4-4. The greater scatter in the DMF data, relative to the NMP data, is probably due to its lower boiling point: 153 °C, versus 202 °C for NMP, which required a larger correction for DMF weight loss. The DMF may also not have been as uniformly distributed in some of the samples. This T_g depression behavior does not follow the

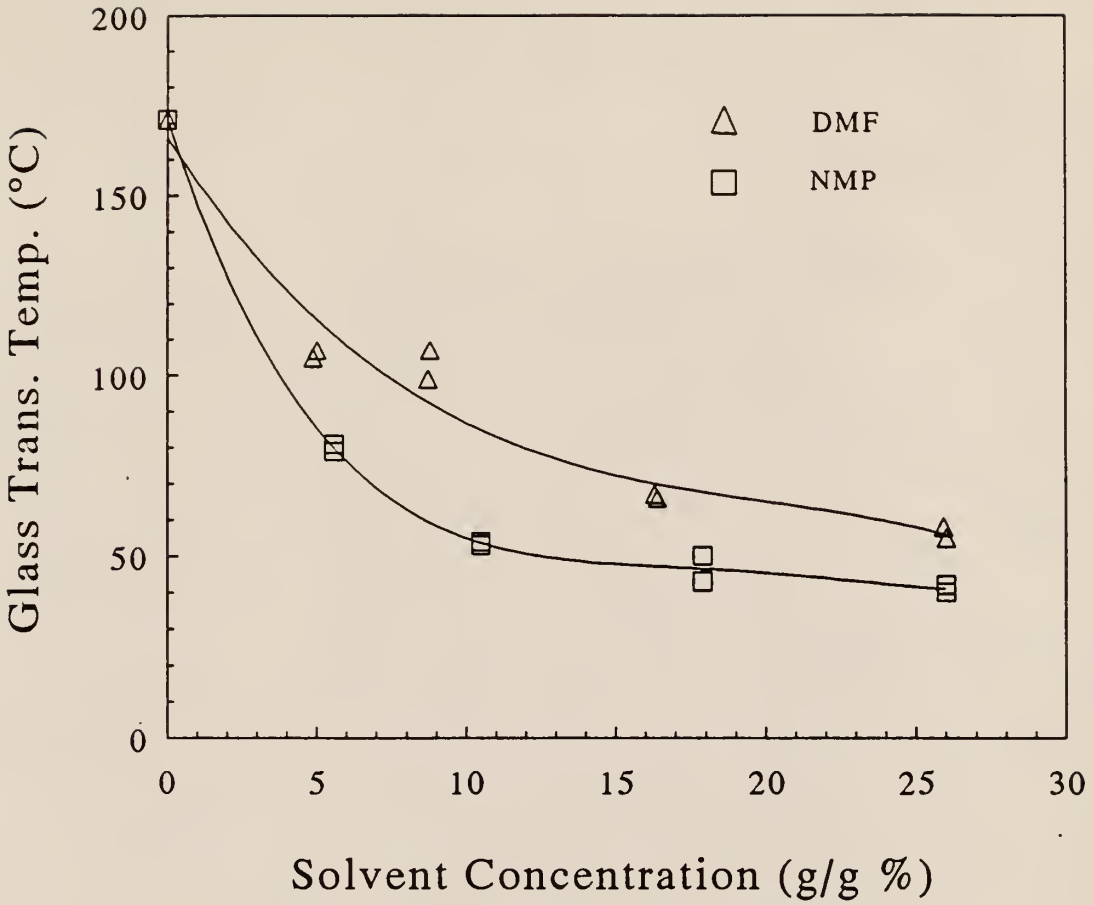

Figure 4-4. Glass Transition Depression for Solvent Plasticized Indulin AT Lignin.

linear models of Ferry [23] and Fujita and Kishimoto [30] because these models are based solely on free volume considerations and do not account for secondary interactions such as hydrogen bonding.

The larger glass transition depression for the NMP plasticized Indulin AT, as compared to the DMF plasticized one, is unexpected. Since both are good lignin solvents, the weaker hydrogen bonding solvent (NMP) should swell lignin less, which would result in less disruption of the lignin structure and less of a decrease in the T_g at a given solvent concentration. In fact, the opposite was observed, and on a molar

basis, the difference between the two is amplified because of the difference in molecular weights: 73.10 for DMF, and 99.13 for NMP.

The real issue may be that NMP is actually a better solvent for Indulin AT lignin, than DMF, based on a comparison of overall Hansen solubility parameters. For lignin, NMP, and DMF, δ_o = approximately 11, 11.2, and 12.1 $(cal/cm^3)^{½}$, respectively. The δ_o s for NMP and lignin are thus much more closely matched than those for DMF and lignin, and the ability of solvents to dissolve or swell a variety of isolated lignins increased as the δ_o s of the solvents approached that of lignin, but as their hydrogen bonding capacities increased [83]. Perhaps, the lower hydrogen bonding capacity, which of course, is incorporated into the δ_o value, may have less of an effect than the better match of δ_o values. Sakata and Senju [82] also observed the maximum depression in thermal softening temperatures for lignins with plasticizers having δ_o s of about 11 $(cal/cm^3)^{½}$, but in the absence of significant hydrogen bonding capacities. Both solvents are single hydrogen bond acceptors, and lignin can act as a proton acceptor as well as a donor [83].

This line of reasoning is supported by a recent study by Birkinshaw et al. [7] on the plasticization of nylon 6,6 by water, methanol, and ethanol. They measured successively larger decreases in the T_g s of the plasticized nylon 6,6 for equal molar concentrations of water, methanol, and ethanol, respectively. This trend in the T_g values followed a progressive decrease in the solvent δ_o and δ_h values as they more closely approached those for nylon 6,6: 11.1, and 6.0 $(cal/cm^3)^{½}$, respectively. The

molecular size of the plasticizing solvents also became progressively larger resulting in a greater disruption of interchain bonding in the nylon structure.

A more specific approach is to investigate the relative strengths of the lignin-DMF and the lignin-NMP hydrogen bonds. Although such specific data has not been found, tabulated hydrogen bond enthalpies for several Lewis acids: t-butanol, p-flourophenol, and p-bromoanaline, in combination with the Lewis bases DMF and NMP, all demonstrate that the acid-NMP hydrogen bond is stronger than the acid-DMF hydrogen bond [46]. This raises questions as to the applicability of the Hansen hydrogen bonding parameter.

In any event, these are complex molecular interactions which we are attempting to explain from a macroscopic point of view with only limited data. In the absence of detailed structural information about this Indulin AT sample, and its hydrogen bonding capacity, it is difficult to reach any firm conclusions to explain this observed difference in T_g s between DMF, and NMP, plasticized Indulin AT.

4.6 Conclusions and Recommendations

4.6.1 Conclusions

The thermal analysis work discussed in this chapter has only been preliminary in nature. Although a reasonable survey of the glass transition temperatures for the dry purified lignins was performed, the work on solvent plasticized lignins has been limited. Nevertheless, some basic conclusions were reached.

1. Glass transition temperatures for the kraft lignins investigated here covered a wide range: 132-171 °C and reflect the effect of the wide range of pulping conditions on the lignin degradation reactions in solution and their effect on the lignin molecular weights.
2. The breadth of the glass transition region was very broad: 44-87 °C and correlated linearly with the polydispersity of the kraft lignins.
3. The glass transition depression was greater for Indulin AT plasticized with NMP, a weaker hydrogen bonding solvent, than with DMF, a stronger hydrogen bonding solvent, over the range of 0-26 wt. % of solvent.

4.6.2 Recommendations for Future Work

Due to the exploratory nature of this study, further work is recommended to extend this work to more lignins and solvents, and to address some of the experimental difficulties that have been encountered.

1. Glass transition temperatures should be determined for the complete set of lignins from the University of Florida pulping experiment for which detailed pulping and molecular weight data is available.
2. At least two additional lignins, such as a hardwood kraft, and an organosolv, should be studied with several plasticizing solvents.
3. The lignin + solvent samples should be prepared in a sigma blade type of mixer, which has twin counterrotating blades, with the desired

solvent concentration determined at the outset. This should result in a more uniform solvent distribution in the lignin, and should lead to more consistent T_g data. The method used here: concentrating a dilute lignin solution by gradually evaporating off the solvent, is indirect and not very accurate; sample uniformity is difficult to achieve.

4. DMF should be replaced by a higher boiling plasticizing solvent because it has too high of a vapor pressure at the analysis temperatures used, and results in significant solvent loss which must be corrected for. Two possible alternatives are DMSO and aniline. Both of these are good lignin solvents and have similar solubility parameters: δ_o, and δ_h, for DMF, DMSO, and aniline are 12.1, and 5.5; 12.9, and 5.0; and 12.0, and 6.0 $(cal/cm^3)^{½}$, respectively. Boiling points for DMSO, and aniline are 189 and 184°C, respectively, as compared to 153°C for DMF.

5. For rheological experiments, a sample of NMP plasticized Indulin AT should be investigated because of the lower T_g s and lower volatility of the solvent will enable the use of lower analysis temperatures in the rheometer.

CHAPTER 5
LIGNIN RHEOLOGY

5.1 Introduction

Rheology is the science that deals with the deformation behavior of materials subjected to certain forces. It is a very extensive area, and the focus of this investigation is limited to the rheometry, or experimental measurement of the rheological properties, of plasticized lignins. These are important, especially viscoelastic ones, because they govern the flow behavior during processing operations such as extrusion for fiber spinning.

The author is not aware of any work on the rheometry of pure or plasticized lignins. However, a small body of work exists on the rheological characterization of black liquors, which may be considered to be complex lignin polymer solutions, and a very extensive body of work exists on the melt rheology of commercially important linear and branched thermoplastic polymers.

In the remainder of this chapter, rheometry theory is discussed in section 5.2, and a brief background on the rheology of black liquors, and synthetic polymer melts, is provided in section 5.3. The experimental work is described in section 5.4, and results and discussion are presented in section 5.5. Finally, conclusions and recommendations for future work are presented in section 5.6.

5.2 Rheometry Theory

5.2.1 Viscometric Flows and Material Functions

Steady simple shear flow is important in applied rheology because it is easy to generate experimentally, and a number of industrial processes, particularly extrusion, approximate it. This flow can be visualized as the rectilinear motion of one flat plate relative to another, where both plates are parallel and the gap spacing between them remains constant. The shear stress tensor then has only three rheologically significant features: the magnitude of the shear stress, τ, and the first and second normal stress differences, N_1, and N_2, respectively [16].

Three material functions: the apparent viscosity, η, and the first and second normal stress coefficients, Ψ_1, and Ψ_2, respectively, can, in principle, be determined:

$$\eta \equiv \tau(\dot{\gamma})/\dot{\gamma} \tag{5-1}$$

$$\Psi_1 \equiv N_1(\dot{\gamma})/\dot{\gamma}^2 \tag{5-2}$$

$$\Psi_2 \equiv N_2(\dot{\gamma})/\dot{\gamma}^2 \tag{5-3}$$

For the special case of a Newtonian fluid, $N_1 = N_2 = 0$, and the shear stress is proportional to the shear rate:

$$\tau = \eta\dot{\gamma} \tag{5-4}$$

Rheometers are designed around 'approximately', or 'partially' viscometric flows, which simulate simple steady shear such that the deformation experienced by a given fluid element is indistinguishable from simple steady shear, in order to

determine one or more of the viscometric functions. One of the most common geometries used in rotational rheometers is a cone and plate, which is pictured in Figures 5-1(a), and (b), for steady shear, and dynamic oscillatory shear operation, respectively. This geometry is usually used to measure η and N_1 in steady shear, and linear viscoelastic properties in dynamic shear.

5.2.2 Steady Shear Operation

During steady shear operation of the cone and plate rheometer, the lower disk is rotated at a constant angular velocity Ω while the upper cone is held stationary. The equations of the cone, and the plate, are $\theta = \pi/2 - \alpha$, and $\theta = \pi/2$, respectively, as seen in Figure 5-1(a), where α is the cone angle (usually less than 0.1 radians (5.73°)). The torque, the total normal force exerted on the cone, and the angular velocity, are routinely measured and can be related to the shear stress, the first normal stress difference, and the shear rate, respectively.

The fundamental equations for this system can then be derived by solving the equations of continuity and motion in spherical coordinates subject to certain simplifying assumptions [16, 76]:

(1) steady-state laminar flow of an incompressible fluid,

(2) isothermal system (constant physical properties),

(3) negligible inertial effects (acceleration terms in the equation of motion can be neglected),

(4) no slip condition at the disk surface,

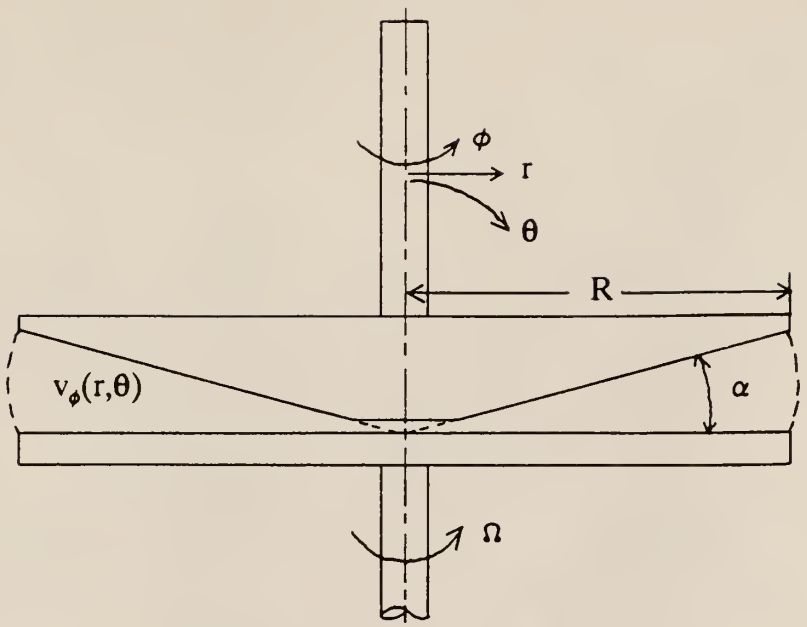

(a)

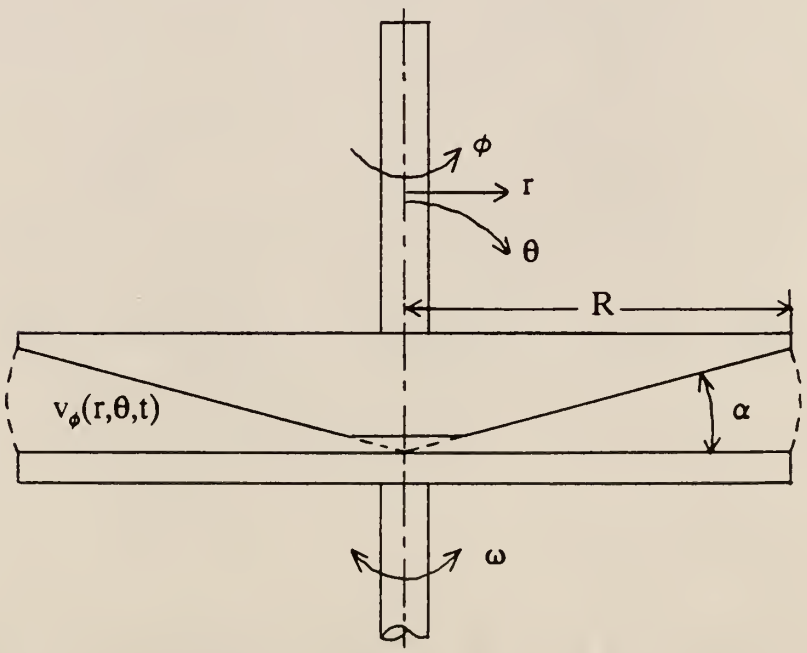

(b)

Figure 5-1. Cone and Plate Geometry. (a) Steady Shear Flow; and (b) Dynamic Oscillatory Shear Flow.

(5) small cone angle so that certain trigonometric identities apply,

(6) negligible surface tension effects at the exposed edge, and

(7) the free surface is spherical in shape with a radius of curvature equal to the cone radius, and the flow pattern is uniform out to this edge.

When the above assumptions are valid, $v_\phi(\theta)$ is the only nonzero velocity component, and the resulting shear rate is uniform throughout the gap:

$$\dot{\gamma} = -\dot{\gamma}_{\theta\phi} = \frac{\Omega}{\alpha} \tag{5-5}$$

The apparent viscosity at the set shear rate can be determined by measuring the torque exerted by the fluid on the cone and relating it to the shear stress by

$$T = \int_0^{2\pi} \int_0^R r^2 \tau_{\theta\phi} dr d\phi \tag{5-6}$$

Since $\tau_{\theta\phi} = \tau(\dot{\gamma})$ is a constant, (5-6) can be integrated directly, and combined with (5-5) to give

$$\eta(\dot{\gamma}) = \tau/\dot{\gamma} = \frac{3T\alpha}{2\pi R^3 \Omega} \tag{5-7}$$

The first normal stress difference can be determined directly by measuring the total normal force, F, exerted by the fluid on the cone (or plate), and relating it to the normal stress, $\tau_{\theta\theta}$ through

$$F = \int_0^R \int_0^{2\pi} \tau_{\theta\theta} r dr d\theta \tag{5-8}$$

With the assumptions in (5-8) that the free surface at r = R is at atmospheric pressure, and that interfacial effects are absent, integrating (5-8) then gives

$$N_1 = \frac{2F}{\pi R^2} \tag{5-9}$$

5.2.3 Dynamic Shear Operation and Linear Viscoelasticity

Dynamic shear operation of the cone and plate rheometer, utilizing small amplitude oscillatory motion of the plate, is commonly used to investigate the linear viscoelatic behavior of materials. In this mode, pictured in Figure 5-1(b), the plate is oscillated sinusoidally with angular frequency ω, and the torque required to maintain the stationary position of the cone is measured.

The input function is the applied strain, γ, which is given by

$$\gamma = \gamma_0 \sin(\omega t) \tag{5-10}$$

where γ_0 is the strain amplitude. The output torque response also varies sinusoidally with frequency ω, but, depending on the nature of the material, may or may not be in phase with the applied strain. If γ_0 is sufficiently small, i.e., if the Boltzmann superposition principle holds and the motion is linearly viscoelastic, the shear stress may be written as

$$\tau = \tau_0 \sin(\omega t + \delta) \tag{5-11}$$

where τ_0 is the shear stress amplitude, and δ is the phase shift relative to the strain.

Two important and equivalent material functions that are commonly used to describe linear viscoelastic behavior are the complex shear modulus, G^*, and the complex viscosity, η^*:

$$G^*(\omega) = \frac{\tau(t)}{\gamma(t)} = G'(\omega) + iG''(\omega) \tag{5-12}$$

$$\eta^*(\omega) = \frac{\tau(t)}{\dot{\gamma}(t)} = \eta'(\omega) - i\eta''(\omega) \tag{5-13}$$

which are related by

$$\eta^* = \eta' - i\eta'' = \frac{G^*}{i\omega} = \frac{G''}{\omega} - i\frac{G'}{\omega} \tag{5-14}$$

Both functions have been separated into real (in phase) and imaginary (out of phase) components [3].

The two components G′ and G″ are referred to as the storage modulus and the loss modulus, respectively. The storage modulus is related to the recoverable energy stored elastically in the material upon deformation, and the loss modulus represents the energy lost due to viscous dissipation within the material. In a similar manner, the dynamic viscosity, η', also represents the viscous dissipation of energy that occurs during flow, and η'' is related to energy stored elastically by the fluid upon deformation [90].

Experimentally, the displacement of the plate is proportional to the strain, and the torque is proportional to the stress. Therefore, the ratio of torque amplitude to displacement amplitude is equivalent to the ratio of stress amplitude to strain amplitude. The phase angle between the stress and the strain is related to the response of the fluid, and for the ideal cases of a purely elastic solid, the stress is in phase with the strain ($\delta = 0$), and for a purely viscous fluid, the stress is 90° out of

phase with the strain ($\delta = 90°$). Most materials, however, exhibit viscoelastic behavior, and for these, $0 < \delta < 90°$ [90].

The material functions can then be calculated for a given frequency with the help of certain trigonometric identities and the stress strain phasors from

$$G' = \frac{\tau_0}{\gamma_0}\cos\delta \tag{5-15}$$

$$G'' = \frac{\tau_0}{\gamma_0}\sin\delta \tag{5-16}$$

Finally, the magnitude of G^* is the amplitude ratio and is defined as the vector sum of G' and G'':

$$G^* = |G^*| = \frac{\tau_0}{\gamma_0} = [(G')^2 + (G'')^2]^{0.5} \tag{5-17}$$

The complex modulus thus provides an indication of the total energy required to deform a material.

Data from steady shear and oscillatory shear experiments on polymer solutions and melts can be compared at corresponding values of shear rate and frequency by means of the Cox-Merz approximation [14]:

$$\eta(\dot{\gamma}) = |\eta^*(\omega)|_{\omega=\dot{\gamma}} \tag{5-18}$$

This empirical relationship is very useful and works well for linear polymers.

5.3 Background and Literature Review

5.3.1 Black Liquor Rheology

The author is unaware of any rheology work on pure or plasticized lignins directly. However, there has been a modest amount of work on the rheological characterization of kraft black liquors, which have been treated as lignin polymer solutions. These are actually complex aqueous solutions containing lignins as the primary high MW polymer, hemicelluloses, sugars, organic acids, other low MW organics extracted from wood, and inorganic sodium salts from the pulping solution. The emphasis has been on studying black liquor shear viscosity as a function of temperature, solids content, and shear rate, which are important parameters in the concentration and processing of black liquors in pulp and paper mills.

Kraft black liquors behave as Newtonian fluids at up to 50% solids at temperatures over 40°C and over a range of shear rates. At higher solids levels, they generally exhibit shear thinning behavior, and the shear viscosity is strongly dependent on lignin concentration, lignin molecular weight, temperature, solids content, and shear rate. At high solids (>75%), black liquors can exhibit some viscoelastic behavior [27, 102].

5.3.2 Polymer Rheology

The rheological properties of polymer melts and solutions have been studied extensively for many years because they form the foundation for the entire range of

polymer processing operations, such as injection molding, blow molding, and extrusion. These materials have often been characterized by cone and plate, parallel plate, and capillary instruments.

Polymer melts and concentrated solutions can be qualitatively compared, and exhibit a wide range of steady shear and dynamic oscillatory shear behavior that is dependent on many factors, such as temperature, shear rate or frequency, MW and MWD, concentration, and structure (linear or branched). Direct quantitative comparisons among different studies are generally not very meaningful, because the results are often method dependent.

In steady shear experiments, amorphous polymers generally exhibit Newtonian behavior at very low shear rates, where the apparent viscosity approaches the zero shear rate viscosity, η_o, and shear thinning behavior at higher shear rates. For polymers with significant long chain branching, and at high concentrations, η_o is usually greater than for linear polymers, but the opposite is usually true for polymers with short chain branching and at low concentrations. First normal stress differences are monotonically increasing functions of $\dot{\gamma}$, are usually nearly linear with a slight downward curvature, and gradually level off at higher shear rates. This behavior has been observed for linear, and four-arm and six-arm star branched polyisoprenes by Graessley et al. [38] using cone and plate rheometry, and has also been noted by Tanner [95].

In dynamic experiments, amorphous polymers can display pronounced viscoelastic properties. Complex viscosities are constant at very low ω, and at higher

ω, log η^* versus log ω is almost linear, in an analogous manner to η_{app} versus $\dot{\gamma}$. The two dynamic moduli: G′ and G″, increase monotonically with increasing ω, and level off at higher ω in a similar manner to N_1 versus $\dot{\gamma}$. This general behavior has been noted by Tanner [95], and observed by Noordermeer et al. [67] for branched polystyrenes with star and comb structures, and by Small [90] for unfilled and filled polystyrenes, which also followed the Cox-Merz approximation over a range of $\dot{\gamma}$ and ω.

5.4 Experimental Work

5.4.1 Sample Preparation

This work was only an exploratory study, and therefore, only one sample: Indulin AT + 28 weight % NMP, was prepared for rheological testing. Indulin AT was chosen because it had a relatively high MW ($\bar{M}_w$ = 49,380 from LALLS), and sufficient quantity was on hand to prepare a large batch. For the plasticizing solvent, NMP was chosen because it had the highest boiling point, and produced the greatest T_g depression as discussed in chapter 4. These solvent characteristics should allow rheological testing at temperatures sufficiently above the T_g of the mixture, but still low relative to the solvent boiling point, so that a large enough operating window will exist in which to run the experiments before solvent evaporation becomes significant.

The Indulin AT + NMP sample was prepared by mixing the two components in a Bramley beken blade mixer (Bramley, Pottstown, PA) which consists of a 475 ml electrically heated chamber with twin blades counterrotating at 30 rpm. Indulin

AT was used as received from Westvaco, without further purification, except that it was first vacuum dried for 12 hours at 50-60°C and then kept desiccated. The dried lignin (146.2 g), and then NMP (41.27 g), were loaded into the mixing chamber and distributed by manually turning the blades. The mixer was then run for 15 min (after a 25 min heat up time) at 80°C with a continuous nitrogen purge of the chamber. As the mixing progressed, the sample became a viscoelastic mass similar to a molten polymer. The mixer was then stopped, and the plasticized lignin scraped off the walls and blades and collected. The net amount recovered was 176.1 g (93.9% yield), and the nominal solvent concentration was 28.2% (mass solvent/mass lignin).

A plaque of this plasticized lignin was prepared by compression molding in a Pasadena Hydraulics model SPW225C press (Pasadena Hydraulics, Inc., El Monte, CA) which has electrically heated and water cooled platens. Some ground up sample (26 g) was spread out in a flat 7" x 8" mold which consisted of two stainless steel plates covered with Teflon sheet (to prevent sample adhesion), and aluminum spacers on the corners to adjust the thickness. This mold was placed into the press, and the two preheated platens were brought together until they just contacted the mold (~0 force). The temperature was maintained at 80°C, and the sample was allowed to thermally equilibrate for 20 min. The sample was then compressed to 4,000 lbs force, held for 3 min, released momentarily to allow any entrapped gases to escape, and then compressed again to 4,000 lbs force, held for 5 min, and then cooled to room temperature with the pressure relieved. The sample plaque (~12 cm in diameter and 1.5 mm thick) was then removed and stored in a desiccator.

Compression forces for this sample were low compared to previous trials (up to 30,000 lbs force), because the sample was spread out too much in the mold, but the sample appeared uniform nevertheless.

5.4.2 Rheometer

The rheological testing and data collection were performed on a Rheometrics RMS-800 mechanical spectrometer (Rheometrics, Inc., Piscataway, NJ). This instrument is capable of both steady shear and dynamic oscillatory shear operation over a wide range of shear rates and with a controlled sample environment over a temperature range of -150°C (with liquid nitrogen cooling) to 350°C. Four measurement geometries were available: 25 and 50 mm diameter parallel plates, and truncated cones and plates with 5.7°, and 1.2° cone angles, respectively.

The general operating principle of the rheometer is that the command motion of the lower disk, by means of a servo motor, is transmitted through the sample to the upper parallel disk or cone, which is connected to a force rebalance transducer (FRT). The FRT then measures the torque required to maintain the position of the transducer shaft, and the normal force required to maintain a constant disk separation. For a more detailed description of the instrument, its capabilities, and operating instructions, the reader is referred to the owner's manual [77].

Sample temperature in the RMS-800 was maintained through the use of a forced gas convection oven, with PID control, which was split into two halves that closed around the sample like a clamshell. Heat was supplied via an electric gun

heater inserted into the oven chamber, and the oven temperature, and the sample temperature (i.e. lower tool temperature), were measured with type J thermocouples. A PRT sensor, also located in the chamber, provided the temperature monitoring required for control. In order to slow down solvent evaporation from the samples, resulting from the forced convection heating, the clamshell oven was modified by adding two small custom made semicircular stainless steel trays. These were packed with cotton balls which were then soaked with NMP and placed into the oven (one in each half) for the duration of a run to serve as a crude humidifier.

5.4.3 Testing Procedures

Rheological properties of the NMP plasticized Indulin AT were measured at 80 and 100 °C, which is sufficiently above the glass transition region for this sample. Test samples approximating the size of the tooling were cut from the plaque and heated in a natural convection oven at 105 °C for at least 30 min until they softened. During this time, the tooling was preheated to 20 °C above the desired run temperature, and the gap was zeroed at the run temperature to account for thermal expansion of the stainless steel tooling.

The preheated sample was quickly loaded onto the lower plate, and the upper cone, or plate, was lowered until contact occurred. The humidifiers, soaked with NMP, were placed in each oven half, the oven was then closed, and heating was resumed. The sample was gradually compressed during heatup until, at the desired run temperature, the proper gap was reached: 0.05 mm minimum for cone and plate,

and 1.0 mm for parallel disks. The oven was then opened, excess sample that was squeezed from the gap was removed, and NMP was lightly dabbed on to the exposed sample edge with a cotton tipped applicator to minimize drying. Finally, the oven was resealed, and reheating was initiated. The samples were then allowed to equilibrate at the run temperature for 5 min before the rheological tests were initiated.

Experimental runs usually consisted of five different tests: (1) a dynamic rate sweep--first set of check data, (2) a dynamic strain sweep to check for the linear viscoelastic region, (3) a dynamic rate sweep--oscillatory shear flow data and second set of check data, (4) a steady rate sweep--steady shear flow data, and (5) a dynamic rate sweep--third set of check data. Torque values in the check data were used to monitor time related changes (e.g. drying) in the sample while in the rheometer.

Dynamic rate sweeps were run over a frequency range of 0.1-100 rad/sec with 5% strain for 80°C, and 1-1,000 rad/sec with 10% strain for 100°C operating temperatures. These strains were in the linear viscoelastic region. Steady rate sweeps were run over a shear rate range of 0.01-1 sec^{-1} at 80°C, and 0.1-10 sec^{-1} at 100°C. Torque values for these sweeps covered the full accurate measuring range of the FRT, and tests were often stopped prematurely because torque readings overloaded the transducer. The total run times for each experiment were 30-35 min, and the total sample heating times were 50-55 min. Finally, standard calibration procedures for torque, normal force, and torque phase were routinely performed on this instrument according to the operating instructions [77].

5.5 Results and Discussion

5.5.1 General Observations

The steady shear and the dynamic oscillatory shear tests on the NMP plasticized Indulin AT sample were performed with all four sets of tooling, i.e., the 25 mm and 50 mm parallel plates, and cones and plates. Unfortunately, the steady shear data, and to a lesser extent, the dynamic shear data, were generally very poor and inconsistent for both 50 mm geometries. This was due to the difficulty in properly loading a sample into the 50 mm tooling and compressing it so that it completely filled the gap, and so that the appropriate gap setting was reached in a timely manner without overloading the FRT. At 80°C, which is just above the end of the sample's glass transition region, this problem was especially acute because the material's compliance approximated that of the FRT's, and it became exceedingly difficult to compress the sample. Extensive heating was often required, but this resulted in premature drying of the sample.

Control of the sample temperature was adequate, but maintaining a constant solvent concentration in the samples, for the duration of the runs, was a persistent problem. The high heat transfer rates from the forced air convection oven promoted rapid drying of the sample, especially at the edge, and the steps taken to minimize this--dabbing NMP on the sample's edge, and placing a crude humidifier in the oven, as described in section 5.4.2--provided only marginal control and a relatively short time window for analysis. Torque profiles from dynamic rate sweeps were monitored

for each sample to insure that solvent evaporation was not significantly affecting the results, but a much more effective temperature and humidity control system is needed before extensive measurements can be undertaken.

The 25 mm parallel plates and cone and plate were much easier to use, and produced very consistent data for dynamic shear experiments, but the cone and plate tooling gave better steady shear results. The cone and plate geometry also directly gives N_1. Therefore, only results from cone and plate rheometry are reported and discussed here.

Upon pulling the tooling elements apart, substantial fiber formation was observed for tests run at 100°C, but only small amounts of fibers were formed for runs at 80°C. This, by itself, is an encouraging sign that the spinning of lignin fibers is feasible at 100°C.

5.5.2 Steady Shear Behavior

Steady shear apparent viscosities and first normal stress differences are presented in Figure 5-2 for both 80 and 100°C run conditions. Although not very consistent, the η_{app} values decrease with increasing $\dot{\gamma}$ and have a strong temperature dependence, as seen by the approximately 1.5 order of magnitude drop in η_{app} for a 20°C increase in temperature. The N_1 values increase with increasing $\dot{\gamma}$, but again, the curves are not smooth. These trends in the η_{app} and N_1 data follow the behavior exhibited by polymer melts and solutions, but since lignins are highly branched, the

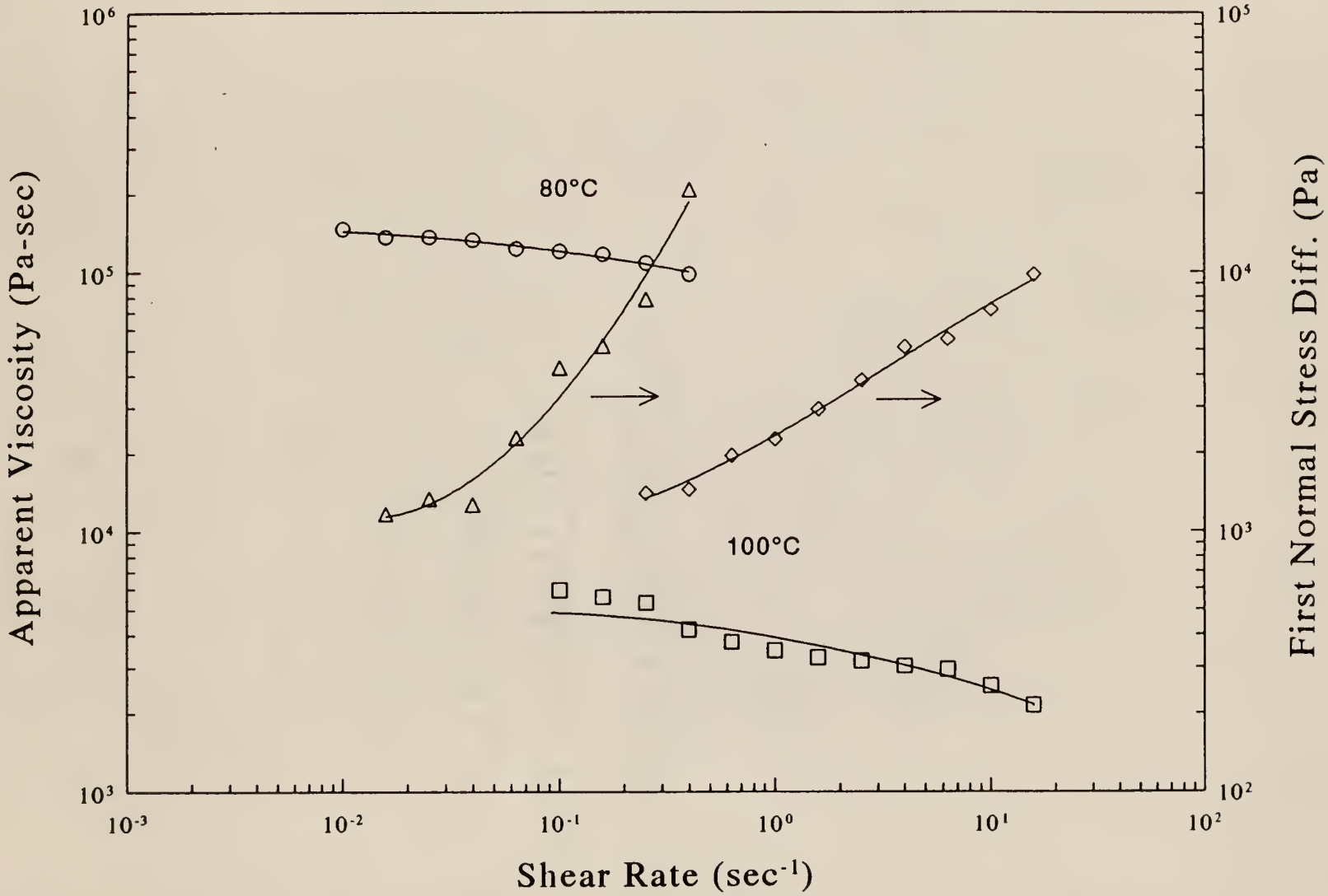

Figure 5-2. Steady Shear Rheometry of Indulin AT + 28% NMP at 80 and 100°C.

decrease in viscosity over a two decade range of $\dot{\gamma}$, is probably less than that for common linear polymers tested under comparable conditions.

The roughness in the curves can be attributed to some nonideal effects, such as edge fracture and breakup, which were a problem at higher shear rates. The steady shear tests were run in both clockwise and counterclockwise directions for each measurement to minimize balling of the material, where some amount of material was literally squeezed out from between the cone and the plate at higher rotational rates.

5.5.3 Dynamic Shear Rheometry

Oscillatory shear experiments were also performed and these were much easier to run because the runs were shorter, and there was no visible sample disruption. Dynamic shear strain sweeps were run to determine that the deformations were within the sample's linear viscoelastic range, and examples of these, for both 80 and 100°C run conditions, are presented in Figure 5-3. These strain sweeps exhibit an extensive linear viscoelastic region, which is somewhat surprising because lignins are highly branched molecules.

Results for the complex viscosity and the storage modulus, as functions of frequency, are presented in Figure 5-4. Both η^* curves decrease smoothly with increasing ω, and exhibit a strong temperature dependence, as seen by the greater than 1.5 order of magnitude drop in η^* with a 20°C increase in temperature. Also, the storage modulus increases smoothly with increasing ω, which indicates some

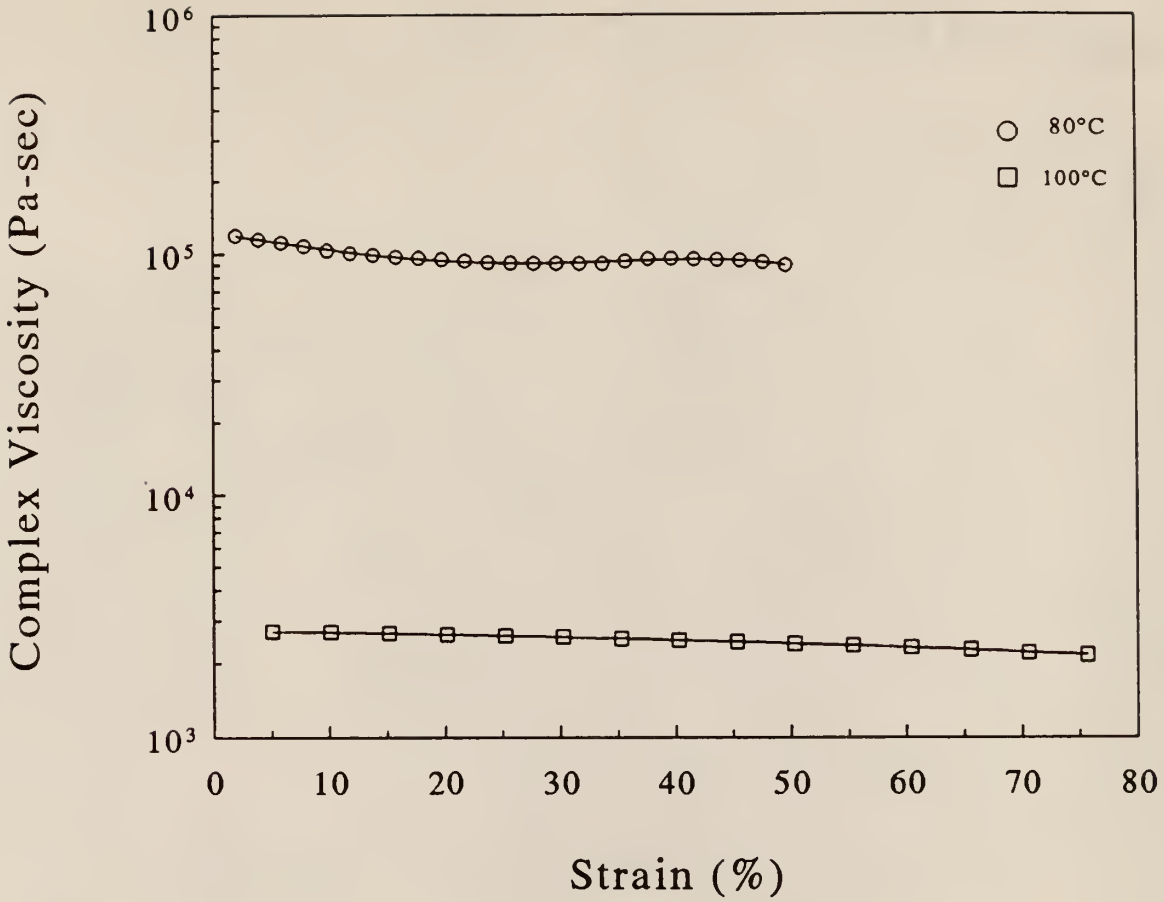

Figure 5-3. Dynamic Oscillatory Shear Strain Sweeps of Indulin AT + 28% NMP. Frequencies were 1.0 rad/sec at 80°C, and 10 rad/sec at 100°C.

degree of viscoelastic behavior. Both η^* and G' follow the same trends in behavior as is seen for polymer melts and solutions, except that η^* for the plasticized Indulin AT probably decreases less than for polymer melts, over a greater than two decade range of frequency, because the lignin is highly branched.

Two correlations that are often observed for polymers, especially linear ones, is the Cox-Merz approximation [14], and the observation that the ratio of N_1 to G', at corresponding values, and low values, for $\dot{\gamma}$, and ω, respectively, is equal to two

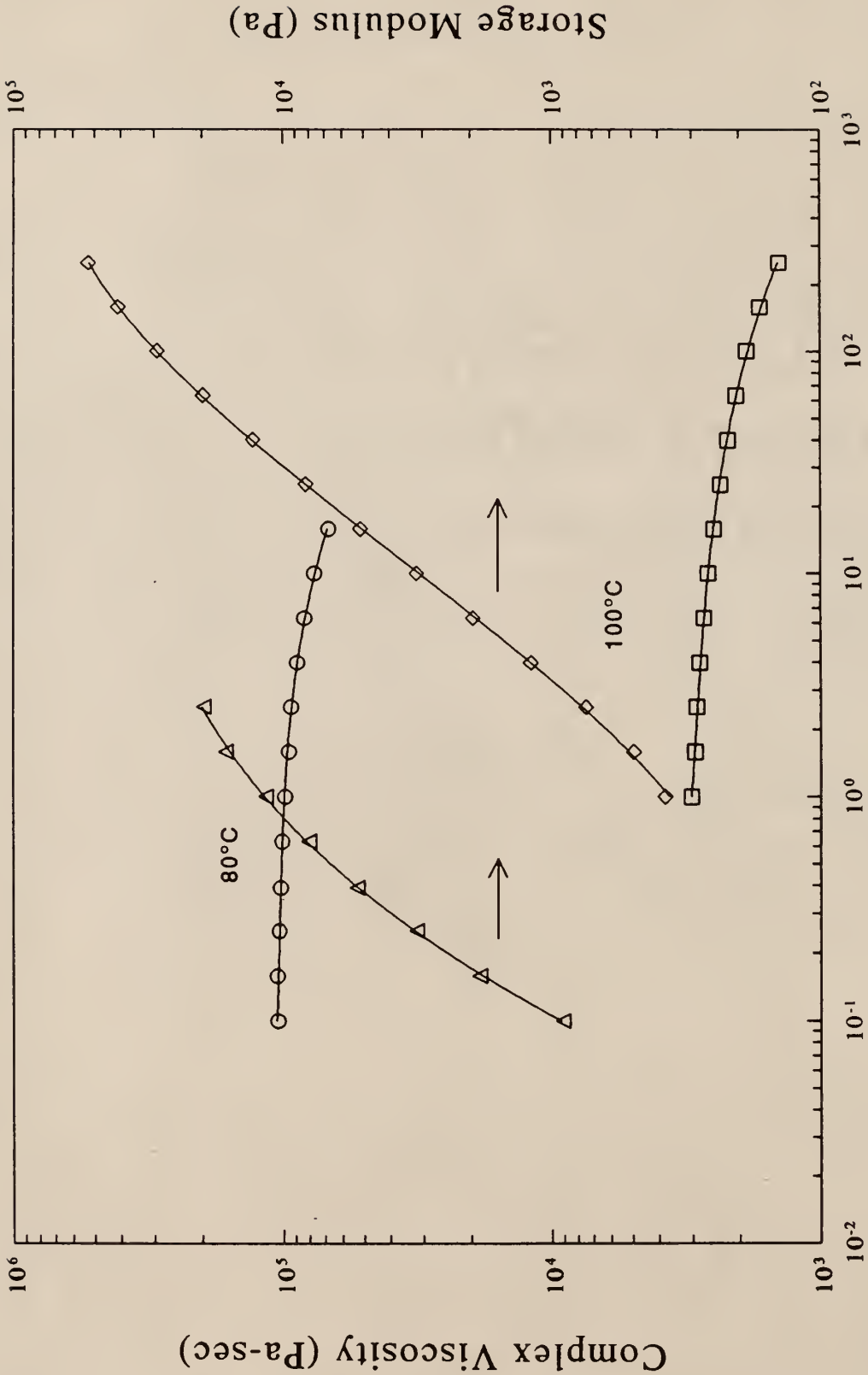

Figure 5-4. Dynamic Oscillatory Shear Rheometry of Indulin AT + 28% NMP at 80 and 100°C.

[23]. A comparison of Figures 5-2 and 5-4 demonstrates a relatively poor overlap for the η_{app} and η^* curves, which is probably due to the inconsistent steady shear viscosity data, and the extensive branching in lignin. The Cox-Merz approximation does not appear to hold in this case.

For the plasticized Indulin AT samples, N_1/G' differs significantly from two at both 80 and 100°C, as seen in Figure 5-5. This poor correlation is probably due to the inconsistent N_1 data from the steady shear measurements, which are shown in Figure 5-2, and this necessarily has a dramatic effect on the values of N_1/G'.

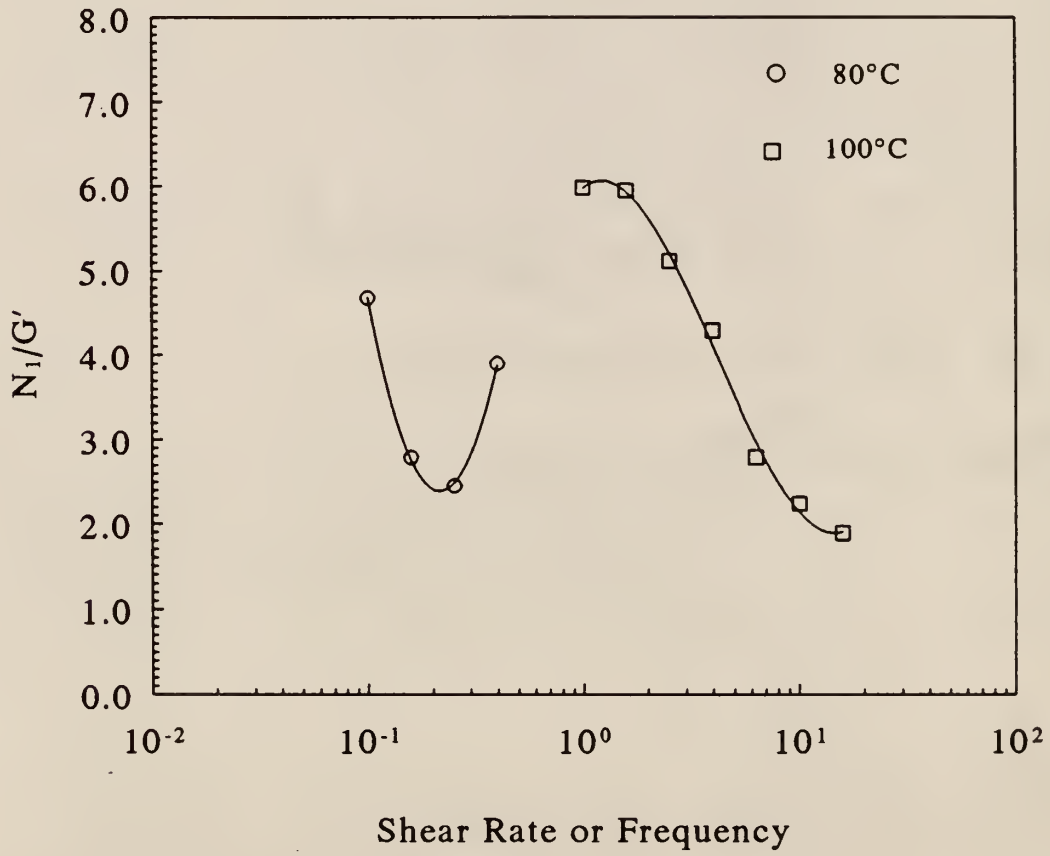

Figure 5-5. A Comparison of First Normal Stress Differences and Storage Moduli, from Steady Shear and Dynamic Shear Rheometry, Respectively.

5.6 Conclusions and Recommendations

5.6.1 Conclusions

The rheological testing of the Indulin AT + 28% NMP sample was exploratory in nature, and only a limited analysis of its behavior was performed. Some of the considerable experimental problems that exist in this type of work have been identified, and the following conclusions were reached:

1. Indulin AT lignin plasticized with NMP exhibited shear thinning behavior, and some degree of viscoelasticity. Both η_{app} and η^* decreased with increasing $\dot{\gamma}$ or ω, and N_1 and G' both increased with increasing $\dot{\gamma}$ or ω. These trends are the same as for synthetic polymer melts and solutions.
2. Solvent evaporation during the rheological testing, resulting in sample drying, was a persistent problem and needs to be minimized.
3. Indulin AT + 28% NMP is capable of forming fibers at 100°C.

5.6.2 Recommendations for Future Work

The numerous experimental problems encountered in this work must first be overcome before any meaningful and consistent rheological data for solvent plasticized lignins can be obtained. Recommendations to improve these experimental procedures, and expand the scope of this work, are discussed below:

1. A more effective apparatus for sample heating and humidity control needs to be developed. The pervasive problem of sample drying must be minimized in order to obtain consistent rheological data. One possibility is to fabricate a circulating hot oil bath similar to the low temperature water bath that was supplied with the RMS-800.

2. If sample drying can be minimized, several solvent concentrations and a wider temperature range should be investigated. Because of the strong temperature dependence of η_{app}, η^*, N_1, G', G'', and other parameters; several more closely spaced analysis temperatures, such as 80, 90, 100, 110, and 120°C, should be investigated. This data can then be shifted by time-temperature superposition to develop master curves for a set of lignins.

3. A plasticized organosolv lignin, and several other plasticized kraft lignins, covering a range of MW s, should be investigated, because of the strong dependence of rheological properties on MW.

4. Based on the observed fiber formation for this sample, lignin fiber spinning experiments should be pursued at 100°C (as a starting point) for this Indulin AT/NMP composition.

CHAPTER 6
LIGNIN FIBER SPINNING AND CARBONIZATION

6.1 Introduction

Lignin-based carbon fibers have been investigated primarily by the Japanese in the 1960's and 1970's, but are currently not commercially important. Background information on production processes, lignin MW s, and rheological properties, is limited and confined mainly to the patent literature. The lignins used have generally been impure, poorly characterized, and resulted in fibers with limited properties.

In the next section, lignin-based carbon fiber production processes are reviewed in rough chronological order. The experimental spinning and carbonization work is described in section 6.3, and results and discussion are presented in section 6.4. Finally, conclusions and recommendations are given in section 6.5.

6.2 Background and Literature Review

6.2.1 Early Japanese Development Work

Lignin-based carbon fibers were first developed by Otani in Japan in 1964*. The Nippon Chemical Co. commercialized this fiber in 1968 for gasket applications

* Otani, S., Personal Communication (21 Sept. 1990).

and was assigned patents for the production process in France [69], and in the United States [72]. Commercial production of this fiber at Nippon Chemical Co. was small: a pilot plant was producing only several tons per year in 1970 [65].

Nippon Chemical's process could use alkali-lignin, thiolignin, or lignin sulfonate as raw materials, and the lignin fiber used could be in the form of a continuous monofilament, short-length or staple fiber, yarn or woven webs, or any other suitable fiber form. Conventional spinning methods such as melt spinning, dry spinning, and wet spinning could be used [72, 88].

In the melt spinning method, originally developed by Otani, alkali-lignin or thiolignin is charged into a melting apparatus and rapidly heated to a temperature of 150-200°C. To prevent oxidation during melting, the melt surface is blanketed with an inert gas such as nitrogen or carbon dioxide. Filaments are spun by continuously extruding the melt from a small nozzle, and short length fibers can be produced by passing the molten lignin through a blower of air or inert gas, or by dropping the melt on to a turning disk [72].

In the dry spinning method, which was commercialized, the lignin raw material is dissolved in an appropriate solvent, e.g., aqueous caustic soda, extruded from a small nozzle, and then dried at a suitable temperature to obtain lignin fiber. High molecular weight polymers such as poly vinylalcohol (PVA) are added to the lignin solution to act as a binder and result in stronger fibers [72].

In the wet spinning method, the lignin is dissolved in a suitable solvent, with an appropriate amount of viscose, spun into a nonsolvent, and dried to produce lignin

fiber. When carbonized, this lignin fiber yields a carbon fiber having a practical strength [72].

The carbonization process, following dry spinning, involves pretreating the lignin fiber in an oxidizing atmosphere, such as air or ozone at 50-400°C, or in a closed vessel at 100-400°C, and then heat treating it under inert gas by ramping up the temperature at less than 50°C per minute. A flame resistant fiber is produced at about 400°C which becomes carbon fiber at temperatures above 700°C. This carbon fiber becomes graphite fiber when subjected to a graphitizing treatment at temperatures in excess of 2,000°C [72].

If no high MW polymers are added to the lignin solution, pretreatment in air or ozone followed by carbonization in an inert gas results in a stronger carbonized fiber. If high MW polymers are added, a stronger carbonized fiber is produced through pretreatment in a closed vessel followed by carbonization under inert gas. Direct activation by activating gases (e.g. air, oxygen, steam), without pretreatment, yields the stronger activated carbonized fiber [72].

Nippon Chemical Co. withdrew from this market in 1973 when it sold the production facilities and the license to the manufacturing technology to a gasket manufacturer. Shortly thereafter, the oil crisis of 1973, and the resulting worldwide recession, forced the project to be abandoned*. Tomizuka** and Johnson***,

---

* Otani, S., Personal Communication (21 Sept. 1990).

** Tomizuka, I., Personal Communication (18 Sept. 1990).

*** Johnson, D.J., Personal Communication (11 July 1990).

however, claim that production of lignin-based carbon fibers was terminated because of poor mechanical properties resulting from impurities in the lignin raw material. This carbon fiber, however, exhibited similar mechanical properties to the general purpose carbon fiber presently used in gaskets, thermal insulators, electrode material for fuel cells, and other applications not requiring high mechanical properties*.

6.2.2 West German Process

A similar production process for lignin-based carbon fibers was developed by Mannsmann et al. [60, 61, 88]. In this process, aqueous solutions of lignin, or lignin salt derivatives such as lignin sulfonate, at a pH of 0 to 6, are dry spun or wet spun. The lignin solutions require the addition of 0.001 to 10 wt. % of at least one fiberforming linear high molecular weight polymer, such as PEO, with a degree of polymerization greater than 2,000, to act as a binder and promote spinnability. This process is claimed to be very versatile and applicable to many other carbon containing starting materials which alone do not form fibers [61].

The spun filaments are taken up on a rotating drum, and the spinning cake is removed from the drum and heated in air from 100°C to 250°C for one hour. The lignin fibers are then dried and mechanically stabilized by heat treatment between 80°C and 400°C. This heat treatment involves ramping up the temperature at 40°C per hour to 400°C in a stream of nitrogen and then carbonizing the fibers by heating them to 1,000°C at a rate of 150°C per hour. Flexible carbon fibers are

---

* Otani, S., Personal Communication (21 Sept. 1990).

obtained with a carbon yield of 36%. In addition, the fibers can be subjected to a graphitization treatment by heating for 2 hours to 2,600°C under an argon atmosphere [61, 88].

6.2.3 Carbon Fibers from Black Liquor

Lockhart and Bortz [58] produced carbon fibers from solutions of concentrated black liquor with appropriate additives such as resins, stabilizers, and plasticizers. Two resins which have been successfully incorporated are PEO and PVA. Poly ethylene oxide at 0.3 wt.% was added to non-fibering liquor containing 60% lignin solids to produce a dope suitable for dry spinning highly extensible fibers.

In the dry spinning process, the spinning dope is pumped from a reservoir into a spinning head to which several spinnerettes are attached. These spinnerettes are metal cups with many fine holes in the bottom through which the liquid is extruded. System pressures of several hundred psi in conjunction with a closely regulated chamber temperature control the liquid flow rate and viscosity. Freshly spun filaments pass downward through a rising current of heated air in a drying tower and are then turned around a drum at the base of the tower and stretched to several times their extruded length to reduce the diameter for improved handling and faster drying. The dried filaments are then wound up on a take up drum in the form of a tow (parallel strands) or twisted into yarn [58].

Lignin fibers do not require special pretreatment because they do not soften during heating and are nominally non-graphitizing. Heating them in an inert

atmosphere to a temperature of 1,000°C will produce a fiber which is completely carbon. Carbonization times as short as 30 minutes may be used without damaging the filament structure, and a carbonization yield of 50% is obtained which is second only to the 90% carbonization yield of pitch-based carbon fibers [58].

6.2.4 Fiber Microstructure

Lignin-based carbon fibers have relatively poor mechanical properties as compared to PAN- or pitch-based fibers which may be due to the presence of numerous microstructural defects in the fibers. Johnson and his colleagues [49, 50, 96] examined two types of fibers obtained from Nippon Chemical Co. which were dry spun from lignin and PVA as plasticizer and carbonized at 1,500°C and 2,000°C, respectively. Tensile strengths and moduli for these fibers were 0.25 and 27 GPa for the 1,500°C carbonized fiber, and 0.29 and 24 GPa for the 2,000°C carbonized fiber, respectively [49].

The microstructure of these fibers was studied by small angle and high angle X-ray scattering and high resolution electron microscopy. Fibers which had been carbonized at 1,500°C had poorly developed fibrillar structures and display a heterogeneous fine structure with many different continuous and discontinuous inclusions of a highly graphitized nature. This heterogeneity was considered to be more pronounced than in other carbon fibers because of the presence of impurities which caused catalytic graphitization [50]. The relatively low values of modulus and

strength were attributed to a lack of both orientation and interlinking between crystallized layer planes [49].

For the fibers carbonized at 2,000°C, the heterogeneous microstructure exhibited a wider range of crystallite size, pore size, and lattice order than is found in most PAN-based carbon fibers heat treated above 2,000°C [49]. These lignin-based fibers also had a much more complex distribution of microvoids than is seen in the equivalent pitch-based fibers [96]. A large number of well graphitized ring-like structures found in these lignin-based fibers may be the result of catalytic graphitization by impurities such as sodium which are known to be present in the precursor [49].

6.2.5 Recent Development Work

Lignin-based carbon fibers have recently been produced by several melt spinning processes developed by Sudo and Shimizu which do not require the addition of synthetic polymers as plasticizers and spinning aids [91, 92, 93]. Two of these processes are very similar and use lignin precursor fibers obtained from steam exploded and methanol extracted birch lignin. This lignin was modified by alkaline hydrogenolysis to make it thermally meltable, and then heat treated at 300-350°C for 30 min to remove volatile and thermally labile compounds which interfere with successful continuous spinning in the molten state. The molecular weight of this modified lignin was low: $\bar{M}_w$ = 950 as determined by SEC using THF on a PS gel with PS calibration [93].

These modified lignin fibers were melt spun at over 100 m/min from a 0.3 mm diameter pinhole on to a 10 cm diameter bobbin, and then carbonized under nitrogen at 5 °C/min from room temperature to 1,000 °C and held there for 20 min [91, 93]. The physical properties of the final fibers classify them as 'general purpose' grade fibers with a diameter of 7.6 ± 2.7 μm, an elongation of 1.63 ± 0.29%, a tensile strength of 660 ± 230 MPa, and a modulus of 40.7 ± 6.3 GPa [93].

Sudo and Shimizu [92] also produced carbon fibers from lignin-phenol reaction products which were prepared by treating lignin with phenol in the presence of 2% p-toluenesulfonic acid for 4 hours at 180 °C under nonoxidizing gas. This material was then melt spun at up to 300 m/min, heat treated at 200 °C, and carbonized at 1,000 °C to yield carbon fibers with a tensile strength of 518 ± 114 MPa, an elongation of 1.06 ± 0.18%, and a modulus of 48.9 ± 6.2 GPa [92].

Finally, Ito and Shigemoto [45] prepared lignin precursor fibers from lignins obtained by digesting wood in a tricresol solution for 3 hours at 185 °C. This lignin was then melt spun at 190 °C, wound at 100 m/min, heated from room temperature to 200 °C at 3 °C/min, and heat treated for 1 hour to give fibers with a tensile strength of 30.4 MPa, an elongation of 1.2%, and a modulus of 2.63 GPa [45].

6.3 Experimental Work

6.3.1 Lignin Fiber Spinning

The experimental set up for fiber spinning is pictured in Figure 6-1 and consists of an Instron capillary rheometer model 3211 (Instron Corp., Canton, MA)

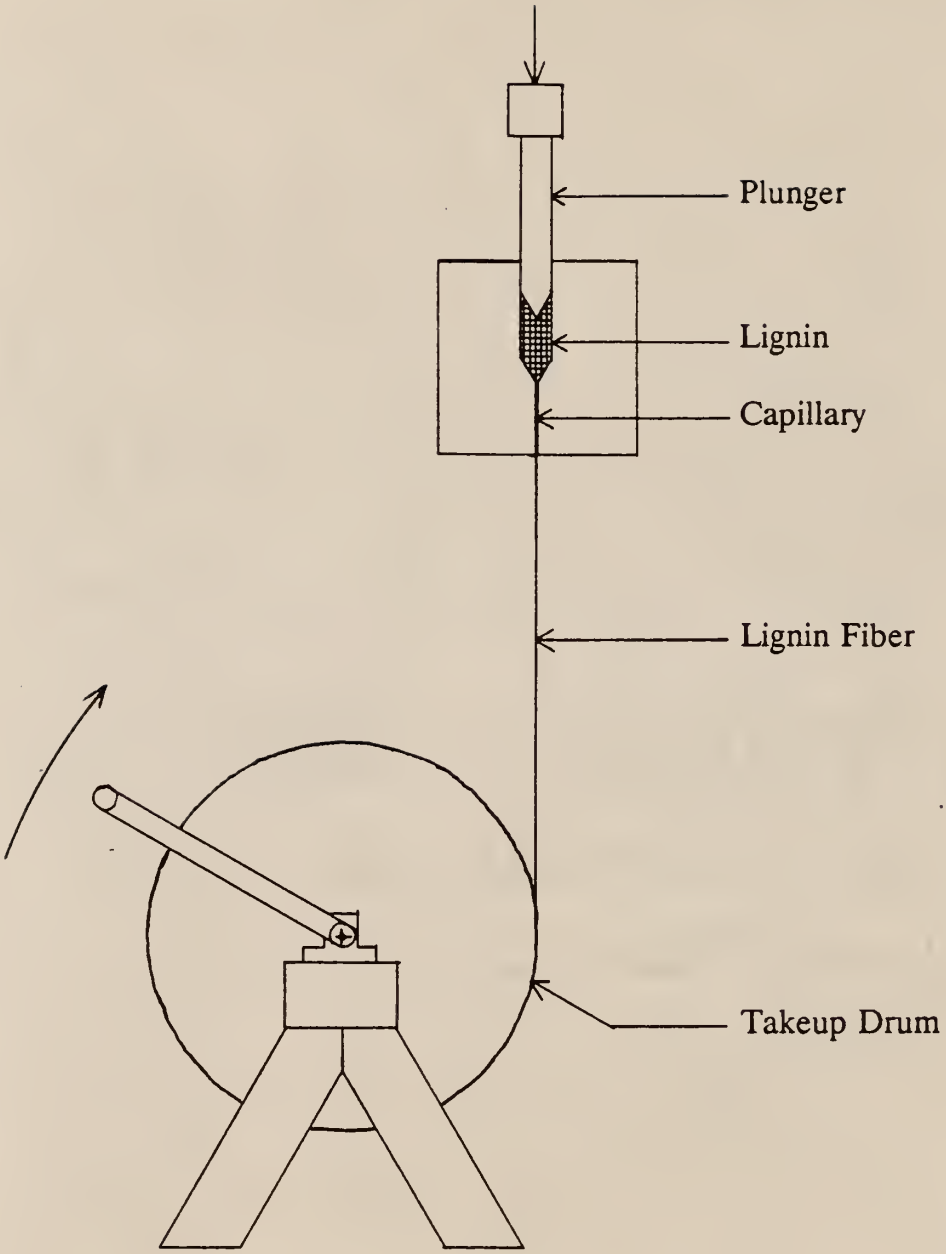

Figure 6-1. Lignin Fiber Spinning Apparatus.

and a manually operated take up drum designed and built by the author. Single fibers were extruded from a capillary die with an internal diameter of 0.5105 mm, and a length of 67.81 mm, and wound up on the take up drum, which has an approximate diameter of 47.5 cm and a circumference of 149.2 cm.

Due to the exploratory nature of this work, only one plasticized lignin sample was investigated for fiber spinning: Indulin AT + 28% NMP. This composition had already been characterized rheologically, as described in chapter 5, and sufficient quantity had already been prepared. Indulin AT was also one of the highest MW lignins available.

Approximately 10-15 g of coarsely ground up Indulin AT/NMP sample were loaded into the barrel for each run. During heat up to the test temperature, the sample was compacted several times to allow entrapped air and water vapor to escape. The plunger was then lowered into the barrel and driven down to extrude a fiber. A range of spinning conditions were investigated and are listed in Table 6-1. Because of the significantly lower viscosities at the higher temperatures, higher extrusion and take up speeds were required to maintain fiber integrity.

6.3.2 Fiber Carbonization

To help establish carbonization conditions for these fibers, samples produced under several different spinning conditions were subjected to thermogravimetric analysis (TGA) in order to determine their weight loss versus temperature profiles. All of the scans were run in a nitrogen atmosphere to prevent sample oxidation.

Table 6-1. Lignin Fiber Spinning Conditions.

Temp. (°C)	Plunger Speed[a] (in/min)	Fiber Extrusion Speed[b] (in/min)	Take-up Speed[c] (in/min)
100	0.02	6.96	~59-118
120	0.0667	23.22	~470
	0.2	69.61	~588; 1,470
	0.3	104.4	2,230
130	0.3	104.4	1,530; 2,290
	1.0	348.1	4,050

Notes: [a] Speed settings on Instron capillary rheometer.
[b] Calculated from barrel/capillary cross sectional area = 348.1.
[c] Calculated from takeup drum rpm.

Fibers spun at 130°C and 348.1 in/min were expected to have the best and most uniform properties because they were wound up at the highest and most consistent takeup speed. These were then selected, cut into 10-15 cm lengths, and carbonized under the conditions described in Table 6-2. The carbonization was carried out by Bill Toreki, in the Department of Materials Science and Engineering at the University of Florida, in a Lindberg model 54233 tube furnace (Watertown, WI) controlled by an Omega temperature controller (Omega Engineering, Inc., Stamford, CT) and with a continuous argon purge.

6.3.3 Fiber Analysis

Mechanical properties of the carbonized fibers--ultimate tensile strength, elongation at break, and modulus of elasticity, were measured by running tensile tests on a MTS 880.14 automated test system (MTS Systems Corp., Minneapolis, MN)

Table 6-2. Lignin Fiber Carbonization Conditions.

Run	Temperature Profile
A	90-800°C @ 5°C/min; isothermal hold for 60 min; Cool
B	90-250°C @ 10°C/min; isothermal hold for 15 min; 250-1,000°C @ 5°C/min; isothermal hold for 60 min; Cool

with a thin beam deflection type load cell (Omega Engineering, Inc., Stamford, CT) having a full scale load of 113 g. These tensile tests were performed in Professor Beatty's laboratory, in the Department of Materials Science and Engineering, with the assistance of David Bennett and using his techniques. The fibers were mounted on to specially designed paper tension forms with Superglue, and these were then attached to the load cell, and the lower clamp of the tensile tester, as shown in Figure 6-2. These tension forms fixed the fiber test length at 15 mm, and supported them to facilitate handling and testing. These carbonized fibers were very brittle and easily broken during mounting and handling, before any measurements were actually made.

Tensile tests were run at a strain rate of 0.020 min^{-1} (2.0%/min), and tensile load versus stroke length data were automatically acquired by a personal computer. To account for expected variations in the values, at least five fibers were tested from each set ("A", and "B"). An estimate of the beam deflection was made by hanging a full scale load of 114.28 g from the load cell and measuring the actual deflection of the beam. Unfortunately, this was only a very approximate determination. The

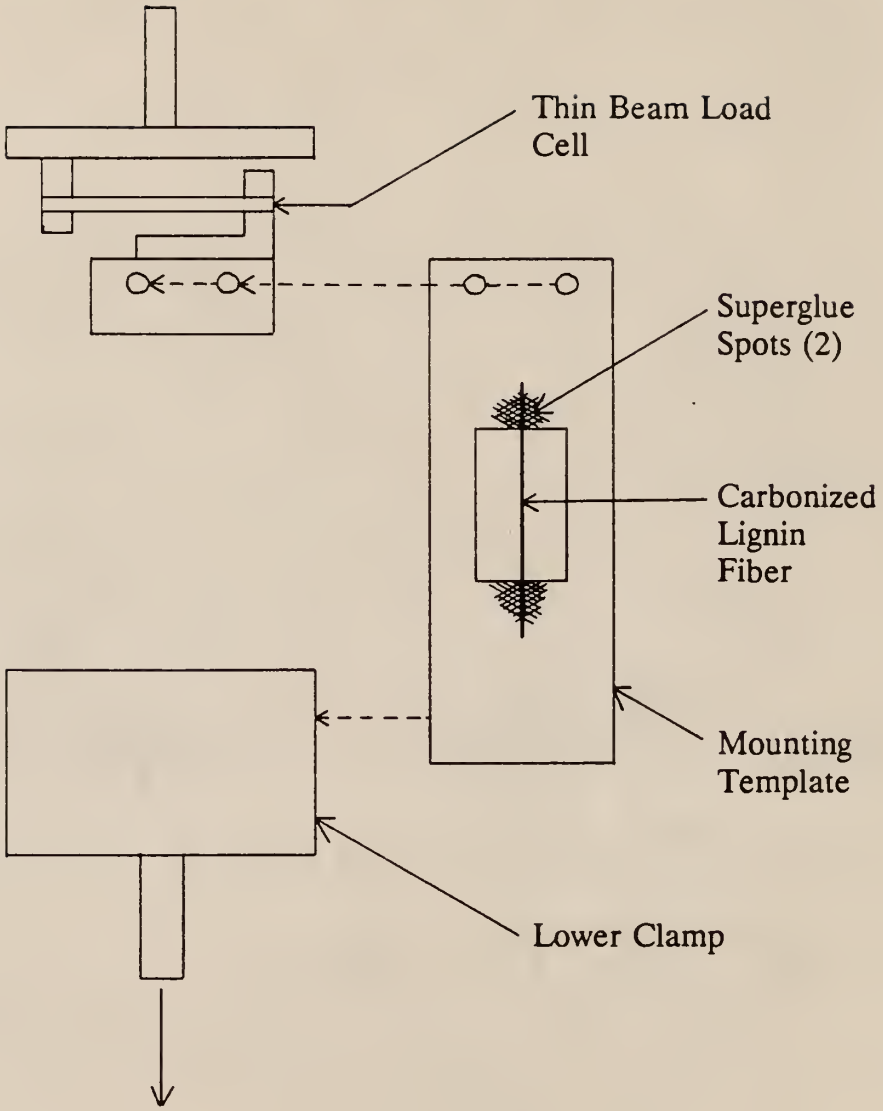

Figure 6-2. Carbonized Lignin Fiber Tensile Testing Apparatus.

fiber diameters were measured with a Nikon optical microscope (Japan) with a length scale in the eyepiece.

Elemental analysis of the fibers was performed to determine their degree of carbonization, and the concentrations of residual impurities such as oxygen and

sulfur. Both the "A", and the "B" fibers were analyzed for total carbon, hydrogen, and nitrogen content by combustion, by Mel Courtney of the Division of Analytical Services in the Chemistry Department at the University of Florida, using a Carlo Erba 1108 elemental analyzer. The "B" fibers were also analyzed for carbon, oxygen, and sulfur by energy dispersive X-ray spectroscopy (EDS) in conjunction with the scanning electron microscopy work discussed below.

Scanning electron microscopy (SEM) was used to visualize the integrity and uniformity of the fiber surface before and after carbonization. Samples were sputtercoated with gold/paladium and submitted to Richard Crockett of the Major Analytical Instrumentation Center at the University of Florida for analysis. Representative micrographs were obtained on a JEOL model JSM 6400 SEM.

6.4 Results and Discussion

6.4.1 Thermogravimetric Analysis

Thermogravimetric analyses of several lignin fiber samples, from different spinning conditions, were performed in order to determine their weight loss versus temperature profiles, and thereby help establish proper carbonization conditions. All of these fiber samples exhibited nearly identical behavior, and a representative TGA scan is given in Figure 6-3. The normal TGA curve indicates the weight % remaining at the corresponding temperature, and the derivative curve denotes the rate of weight loss. For comparison, a normal TGA scan for a dried, purified kraft softwood lignin by Masse [62] has also been included.

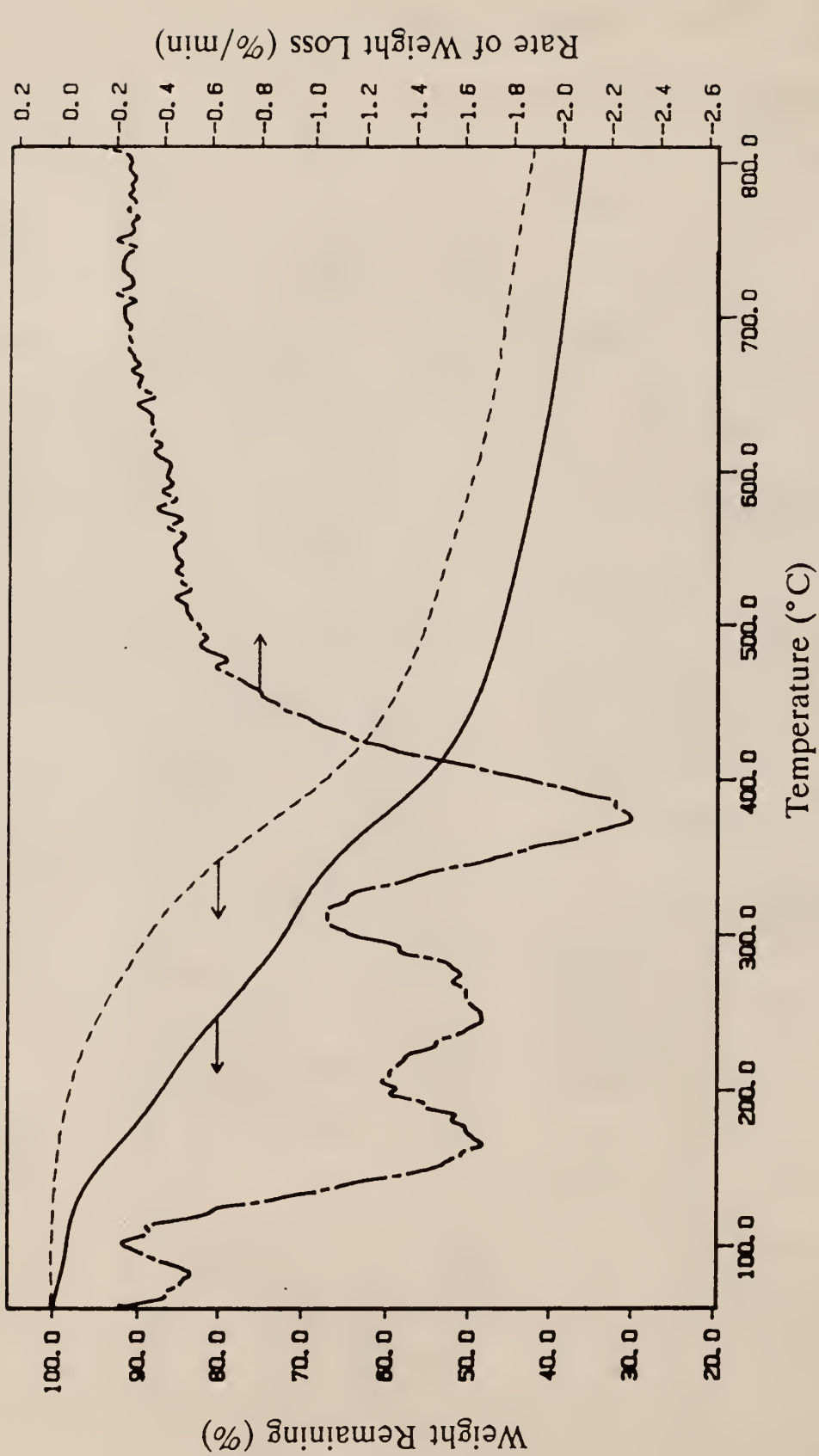

Figure 6-3. Thermogravimetric Analysis of Fibers Spun from Indulin AT + 28% NMP. Normal TGA Curve for Softwood Kraft Lignin (----) by Masse [62]. Heating Rate = 10°C/min in Nitrogen.

The TGA curve for lignin fibers in Figure 6-3 can be divided into several overlapping weight loss regions, with each one accompanied by a negative peak in the derivative curve, which denotes the maximum rate of weight loss. Up to about 100°C, the small weight loss is due to evaporation of absorbed water, and then on up to about 205°C, the residual NMP solvent volatilizes (normal boiling point 202°C). Above 200°C, lignin decomposition and condensation reactions become significant, and extend to over 500°C where the TGA and derivative curves both flatten out indicating only a gradual rate of weight loss. These reactions lead to the accumulation of highly carbonized aromatic condensation products [68].

The general shape of the weight loss curve, and the maximum rate of weight loss at about 375°C, corresponds well to Masse's results [62] for a dried, purified kraft softwood lignin, as seen in Figure 6-3. The different amounts of mass lost for the two lignins is at least partially due to the extra mass of solvent which was evaporated from our plasticized Indulin AT fiber sample. These run conditions were later used for carbonization condition "A".

6.4.2 Surface Morphology

Fiber surface morphology, as seen in SEM micrographs, changed dramatically as a result of carbonization. Comparing the two fibers in Figure 6-4, the uncarbonized "green" fiber in (a) is very brittle and exhibits tensile failure, as seen by the clean fracture plane at the break, and has a relatively smooth surface with distinct axial lines resulting from fiber drawing and takeup. The "B" carbonized fiber

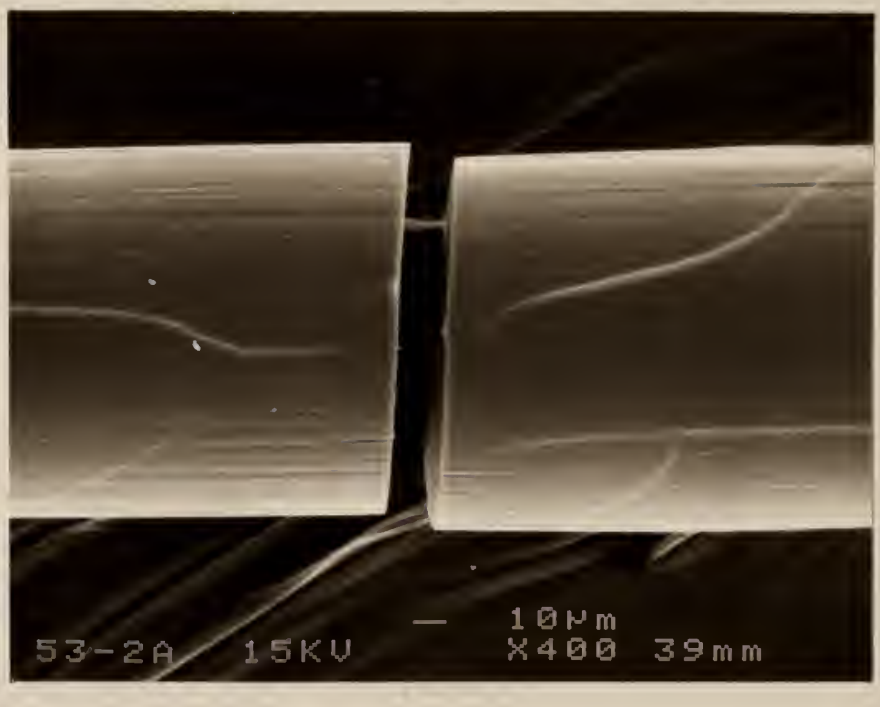

(a)

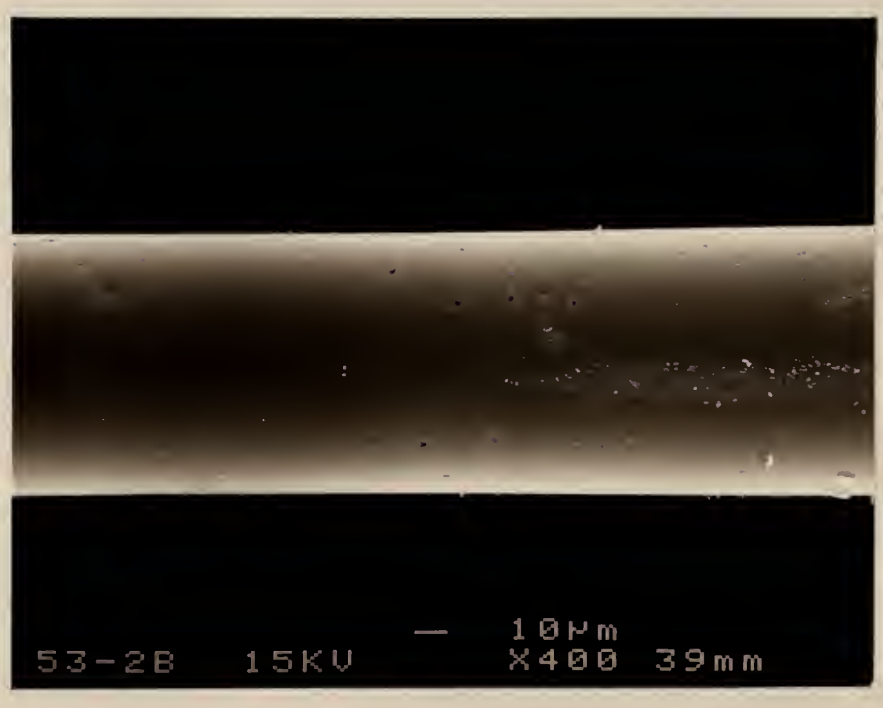

(b)

Figure 6-4. SEM Micrographs for Lignin Fiber. (a) Uncarbonized "Green" Fiber; (b) Carbonized "B" Fiber.

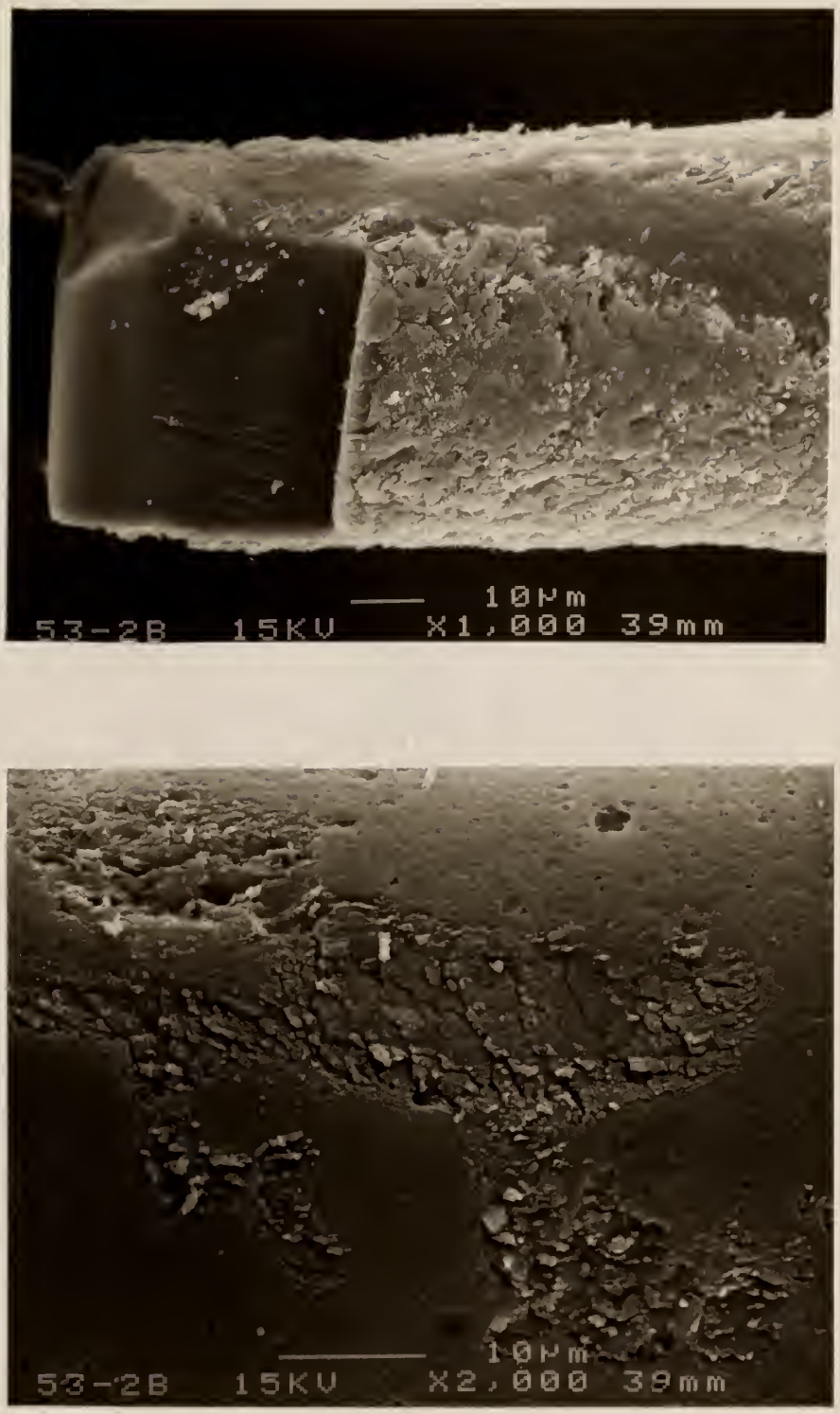

Figure 6-5. SEM Micrographs for "B" Carbonized Lignin Fiber.

in (b) exhibits a porous and almost spongy surface texture with noticeable pinholes. Two more micrographs of this "B" fiber surface, at a higher magnification, are presented in Figure 6-5 and show the porous surface texture, as well as extensive surface roughness and fracturing. In the upper picture in Figure 6-5, the fiber failed in flexure. The clean fracture planes at the break also attest to the brittle nature of this fiber.

The surface features displayed in Figure 6-5 are gross imperfections and flaws and predominate in 'as-prepared' carbon fibers. These surface flaws are routinely observed in most fibers, and control the strength of carbon fibers which have not been heat treated beyond 1,000 - 1,200°C [19]. A detailed look at the fiber cross section by SEM would probably show numerous internal flaws such as voids and inclusions, which are more pronounced in lignin-based fibers than in other ones [50].

The major cause of these flaws is contamination by impurities, such as inorganic salts in the lignin raw material. Microscopic dust and dirt are also common contaminants in the average laboratory environment, and have been shown to adversely affect carbon fiber strength properties [19]. In our laboratory, dust contamination of the lignin precursor fibers during preparation, spinning, and handling, is essentially unavoidable. Clean-room conditions would be necessary in order to realistically minimize dust contamination problems. Also, physical damage of the fiber surface during the numerous handling steps is entirely possible. These impurities react during carbonization and heat treatment to form surface pitting and internal voids and inclusions [19].

The microporous surface features may also have been caused by vaporization of the residual NMP solvent, and by escaping gases that evolved during the multitude of decomposition and condensation reactions that occurred during various stages of the carbonization process. Surface area and density measurements could be used to determine the porosity and internal voidage of the fibers, and help establish whether the observed surface features are truly microporous in nature. Spinning much smaller fibers (on the order of ~10 μm in diameter) would greatly reduce the gas diffusion distances within the fibers and may minimize this phenomenon. Increasing the heat treatment temperature anneals out most of the pores and reduces the porosity open to the surface resulting in a decrease in surface area [19].

Referring back to Figure 6-4, there is also a significant reduction in fiber diameter: from ~125 μm for the uncarbonized fiber, to ~89 μm for the "B" fiber, which corresponds to a 49% reduction in fiber cross-sectional area, and is due to the mass lost during carbonization.

6.4.3 Elemental Composition

The results of the elemental analysis for both sets of carbonized fibers are summarized in Table 6-3. The degree of carbonization is higher for the "B" fibers than for the "A" fibers, which we expected, since the carbonization temperature was 200°C higher. The combustion results are more accurate than the EDS results, but only carbon, hydrogen, and nitrogen were determined this way, whereas EDS also provided us with values for oxygen and sulfur. The sulfur is bound to the lignin

Table 6-3. Elemental Composition of Lignin Carbon Fibers.

Element	Composition[a] "A" Fibers[b]	"B" Fibers[c]		
Carbon	84.00 ± 0.29	87.49 ± 0.68	91.90 ± 0.26	90.99 ± 0.71
Hydrogen	0.88 ± 0.15	0.77 ± 0.03		0.80 ± 0.03
Nitrogen	1.28 ± 0.01	1.13 ± 0.01		1.18 ± 0.02
Oxygen			6.54 ± 0.23	6.48 ± 0.24
Sulfur			0.56 ± 0.07	0.55 ± 0.07
Carbon/ Hydrogen	8.16 ± 1.3	9.50 ± 0.38		

Notes: [a] Composition values in weight %, except carbon/hydrogen atomic ratio.
[b] From combustion analysis.
[c] From combustion analysis (left column), EDS (middle column), and combined combustion analysis and EDS, normalized to 100% (right column).

during the degradation and condensation reactions that occur during pulping, and comes from the sodium sulfide and sodium sulfate salts present in the white liquor.

By comparison to commercial PAN-based and pitch-based carbon fibers, our lignin-based carbon fibers are still relatively impure. Carbon contents for PAN-based fibers range from 92-95% for high strength fibers, to 99+% for ultrahigh modulus fibers with nitrogen and hydrogen as the primary impurities. Pitch-based fibers have carbon contents of 99% for high strength and high modulus fibers, and 99+% for ultrahigh modulus fibers [20].

6.4.4 Mechanical Properties

The mechanical properties of these carbonized fibers are probably the most important ones for evaluating their possible applications. Sample tensile tests for both "A", and "B" fibers are given in Figures 6-6, and 6-7, respectively, and the

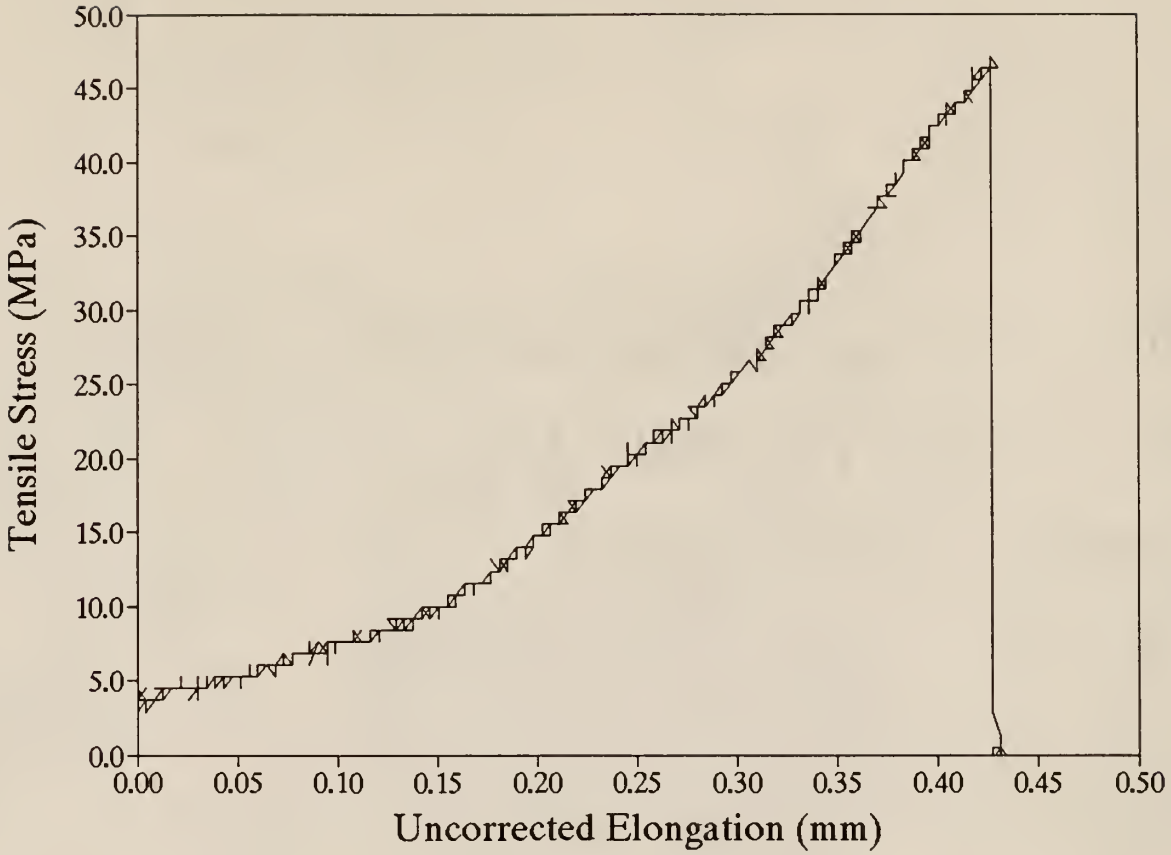

Figure 6-6. Tensile Test for Carbonized Lignin Fiber "A".

calculated tensile properties for both sets of fibers are summarized in Table 6-4. In addition, tensile properties for a general purpose lignin-based carbon fiber developed by Sudo and Shimizu [93], and a Hercules PAN-based fiber tested by David Bennett, who developed the apparatus and test methods used in this study, have also been included for comparison.

The much lower elongation (ultimate strain), and consequently the much higher modulus, for the "B" fibers, as compared to the "A" fibers, is partially due to the uncertainty in correcting for the deflection of the thin beam load cell. These

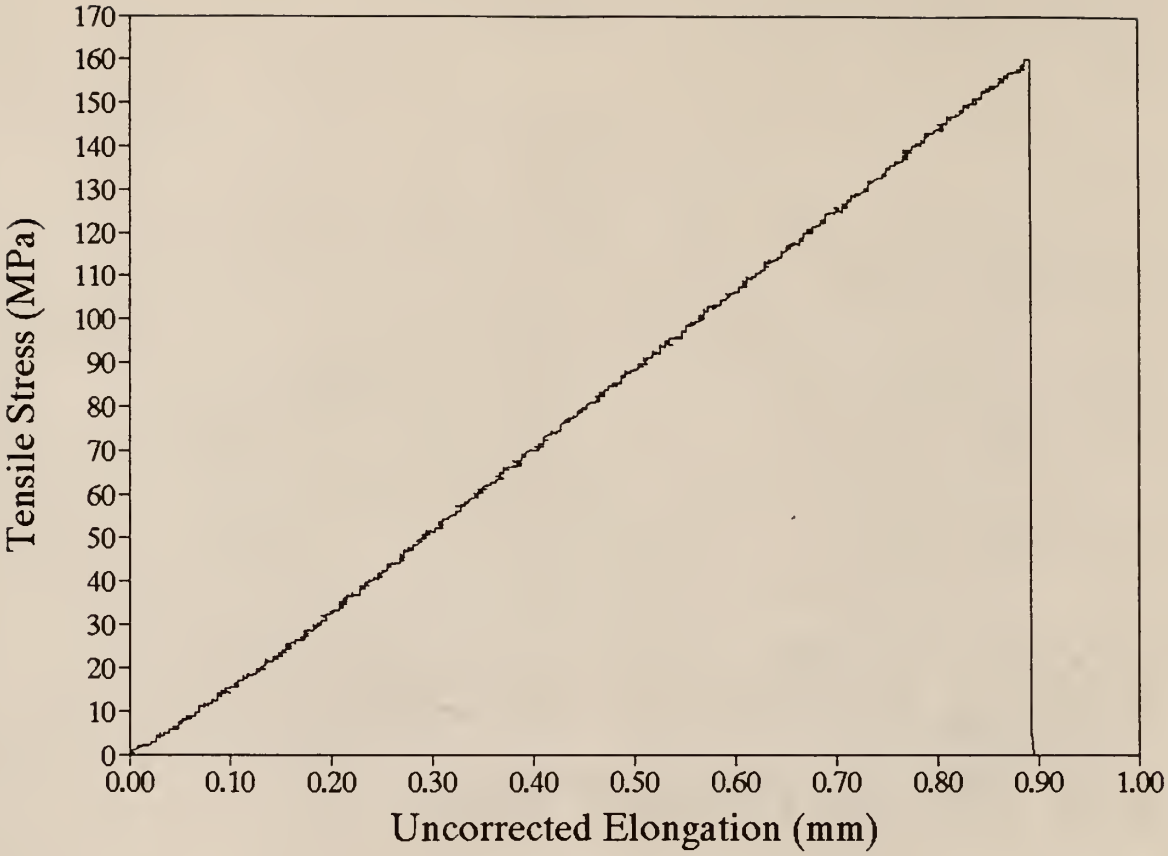

Figure 6-7. Tensile Test for Carbonized Lignin Fiber "B".

elongation values are probably too low and should more realistically be on the order of 1.0 - 1.5 %, which would then give modulus values in the range of 10 - 15 GPa. This would still be a significant improvement over the "A" fibers. The ultimate tensile strength values are realistic. The variation in fiber diameter is probably due to speed variations in the rotating takeup drum, which was manually operated by the author, and therefore, diameter differences between the "A" and "B" fibers are not significant. The substantial increase in strength of the "B" fibers, relative to the "A"

Table 6-4. Mechanical Properties of Lignin-Based and PAN-Based Carbon Fibers.

Carbon Fiber	Diameter (μm)	Tensile Strength (Mpa)	Modulus (Gpa)	Ultimate Strain (%)
"A"	94.5 ± 16.4	58.3 ± 35.2	4.40 ± 1.77	1.57 ± 1.08
"B"	103 ± 3.5	150 ± 20	49.1 ± 14.4	0.32 ± 0.11
General purpose lignin-based[a]	7.6 ± 2.7	660 ± 230	40.7 ± 6.3	1.63 ± 0.29
Hercules PAN-based[b]	7.6 ± 0.42	2,675 ± 668	150 ± 25	1.84 ± 0.61

Notes: [a]Modified lignin-based carbon fibers produced by Sudo and Shimizu [93]
[b]Commercial fibers tested by David Bennett (unpublished data).

fibers, can be attributed to their higher degree of carbonization resulting from the higher processing temperature and longer time.

Compared to the lignin-based fiber developed by Sudo and Shimizu [93], our "B" fiber is quite inferior, having only one fourth of its strength. The PAN-based fiber has 18 times the strength of our "B" fibers, and an order of magnitude greater modulus, if we assume a more realistic value for the elongation of the "B" fibers. This is not surprising because both of these fibers (general purpose lignin-based and PAN-based) were spun from purer starting materials to an order of magnitude smaller diameter: about 8 μm, compared to 100 μm for the "B" fibers. Sudo and Shimizu's lignin was obtained by methanol extraction from steam exploded birch wood, which avoids the inorganic impurities that are present in kraft lignins, and the PAN-based fiber was heat treated, and stretched during carbonization.

These processing steps for commercial fibers are necessary, because it is well recognized that stretching carbon fibers during one of the processing stages improves

the modulus by enhancing the preferred orientation of the carbon crystallites along the fiber axis. The tensile strength has also been shown to vary inversely with the fiber diameter. This is due to the fact that carbon fibers have a composite structure with a sheath consisting of well-oriented crystallites and a core composed of less-oriented material [19]. Reducing the diameter thus increases the proportion of fiber volume composed of the more oriented material, and also reduces the incidence of random internal flaws resulting from contamination by impurities, thereby increasing the strength. Cracks thus have less of a chance of propagating in the smaller diameter, more oriented fibers. Reducing the diameter also reduces the gas diffusion distances, which minimizes the internal pressure buildup due to solvent volatilization (in the case of dry spinning), and gas evolution from the carbonization reactions, which can lead to microcracking and microvoid formation [19].

In light of the preceding discussion, it is obvious that our "B" fibers were spun and carbonized using a very simple procedure, without the modulus and strength enhancing processing steps described above. Considering that this was only an exploratory study utilizing a relatively impure lignin, the results are encouraging.

6.5 Conclusions and Recommendations

6.5.1 Conclusions

The preliminary development work on lignin-based carbon fibers discussed in this chapter has, unfortunately, been very limited. Nevertheless, this study has produced some significant results, and the following conclusions were reached:

1. Lignin fibers can be extruded and drawn at up to 100 m/min at 130°C by thoroughly mixing lignin powder with a good solvent, such as NMP, in sufficient quantity, to act as a plasticizer to lower the lignin T_g far below the degradation temperature.
2. Single fibers of NMP plasticized Indulin AT were carbonized at up to 1,000°C under argon to give fibers with a carbon content of 91%. Mechanical properties--diameter, tensile strength, modulus, and elongation--were 103 ± 3.5 μm, 150 ± 20 MPa, 49.1 ± 14.4 GPa, and 0.32 ± 0.11%, respectively, which are very inferior to commercially available PAN-based and pitch-based carbon fibers.
3. At this point, producing carbon fibers from kraft lignins is not a viable alternative application. However, considering that the Indulin AT lignin was not very pure, and the fiber spinning and carbonization procedures were very simple, the results obtained in this study are encouraging.

6.5.2 Recommendations for Future Work

Numerous refinements to this relatively crude fiber spinning and carbonization process readily come to mind, and some recommendations for future work, to increase the fibers' mechanical properties, are presented below:

1. The Indulin AT lignin raw material should be further purified, and cleaner sample preparation, spinning, and handling procedures should be followed in order to minimize contamination.
2. Smaller diameter fibers (< 10 μm, or as small as possible) should be spun, and the fibers should be stretched during carbonization to see if mechanical properties are improved.
3. Measurements of fiber surface area and density should be made in order to determine the fiber porosity, and SEM micrographs of a fiber cross section should be taken to see if any internal flaws are visible.
4. Subject the fibers to a higher temperature heat treatment, such as 1,500°C, to see if the gross surface flaws and microporous features observed for the "B" fibers are annealed out.
5. Finally, two other types of lignins, such as a high MW lignin sulfonate, and the Repap organosolv lignin, should be investigated as possible raw materials. The lignin sulfonate should be easier to purify than the kraft lignin, and the organosolv lignin should not have any inorganic impurities, but it does have a much lower molecular weight than the Indulin AT lignin investigated here.

CHAPTER 7
OVERALL CONCLUSIONS AND RECOMMENDATIONS

7.1 Summary

In this experimental study there were two principal objectives: (1) to characterize purified lignins, from a statistically designed kraft pulping experiment, and from commercial sources, for molecular weights and molecular weight distribution by SEC, and (2) to investigate the feasibility of producing carbon fibers from these lignins. These two objectives were semi-independent and reflected the dual nature of this work: basic lignin material properties characterization, and applications development for purified lignins.

The molecular weight characterization work was designed to support a much larger overall study of kraft black liquor physical and chemical properties to benefit the pulp and paper industry in its long term plan to more efficiently process black liquors. A lengthy mobile phase/column selection process was undertaken to develop a new SEC method for lignin analysis which overcame persistent lignin association and adsorption problems. The development of lignin-based carbon fibers was investigated to provide an alternative high value use for lignins, as compared to its current predominantly low value fuel use.

There were also two secondary objectives: the determination of glass transition temperatures for dry and solvent plasticized lignins by DSC, and rheological characterization of solvent plasticized lignins by steady and dynamic shear rheometry. These studies were carried out to support the lignin fiber spinning work. Three primary types of lignins were studied: kraft softwood, kraft hardwood, and organosolv lignins.

7.2 Conclusions

Based on the work presented and discussed in the preceding chapters, some important conclusions were drawn.

1. An effective SEC method for comparative lignin molecular weight distribution characterization has been developed and consists of DMSO + 0.1M lithium bromide running at 85°C in a specially designed "deactivated" column set (Jordi Gel GBR series) with sample detection by UV at 280 nm. This mobile phase/column combination minimizes the prevalent adsorption and association problems that have been encountered in the past, and consequently eliminates the need to derivatize the lignins in order to overcome unfavorable adsorption interactions.
2. Accurate and convenient column calibration methods must still be perfected. Calibration with narrow MWD polysaccharide standards

resulted in $\overline{M}_w$ s for kraft lignins being lower by a factor of 3-15 as compared to fully corrected absolute $\overline{M}_w$ values determined by LALLS.

3. Glass transition temperatures for dry purified lignins ranged from 130 to 170°C, and reflect the variation in MW resulting from the range of pulping conditions. The breadth of the glass transition region for kraft lignins was broad: 44-87°C, and correlated linearly with polydispersity of molecular weight.

4. The T_g depression was greater for Indulin AT plasticized with NMP, a weaker hydrogen bonding solvent, than with DMF, a stronger hydrogen bonding solvent, over the range of 0-26 wt. % of solvent. These results do not agree with traditional polymer/solvent glass transition behavior, which is based solely on free volume concepts, but are similar to results from a study involving nylon 6,6 plasticization by different hydrogen bonding solvents [7].

5. Indulin AT plasticized with 28% NMP exhibited shear thinning behavior and some degree of viscoelasticity. Both η_{app} and η^* decreased with increasing $\dot{\gamma}$ or ω, and N_1 and G' both decreased with increasing $\dot{\gamma}$ or ω. These trends are the same as for synthetic polymer melts and solutions.

6. Fibers were easily spun from Indulin AT plasticized with 28% NMP at up to 100 m/min at 130°C, and resulted in carbonized fibers with a carbon content of 91% after carbonization at 1,000°C under argon.

Mechanical properties--diameter, tensile strength, modulus, and elongation--were 103 ± 3.5 μm, 150 ± 20 MPa, 49.1 ± 14.4 GPa, and 0.32 ± 0.11%, respectively. Producing carbon fibers from kraft lignins is currently not a viable alternative application; however, considering the impure raw material, and the simple spinning and carbonization procedures that were employed, the results are encouraging.

7.3 Recommendations for Future Work

Due to the exploratory nature of some of the work presented and discussed in this experimental study, recommendations for future work include expanding this work, and addressing some of the experimental problems that have been identified.

1. The remaining UF kraft softwood lignins should be evaluated using the newly developed SEC method to characterize their MWD s. Once absolute $\overline{M}_n$ values for these lignins have been measured by VPO, the resolution of moments calibration procedure should be pursued further to develop more accurate column calibrations.
2. Glass transition temperatures should be determined for the complete set of lignins from the UF pulping experiment for which detailed pulping and MW data are available. At least two additional lignins (e.g. hardwood kraft, and organosolv), should be studied with several plasticizing solvents. The sample preparation procedure must be revised to insure dry lignins and water free solvents, and the lignin +

solvent samples should be mixed in a sigma blade type of mixer to achieve a more uniform solvent distribution in the sample.

3. For rheological testing of plasticized lignins, a more effective temperature and humidity control system must first be developed so that sample drying is minimized and more consistent rheological data can be obtained. The rheological work should be expanded to include several lignins of different MW s, and several solvent concentrations and temperatures, so that time-temperature superposition can be used to develop master curves for a set of lignins.

4. For producing lignin-based carbon fibers, Indulin AT should be further purified, and cleaner sample preparation, spinning, and handling procedures should be followed to minimize contamination. Smaller diameter fibers ($< 10\ \mu m$, or as small as possible) should be spun, and the fibers should be stretched during carbonization to see if mechanical properties are improved. The fiber porosity should be determined, and SEM micrographs of a fiber cross section should be taken to see if any internal flaws are visible. Higher temperature heat treatments (e.g. to 1,500°C) should be attempted to see if the observed gross surface flaws and microporous features are annealed out. Finally, two other types of lignins, such as a high MW lignin sulfonate, and an organosolv lignin, should be investigated as possible raw materials.

REFERENCES

1. Aho, W.O., "Advances in Chemical Pulping Processes", in Progress in Biomass Conversion, Vol. 4, ed. D.A. Tillman, and E.C. Jahn. New York: Academic Press, 1983, pp. 149-181.

2. Back, E.L., and N.L. Salmén, "Glass Transitions of Wood Components hold Implications for Molding and Pulping Processes", Tappi, 65(7), 107-110 (1982).

3. Barnes, H.A., J.F. Hutton, and K. Walters. An Introduction to Rheology. Amsterdam: Elsevier, 1989, pp. 37-54.

4. Barth, H.G., "Nonsize Exclusion Effects in High-Performance Size Exclusion Chromatography", ch. 2 in Detection and Data Analysis in Size Exclusion Chromatography, ed. T. Provdor. Washington, DC: American Chemical Society, 1987, pp. 29-46.

5. Barton, A.F.M. CRC Handbook of Solubility Parameters and Other Cohesion Parameters. Boca Raton, FL: CRC Press, Inc., 1983, pp. 165-170.

6. Billmeyer, Jr., F.W. Textbook of Polymer Science, 3rd ed. New York: John Wiley & Sons, Inc., 1984, pp. 7, 242-243, 321-322, 339-340, 491-497.

7. Birkinshaw, C., M. Buggy, and S. Daly, "Plasticization of Nylon 66 by Water and Alcohols", Polymer Communications, 28, 286-288 (1987).

8. Brandrup, J., and E.H. Immergut, eds. Polymer Handbook, 3rd ed. New York: John Wiley & Sons, Inc., 1989, p. VII-520.

9. Brunow, G., and G. Miksche, "Some Reactions of Lignin in Kraft and Polysulfide Pulping", Applied Polymer Symposia, 28, 1155-1168 (1976).

10. Chum, H.L., D.K. Johnson, M.P. Tucker, and M.E. Himmel, "Some Aspects of Lignin Characterization by High Performance Size Exclusion Chromatography Using Styrene Divinylbenzene Copolymer Gels", Holzforschung, 41(2), 97-108 (1987).

11. Connors, W.J., "Gel Chromatography of Lignins, Lignin Model Compounds, and Polystyrenes Using Sephadex LH-60", Holzforschung, 32(4), 145-147 (1978).

12. Connors, W.J., L.F. Lorenz, and T.K. Kirk, "Chromatographic Separation of Lignin Models by Molecular Weight Using Sephadex LH-20", Holzforschung, 32(3), 106-108 (1978).

13. Conners, W.J., S. Sarkanen, and J.L. McCarthy, "Gel Chromatography and Association Complexes of Lignin", Holzforschung, 34(3), 80-85 (1980).

14. Cox, W.P., and E.H. Merz, "Correlation of Dynamic and Steady Flow Viscosities", Journal of Polymer Science, 28, 619-622 (1958).

15. Dealy, J.M. Rheometers for Molten Plastics. New York: Van Nostrand Reinhold Co., 1982, pp. 190-197.

16. Dealy, J.M., and K.F. Wissbrun. Melt Rheology and its Role in Plastics Processing: Theory and Applications. New York: Van Nostrand Reinhold, 1990.

17. Dong, D.-J., and A.L. Fricke, "Investigation of Optical Effects of Lignin Solutions and Determination of $\overline{M}_w$ of Kraft Lignins by LALLS", submitted for publication.

18. Donnet, J.-B., and R.C. Bansal. Carbon Fibers. Vol. 3 in "International Fiber Science and Technology Series". New York: Marcel Dekker, Inc., 1984, pp. 9-12.

19. Donnet, J.-B., and R.C. Bansal. Carbon Fibers, 2nd ed. Vol. 10 in "International Fiber Science and Technology Series". New York: Marcel Dekker, Inc., 1990, pp. 1-82, 205-212, 267-314, 367-372, 406-446.

20. Dresselhaus, M.S., G. Dresselhaus, K. Sugihara, I.L. Spain, and H.A. Goldberg. Graphite Fibers and Filaments. Vol. 5 in "Springer Series in Materials Science". Berlin: Springer-Verlag, 1988, pp. 12-18, 304-339.

21. Eastman Kodak Co. Eastman Solvent Selector Chart. Publication no. M-167P. Eastman Kodak Co., 1989.

22. Fengel, D., and G. Wegener. Wood: Chemistry, Ultrastructure, Reactions. Berlin: Walter de Gruyter, 1984, pp. 132-181, 414-481, 526-566.

23. Ferry, J.D. Viscoelastic Properties of Polymers, 2nd ed. New York: John Wiley & Sons, Inc., 1970, pp. 518-557.

24. Forss, K.G., R. Kokkonen, and P.-E. Sågfors, "Determination of the Molar Mass Distribution of Lignins by Gel Permeation Chromatography", ch. 9 in Lignin: Properties and Materials, ed. W.G. Glasser, and S. Sarkanen. ACS Symposium Series No. 397. Washington, DC: American Chemical Society, 1989, pp. 124-133.

25. Forss, K.G., B.G. Stenlund, and P.-E. Sågfors, "Determination of the Molecular-Weight Distribution of Lignosulphonates and Kraft Lignin", Journal of Applied Polymer Science: Applied Polymer Symposium, 28, 1185-1194 (1976).

26. Fricke, A.L. A Comprehensive Program to Develop Correlations for the Physical Properties and Composition of Black Liquors from a Data Base of Experimental and Mill Kraft Black Liquors. A Proposal to the Department of Energy and Industry, University of Florida, Gainesville, FL (1987).

27. Fricke, A.L. Physical Properties of Kraft Black Liquor: Summary Report-Phases I and II. DOE report no. DOE/CE/40606-T5 (DE88002991) (Sept. 1987).

28. Fricke, A.L. A Comprehensive Program to Develop Correlations for the Physical Properties of Kraft Black Liquors: Interim Report No. 1. DOE report no. DOE/CE/40740-T4 (DE89016404) (July 1989).

29. Froment, P., and F. Pla, "Determinations of Average Molecular Weights and Molecular Weight Distributions of Lignin", ch. 10 in Lignin: Properties and Materials, ed. W.G. Glasser, and S. Sarkanen. ACS Symposium Series No. 397. Washington, DC: American Chemical Society, 1989, pp. 134-143.

30. Fujita, H., and A. Kishimoto, "Diffusion-Controlled Stress Relaxation in Polymers. II. Stress Relaxation in Swollen Polymers", Journal of Polymer Science, 28, 547-567 (1958).

31. "Gel Permeation Chromatographic Analysis of Cellulose", Polymer Notes, 1(3). Milford, MA: Waters Division of Millipore Corp., 1986.

32. Glasser, W.G., C.A. Barnett, P.C. Muller, and K.V. Sarkanen, "The Chemistry of Several Novel Bioconversion Lignins", Journal of Agricultural and Food Chemistry, 31(5), 921-930 (1983).

33. Glasser, W.G., and S.S. Kelley, "Lignin", in The Concise Encyclopedia of Polymer Science and Engineering, ed. J.I. Kroschwitz. New York: John Wiley & Sons, Inc., 1990, pp. 544-547.

34. Glasser, W.G., and S. Sarkanen, eds. Lignin: Properties and Materials. ACS Symposium Series No. 397. Washington, DC: American Chemical Society, 1989.

35. Goring, D.A.I., "Thermal Softening of Lignin, Hemicellulose, and Cellulose", Pulp and Paper Magazine of Canada, 64(12), T517-T527 (1963).

36. Goring, D.A.I., "Polymer Properties of Lignin and Lignin Derivatives", ch. 17 in Lignins: Occurence, Formation, Structure, and Reactions, ed. K.V. Sarkanen and C.H. Ludwig. New York: Wiley-Interscience, 1971, pp. 695-768.

37. Goring, D.A.I., "The Lignin Paradigm", ch. 1 in Lignin: Properties and Materials, ed. W.G. Glasser, and S. Sarkanen. ACS Symposium Series No. 397. Washington, DC: American Chemical Society, 1989, pp. 2-10.

38. Graessley, W.W., T. Masuda, J.E.L. Roovers, and N. Hadjichristidis, "Rheological Properties of Linear and Branched Polyisoprenes", Macromolecules, 9(1), 127-141 (1976).

39. Hatakeyama, T., K. Nakamura, and H. Hatakeyama, "Studies on Heat Capacity of Cellulose and Lignin by Differential Scanning Calorimetry", Polymer, 23, 1801-1804 (1982).

40. Himmel, M.E., K.K. Oh, D.W. Sopher, and H.L. Chum, "High Performance Size Exclusion Chromatography of Low-Molecular Weight Lignins and Model Compounds", Journal of Chromatography, 267, 249-265 (1983).

41. Himmel, M.E., and P.G. Squire, "Size Exclusion Parameters", ch. 1 in Aqueous Size-Exclusion Chromatography, ed. P.L. Dubin. Amsterdam: Elsevier, 1988, pp. 3-22.

42. Himmel, M.E., K. Tatsumoto, K. Grohmann, D.K. Johnson, and H.L. Chum, "Molecular Weight Distribution of Aspen Lignins from Conventional Gel Permeation Chromatography, Universal Calibration and Sedimentation Equilibrium", Journal of Chromatography, 498, 93-104 (1990).

43. Himmel, M.E., K. Tatsumoto, K.K. Oh, K. Grohmann, D.K. Johnson, and H.L. Chum, "Molecular Weight Distribution of Aspen Lignins Estimated by Universal Calibration", ch. 6 in Lignin: Properties and Materials, ed. W.G.

Glasser, and S. Sarkanen. ACS Symposium Series No. 397. Washington, DC: American Chemical Society, 1989, pp. 82-99.

44. Irvine, G.M., "The Glass Transitions of Lignin and Hemicellulose and their Measurement by Differential Thermal Analysis", Tappi Journal, 67(5), 118-121 (1984).

45. Ito, K., and T. Shigemoto, "Manufacture of Lignin Precursor Fibers for Carbon Fibers", Japanese patent JP 01239114 A2, 25 September 1989.

46. Joesten, M.D., and L.J. Schaad. Hydrogen Bonding. New York: Marcel Dekker, Inc., 1974, pp. 304, 335, 343, 365, 366, 371, 372.

47. Johansson, A., O. Aaltonen, and P. Ylinen, "Organosolv Pulping--Methods and Pulp Properties", Biomass, 13, 45-65 (1987).

48. Johnson, D.J., "Carbon Fibers: Manufacture, Properties, Structure and Applications", ch. 6 in Introduction to Carbon Science, ed. Harry Marsh. London: Butterworths & Co. Ltd., 1989, pp. 197-228.

49. Johnson, D.J., and I. Tomizuka, "The Fine Structure of Lignin- and Pitch-Based Carbon Fibers", Plastics & Polymers Conference Supplement no. 6, 20-24 (1974).

50. Johnson, D.J., I. Tomizuka, and O. Watanabe, "The Fine Structure of Lignin-Based Carbon Fibers", Carbon, 13, 321-325 (1975).

51. Johnson, D.K., H.L. Chum, and J.A. Hyatt, "Molecular Weight Distribution Studies Using Lignin Model Compounds", ch. 8 in Lignin: Properties and Materials, ed. W.G. Glasser, and S. Sarkanen. ACS Symposium Series No. 397. Washington, DC: American Chemical Society, 1989, pp. 109-123.

52. Kim, H.K. The Effect of Kraft Pulping Conditions on Molecular Weights of Kraft Lignins. Ph.D. Dissertation, University of Maine, Orono, ME (1985).

53. Kolpak, F.J., D.J. Cietek, W. Fookes, and J.J. Cael, "Analysis of Lignins from Spent Alkaline Pulping Liquors by Gel Permeation Chromatography/ Low-Angle Laser Light Scattering (GPC/LALLS)", Journal of Applied Polymer Science: Applied Polymer Symposium, 37, 491-507 (1983).

54. Kristersson, P., K. Lundquist, R. Simonson, and K. Tingsvik, "Gel Permeation Chromatography of Lignin Carbohydrate Compounds", Holzforschung, 37(1), 51-53 (1983).

55. Kuo, C.-Y., and T. Provdor, "An Overview of Size Exclusion Chromatography for Polymers and Coatings", ch. 1 in Detection and Data Analysis in Size Exclusion Chromatography, ed. T. Provdor. Washington, DC: American Chemical Society, 1987, pp. 2-28.

56. Lin, S.Y., "Lignin Utilization: Potential and Challenge", in Progress in Biomass Conversion, Vol. 4, ed. D.A. Tillman, and E.C. Jahn. New York: Academic Press, 1983, pp. 31-78.

57. Lindberg, J.J., T.A. Kuusela, and K. Levon, "Specialty Polymers from Lignin", ch. 14 in Lignin: Properties and Materials, ed. W.G. Glasser, and S. Sarkanen. ACS Symposium Series No. 397. Washington, DC: American Chemical Society, 1989, pp. 190-204.

58. Lockhart, R.J., and S.A. Bortz, "Development of Carbon Products from Lignin (Paper Mill) Wastes", in Proceedings of the 3rd Mineral Waste Utilization Symposium, ed. M.A. Schwartz. Chicago: Illinois Institute of Technology Research Institute, 1972, pp. 79-94.

59. Lora, J.H., C.F. Wu, E.K. Pye, and J.J. Balatinecz, "Characteristics and Potential Applications of Lignin Produced by an Organosolv Pulping Process", ch. 23 in Lignin: Properties and Materials, ed. W.G. Glasser, and S. Sarkanen. ACS Symposium Series No. 397. Washington, DC: American Chemical Society, 1989, pp. 312-323.

60. Mansmann, M., "Stable Lignin and Carbon Fibers", German patent DE 2118488, 26 October 1972.

61. Mansmann, M., G. Winter, G. Pampus, H. Schnooring, and N. Schon, "Process for the Production of Carbon Fibers", U.S. patent 3,723,609, 27 March 1973.

62. Masse, M.A. Thermal Analyses of Kraft Black Liquor. M.S. Thesis, University of Maine, Orono, ME (1984).

63. Meares, P. Polymers: Structure and Bulk Properties. London: Van Nostrand & Co., Ltd., 1965, pp. 266-267.

64. Middleman, S. Fundamentals of Polymer Processing. New York: McGraw-Hill, Inc., 1977, pp. 231-248.

65. Mikawa, S., "Lignin-Based Carbon Fiber", Chemical Economy and Engineering Review, 2(8), 43-46 (1970).

66. Miller, M.L. The Structure of Polymers. New York: Reinhold Book Corp., 1966, pp. 6-9.

67. Noordermeer, J.W.M., O. Kramer, F.H.M. Nestler, J.L. Schrag, and J.D. Ferry, "Viscoelastic Properties of Polymer Solutions in High-Viscosity Solvents and Limiting High-Frequency Behavior. II. Branched Polystyrenes with Star and Comb Structures", Macromolecules, 8(4), 539-544 (1975).

68. Nguyen, T., E. Zavarin, and E.M. Barrall II, "Thermal Analysis of Lignocellulosic Materials. Part I. Unmodified Materials", Journal of Macromolecular Science-Reviews in Macromolecular Chemistry, C20(1), 1-65 (1981).

69. Nippon Kayaku Co., Ltd, "Carbonized Fibers from Lignins", French patent 1,458,725, 10 November 1966.

70. Obiaga, T.I., and M. Wayman, "Improved Calibration Procedure for Gel Permeation Chromatography of Lignins", Journal of Applied Polymer Science, 18, 1943-1952 (1974).

71. Obst, J.R., "Lignins: Structure and Distribution in Wood and Pulp", in Materials Interactions Relevant to the Pulp, Paper, and Wood Industries, ed. D.F. Caulfield, J.D. Passaretti, and S.F. Sobczynski, Materials Research Society Symposium Proceedings, Vol. 197. Pittsburgh, PA: Materials Research Society, 1990, pp. 11-20.

72. Otani, S., Y. Fukuoka, B. Igarashi, and K. Sasaki, "Method for Producing Carbonized Lignin Fiber", U.S. patent 3,461,082, 12 August 1969.

73. Pellinen, J., and M. Salkinoja-Salonen, "Aqueous Size Exclusion Chromatography of Industrial Lignins", Journal of Chromatography, 322, 129-138 (1985).

74. Pellinen, J., and M. Salkinoja-Salonen, "High-Performance Size-Exclusion Chromatography of Lignin and its Derivatives", Journal of Chromatography, 328, 299-308 (1985).

75. Perkin-Elmer Corp. DSC 7 Differential Scanning Calorimeter. Publication no. 0993-7119. Norwalk, CT: Perkin-Elmer Corp., 1985.

76. Powell, R.L., "Rotational Viscometry", ch. 9 in Rheological Measurement, ed. A.A. Collyer, and D.W. Clegg. London: Elsevier Applied Science, 1988, pp. 247-296.

77. Rheometrics, Inc. Mechanical Spectrometer Model RMS-800 and Dynamic Spectrometer Model RDS-II: Operating Instructions. Publication no. 902-00001. Piscataway, NJ: Rheometrics, Inc., June 1986.

78. Rials, T.G., and W.G. Glasser, "Engineering Plastics from Lignin. X. Enthalpy Relaxation of Prepolymers", Journal of Wood Chemistry and Technology, 4(3), 331-345 (1984).

79. Richardson, M.J., "Thermal Analysis of Polymers using Quantitative Differential Scanning Calorimetry", Polymer Testing, 4, 101-115 (1984).

80. Rosen, S.L. Fundamental Principles of Polymeric Materials. New York: John Wiley & Sons, Inc., 1982, p. 84.

81. Rowell, R.M., "Materials Science of Lignocellulosics", in Materials Interactions Relevant to the Pulp, Paper, and Wood Industries, ed. D.F. Caulfield, J.D. Passaretti, and S.F. Sobczynski, Materials Research Society Symposium Proceedings, Vol. 197. Pittsburgh, PA: Materials Research Society, 1990, pp. 3-9.

82. Sakata, I., and R. Senju, "Thermoplastic Behavior of Lignin with Various Synthetic Plasticizers", Journal of Applied Polymer Science, 19, 2799-2810 (1975).

83. Schuerch, C., "The Solvent Properties of Liquids and Their Relation to the Solubility, Swelling, Isolation and Fractionation of Lignin", Journal of the American Chemical Society, 74, 5061-5067 (1952).

84. Scott, W.E. Properties of Paper: An Introduction. Atlanta: TAPPI Press, 1989, p. 5.

85. Shugar, G.J., R.A. Shugar, and L. Bauman. Chemical Technicians' Ready Reference Handbook. New York: McGraw-Hill, 1973, p. 113.

86. Siochi, E.J., M.A. Haney, W. Mahn, and T.C. Ward, "Molecular Weight Determination of Hydroxypropylated Lignins", ch. 7 in Lignin: Properties and Materials, ed. W.G. Glasser, and S. Sarkanen. ACS Symposium Series No. 397. Washington, DC: American Chemical Society, 1989, pp. 100-108.

87. Siochi, E.J., T.C. Ward, M.A. Haney, and B. Mahn, "The Absolute Molecular Weight Distribution of Hydroxypropylated Lignins", Macromolecules, 23, 1420-1429 (1990).

88. Sittig, M., ed. Carbon and Graphite Fibers: Manufacture and Applications. Park Ridge, NJ: Noyes Data Corporation, 1980, pp. 27, 155-156, 336-408.

89. Sjöström, E. Wood Chemistry: Fundamentals and Applications. New York: Academic Press, 1981, pp. 104-145.

90. Small, J.D. An Experimental Investigation of the Rheological Properties of Various Polystyrene Composites. Ph.D. Dissertation, University of Florida, Gainesville, FL (1989).

91. Sudo, K., and K. Shimizu, "Lignin-Based Carbon Fiber Manufacture", Japanese patent JP 62-110922 A2, 22 May 1987.

92. Sudo, K., and K. Shimizu, "Lignin-Phenol Reaction Products for Manufacture of Carbon Fibers", Japanese patent JP 01306618 A2, 11 December 1989.

93. Sudo, K., and K. Shimizu, "A New Carbon Fiber from Lignin", Journal of Applied Polymer Science, 44, 127-134 (1992).

94. Tadmor, Z., and C.G. Gogos. Principles of Polymer Processing. New York: John Wiley & Sons, Inc., 1979, pp. 542-545.

95. Tanner, R.I. Engineering Rheology, rev. ed. Oxford: Clarendon Press, 1988, pp. 114-127.

96. Tomizuka, I., and D.J. Johnson, "Microvoids in Pitch-Based and Lignin-Based Carbon Fibers as Observed by X-Ray Small-Angle Scattering", Yogyo-Kyokai-Shi, 86(4), 186-192 (1978).

97. Wagner, B.A., T. Thanh, D.E. Teller, and J.L. McCarthy, "Estimation of the Distribution of Molecular Weights of Lignins by Use of Low Pressure Size Exclusion Chromatography", Holzforschung, 40 Supplement, 67-73 (1986).

98. Walsh, A.R., and A.G. Campbell, "HPSEC Analysis of Kraft Lignin on a Bondagel Column", Holzforschung, 40(5), 263-266 (1986).

99. Waters Division of Millipore Corp. Waters 150C ALC/GPC: Operator's Manual. Manual no. 82916, rev. A, Sept. 1987. Milford, MA: Waters Publications, 1981.

100. Waters Division of Millipore Corp. Waters 486 Tunable Absorbance Detector: Operator's Manual. Manual no. 80610, rev. 0, August 1990. Milford, MA: Waters Publications, 1990.

101. Wendlandt, W.W., and P.K. Gallagher, "Instrumentation", ch. 1 in Thermal Characterization of Polymeric Materials, ed. E.A. Turi. New York: Academic Press, 1981, pp. 1-90.

102. Wight, M.O. An Investigation of Black Liquor Rheology versus Pulping Conditions. Ph.D. Dissertation, University of Maine, Orono, ME (1985).

103. Williamson, P.N., "Repap's ALCELL™ Process: How it Works and What it Offers", Pulp & Paper Canada, 88(12), (1987).

104. Wunderlich, B., "The Basis of Thermal Analysis", ch. 2 in Thermal Characterization of Polymeric Materials, ed. E.A. Turi. New York: Academic Press, 1981, pp. 91-234.

105. Yau, W.W., J.J. Kirkland, and D.D. Bly. Modern Size Exclusion Liquid Chromatography. New York: John Wiley & Sons, Inc., 1979, pp. 4-12, 19-51, 294-302.

106. Yoshida, H., R. Morck, and K.P. Kringstad, "Fractionation of Kraft Lignin by Successive Extraction with Organic Solvents. II. Thermal Properties of Kraft Lignin Fractions", Holzforschung, 41(3), 171-176 (1987).

BIOGRAPHICAL SKETCH

Gerald Wolfgang Schmidl was born in Long Branch, NJ, on January 6, 1961, and grew up in nearby Tinton Falls. He attended public school there, and graduated from Monmouth Regional High School as valedictorian of his class in June, 1979.

The author enrolled at Virginia Tech in September, 1979, and graduated with a B.S. in chemical engineering in June, 1984. From September, 1980, through December, 1982, he participated in the Cooperative Education Program, working alternate quarters at Union Carbide Corporation's research and development center in Bound Brook, NJ. This experience sparked the author's interest in polymers.

Seeking a change of scenery, the author headed south in August, 1984, to sunny Florida to pursue a graduate degree in chemical engineering at the University of Florida. After completing a M.S. degree in chemical engineering in August, 1985, he switched over to the Materials Science & Engineering Department for a Ph.D., where he studied biomedical polymers for implants. He became disillusioned with this career path, and in September, 1987, returned to the Chemical Engineering Department to pursue a Ph.D. with Professor Arthur L. Fricke on lignin characterization. He is currently a candidate for the Doctor of Philosophy degree in chemical engineering from the University of Florida in December, 1992. Only time will tell if this long and painful struggle has all been worth it.

I certify that I have read this study and that in my opinion it conforms to acceptable standards of scholarly presentation and is fully adequate, in scope and quality, as a dissertation for the degree of Doctor of Philosophy.

Arthur L. Fricke, Chairman
Professor of Chemical Engineering

I certify that I have read this study and that in my opinion it conforms to acceptable standards of scholarly presentation and is fully adequate, in scope and quality, as a dissertation for the degree of Doctor of Philosophy.

Charles L. Beatty
Professor of Materials Science and Engineering

I certify that I have read this study and that in my opinion it conforms to acceptable standards of scholarly presentation and is fully adequate, in scope and quality, as a dissertation for the degree of Doctor of Philosophy.

Russell S. Drago
Graduate Research Professor of Chemistry

I certify that I have read this study and that in my opinion it conforms to acceptable standards of scholarly presentation and is fully adequate, in scope and quality, as a dissertation for the degree of Doctor of Philosophy.

Gar B. Hoflund
Professor of Chemical Engineering

I certify that I have read this study and that in my opinion it conforms to acceptable standards of scholarly presentation and is fully adequate, in scope and quality, as a dissertation for the degree of Doctor of Philosophy.

Chang W. Park
Assistant Professor of Chemical Engineering

This dissertation was submitted to the Graduate Faculty of the College of Engineering and to the Graduate School and was accepted as partial fulfillment of the requirements for the degree of Doctor of Philosophy.

December 1992

for Winfred M. Phillips
Dean, College of Engineering

Madelyn M. Lockhart
Dean, Graduate School